Machine-learning assisted workflows for inorganic molecular discovery

Jon Paul Janet [1] Chenru Duan[2] Aditya Nandy[2]
Heather Kulik [1]

[1]Department of Chemical Engineering, Massachusetts Institute of Technology

[2]Department of Chemistry, Massachusetts Institute of Technology

Machine Learning and Informatics for Chemistry and Materials

10.02.19

Motivation: chemical discovery

How can we design new materials using computers?

The space of possible chemistries is incredibly vast, with $\mathcal{O}(10^{60})$ small organic molecules.

All potentially undiscovered medicines, catalysts and materials are somewhere, out in this huge space.

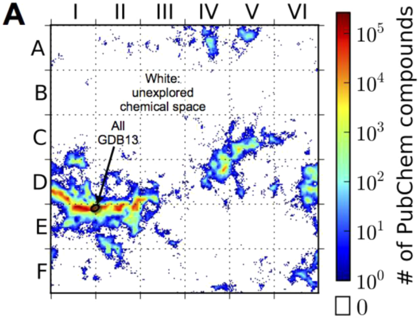

Virshup *et al.*, *J. Am. Chem. Soc.*, 135(19): 7296–7303, 2013.

Motivation: chemical discovery

How can we design new materials using computers?

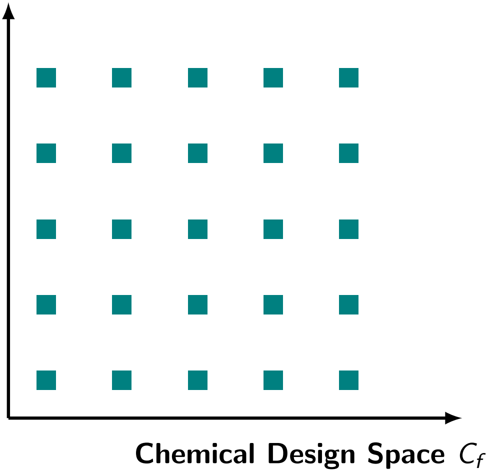

Motivation: chemical discovery

How can we design new materials using computers?

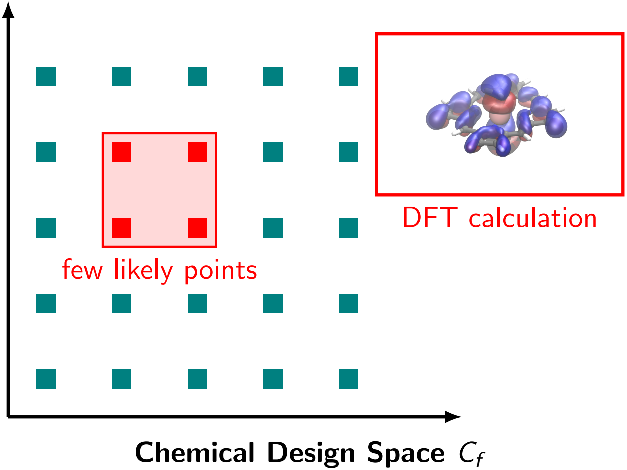

Motivation: chemical discovery

How can we design new materials using computers?

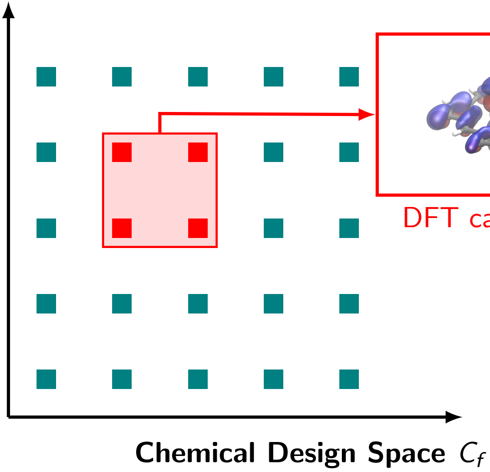

Motivation: chemical discovery

How can we design new materials using computers?

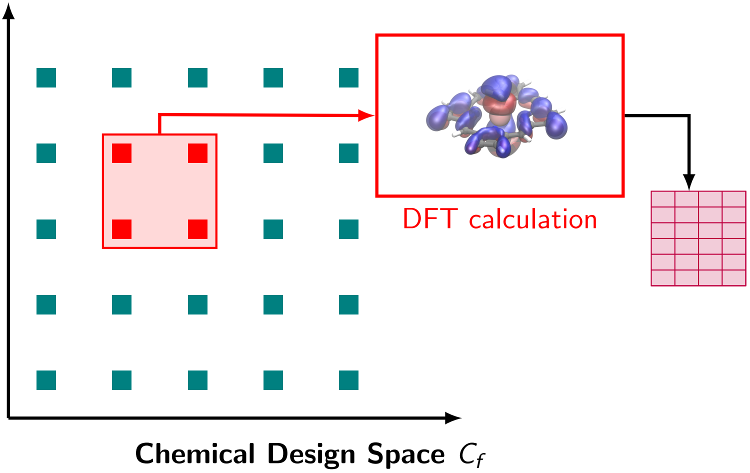

Motivation: chemical discovery

How can we design new materials using computers?

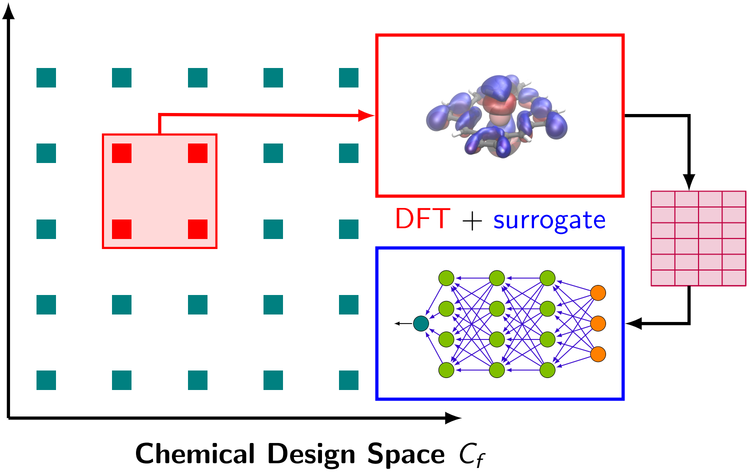

Motivation: chemical discovery

How can we design new materials using computers?

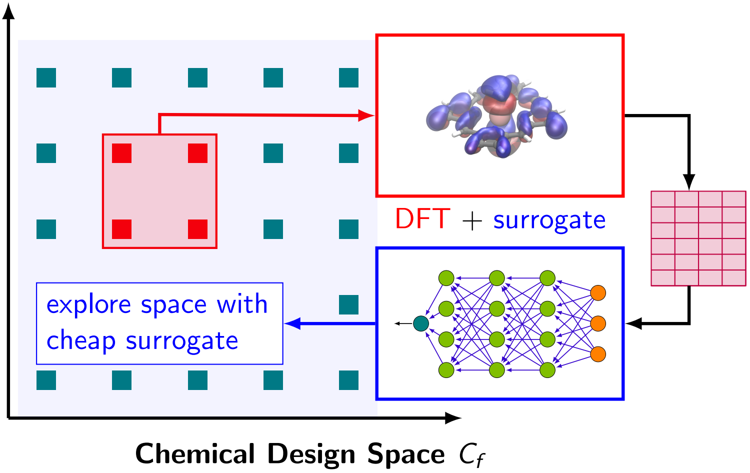

Motivation: chemical discovery

How can we design new materials using computers?

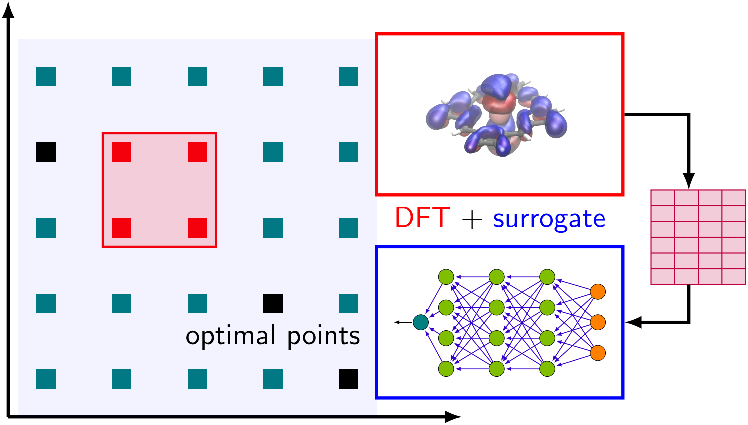

Chemical Design Space C_f

Motivation: chemical discovery

How can we design new materials using computers?

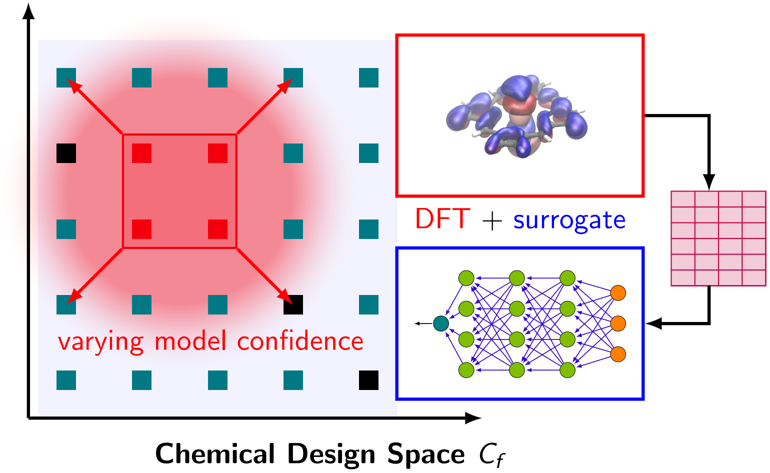

Transition metal complexes

Transition metal complexes

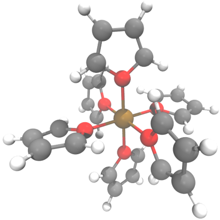

Transition metal complexes

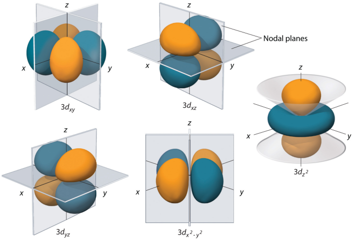

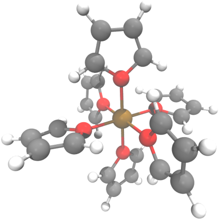

Transition metal complexes

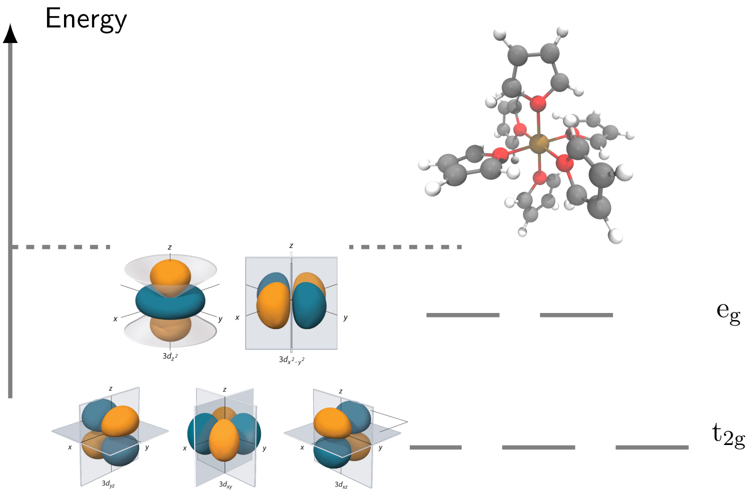

Transition metal complexes

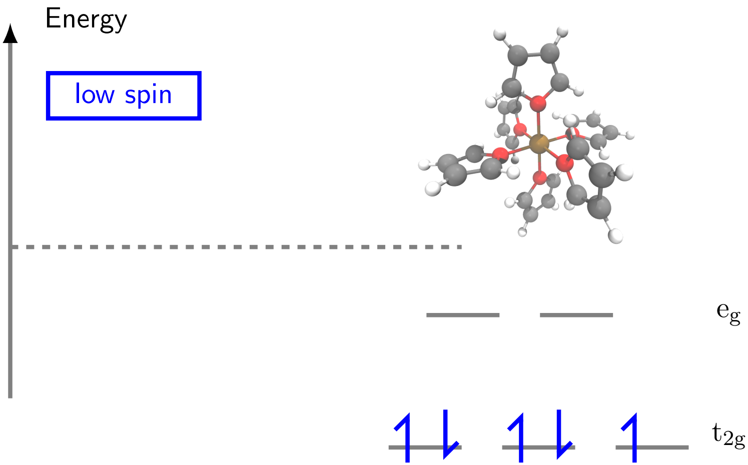

Transition metal complexes

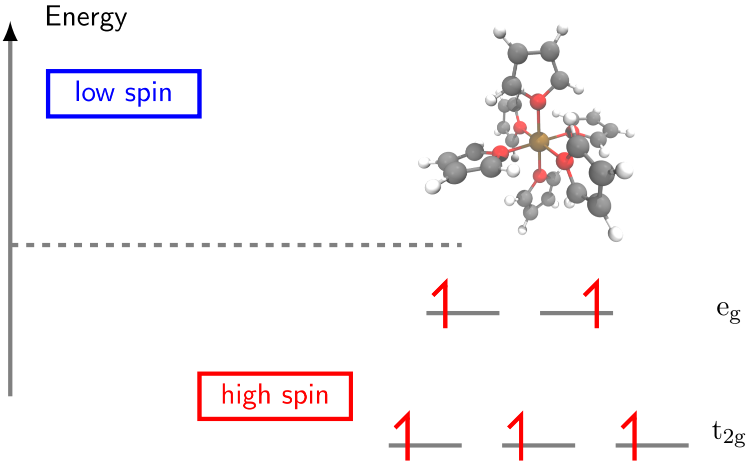

Transition metal complexes

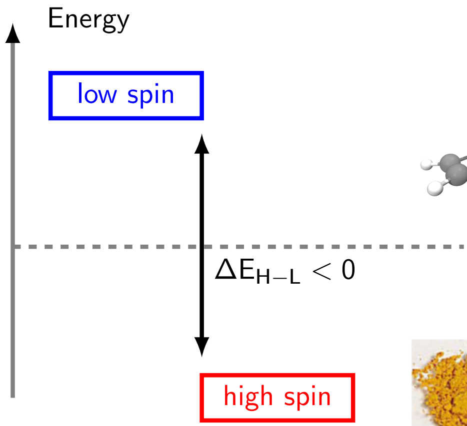

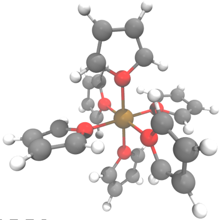

Transition metal complexes

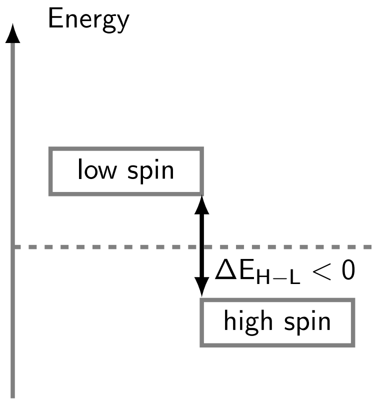

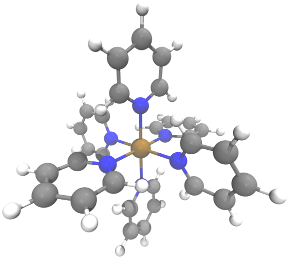

Transition metal complexes

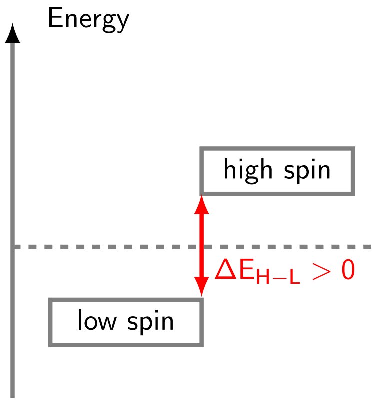

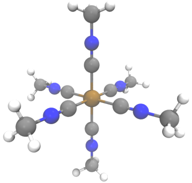

Transition metal complexes

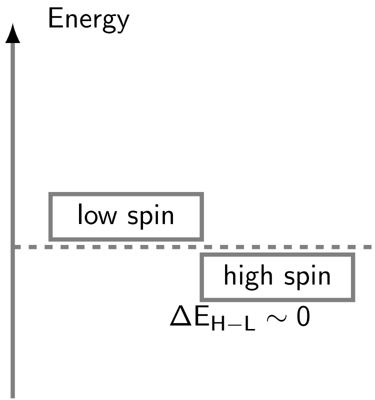

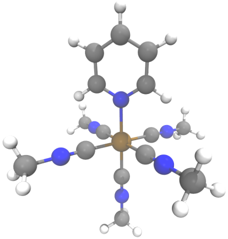

Transition metal complexes

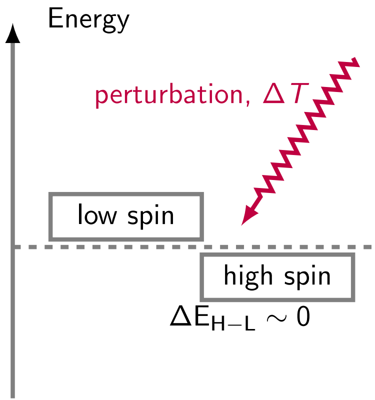

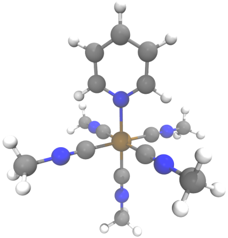

Transition metal complexes

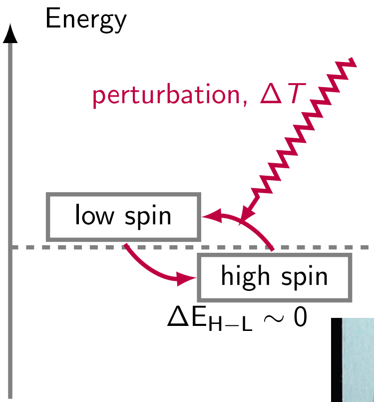

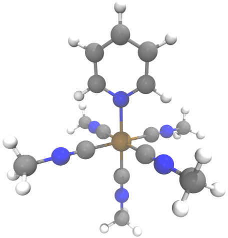

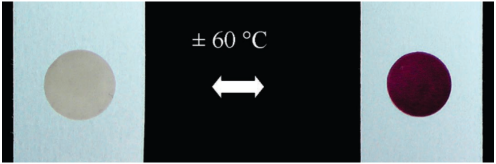

Seredyuk, M *et al.*, *Chem. Mater.*, 18(10):2513–2519, 2006.

Transition metal complexes

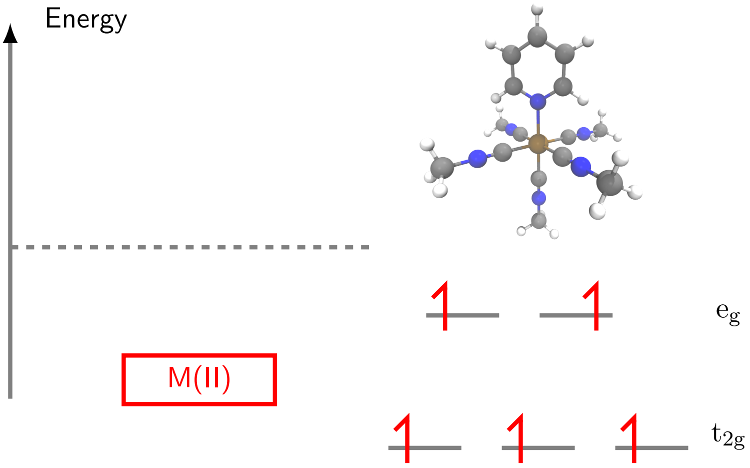

Transition metal complexes

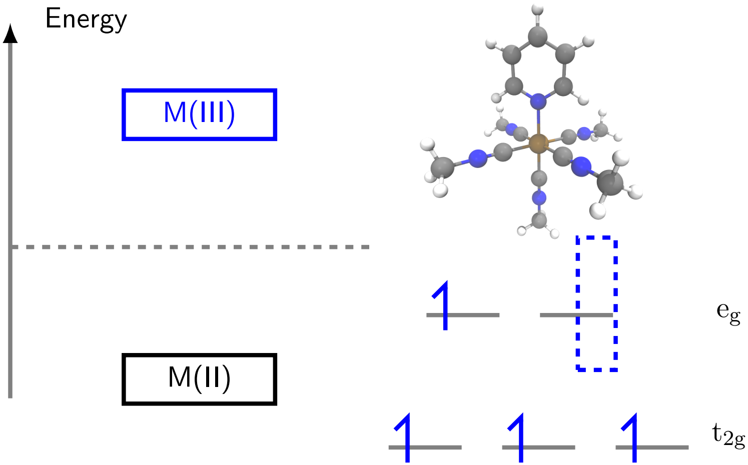

Transition metal complexes

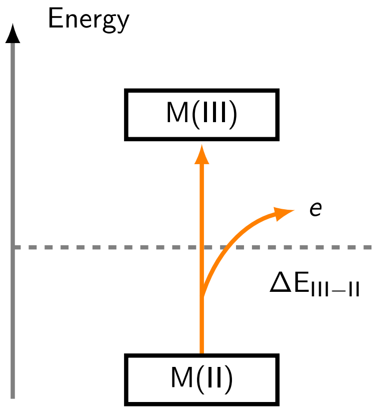

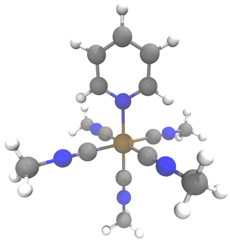

Algorithmic chemical discovery

design space

candidate materials

Algorithmic chemical discovery

Algorithmic chemical discovery

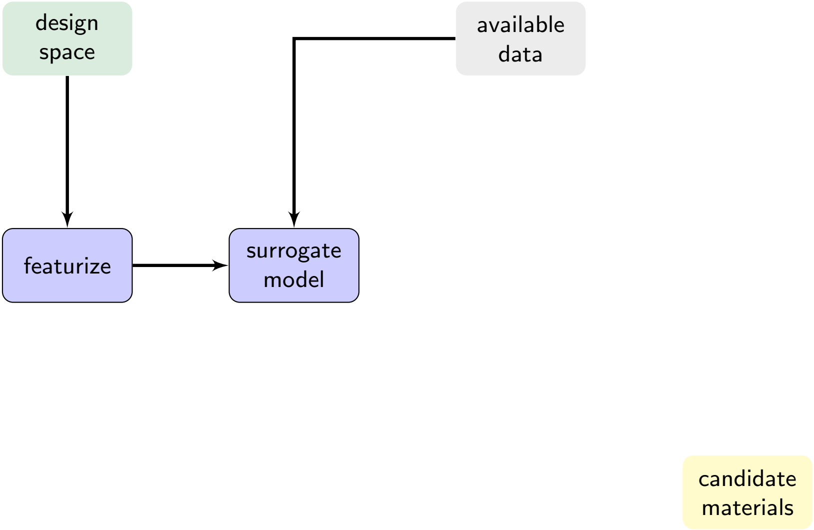

Algorithmic chemical discovery

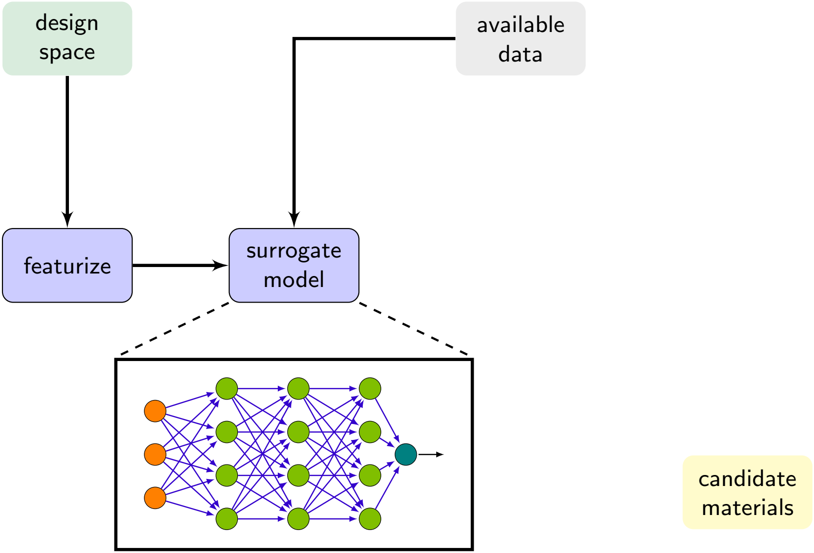

Algorithmic chemical discovery

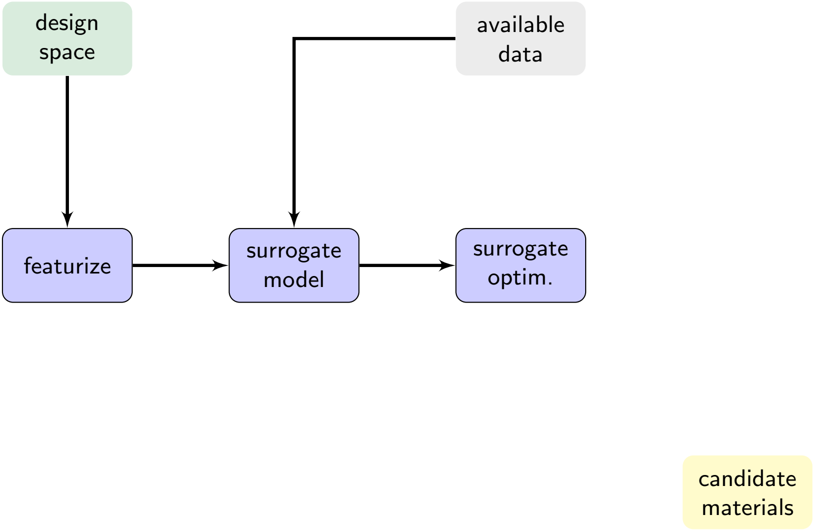

Algorithmic chemical discovery

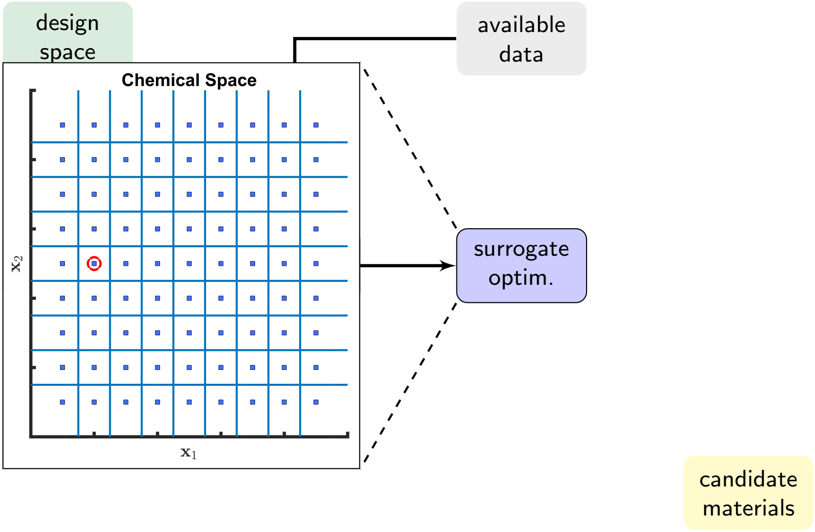

Algorithmic chemical discovery

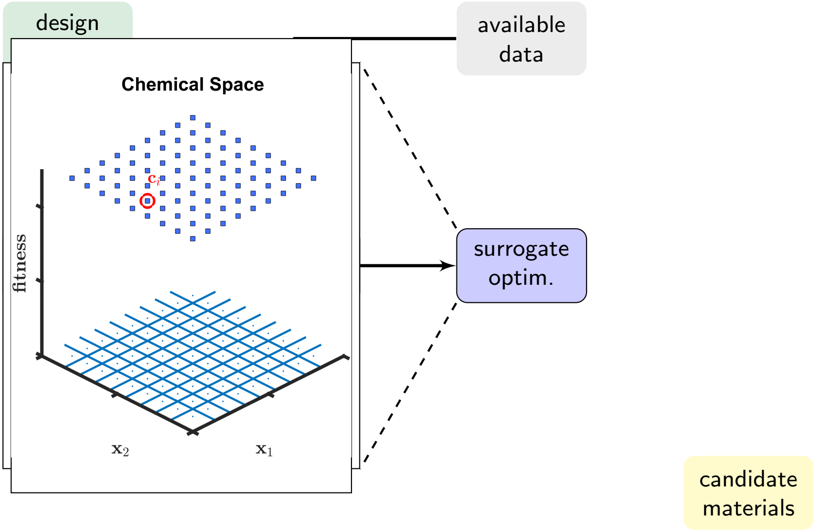

Algorithmic chemical discovery

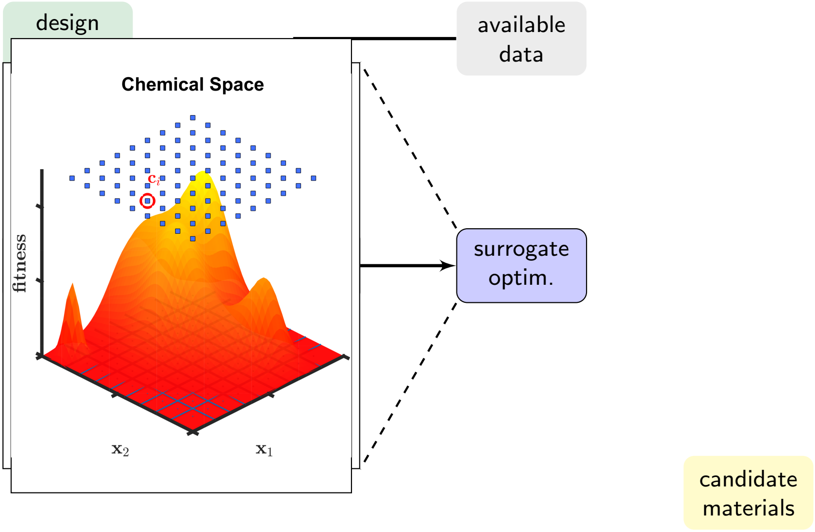

Algorithmic chemical discovery

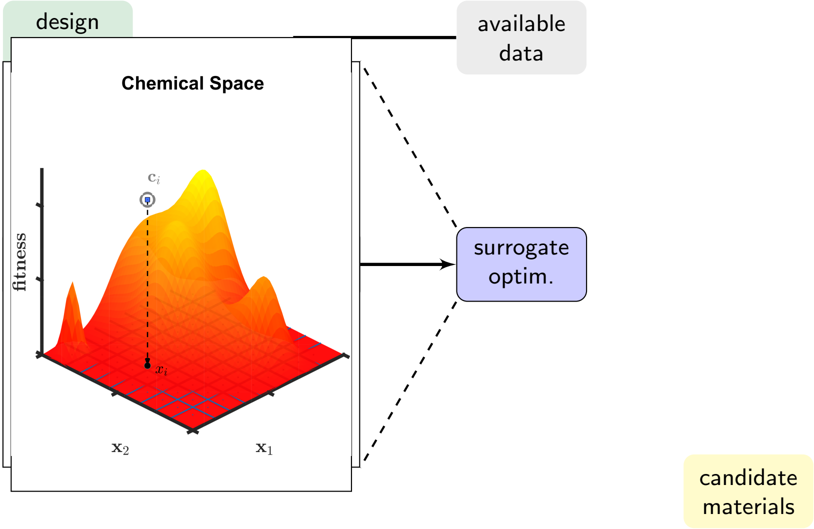

Algorithmic chemical discovery

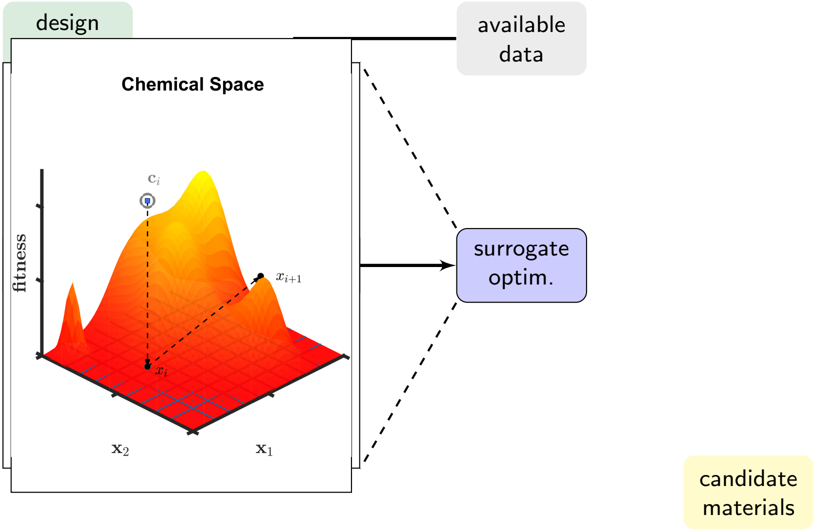

Algorithmic chemical discovery

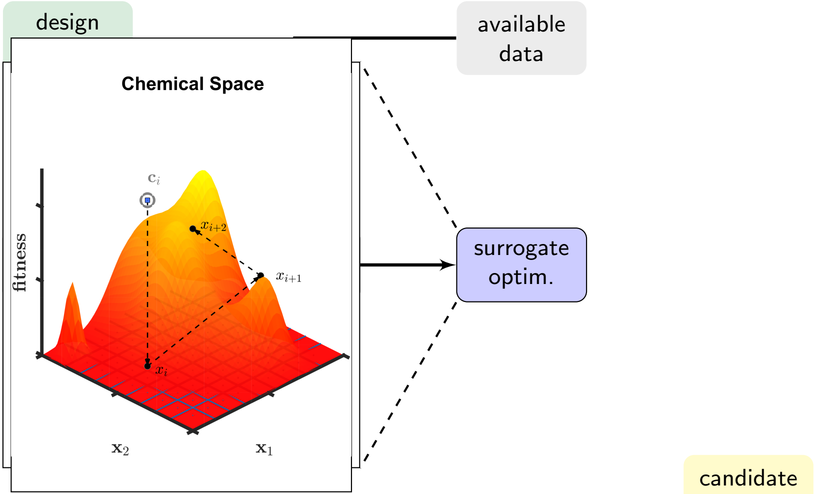

Algorithmic chemical discovery

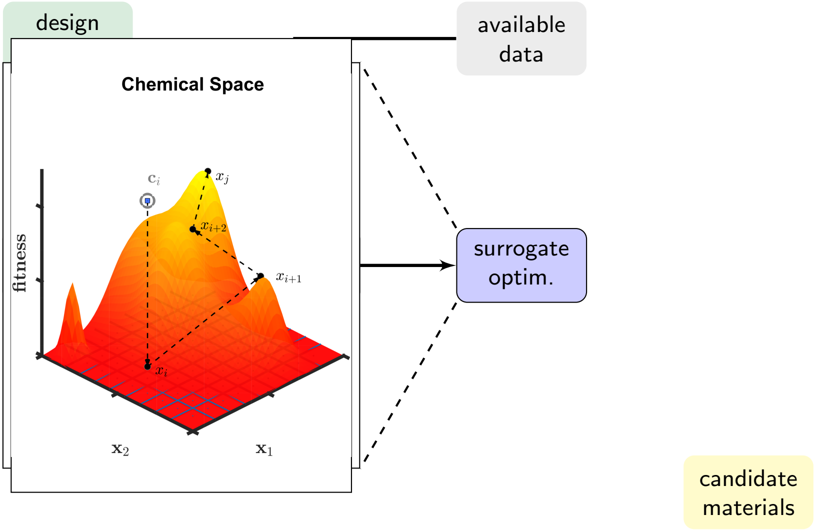

Algorithmic chemical discovery

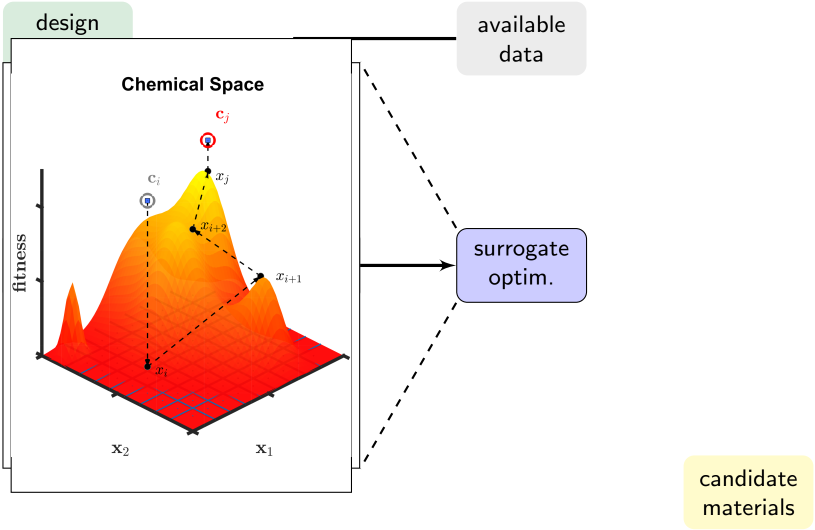

Algorithmic chemical discovery

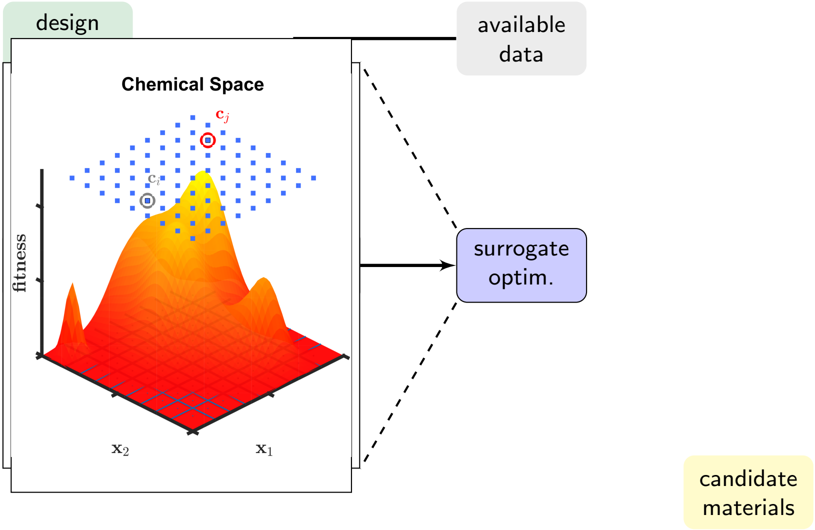

Algorithmic chemical discovery

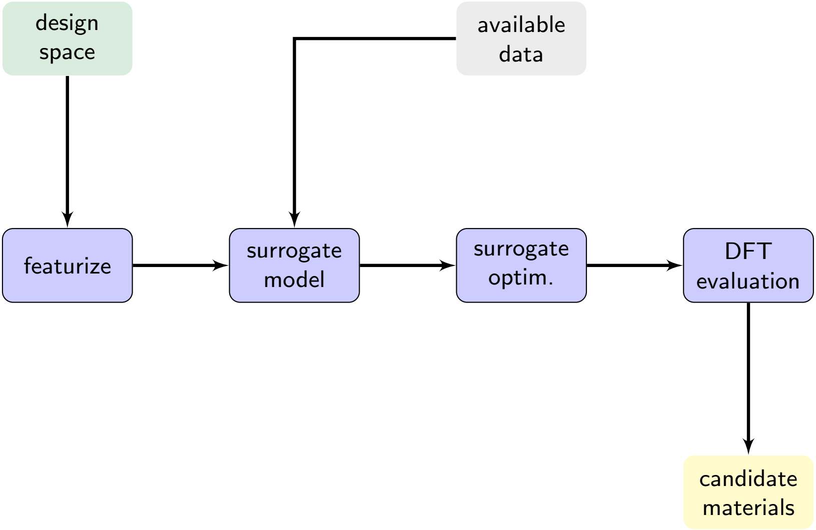

Algorithmic chemical discovery

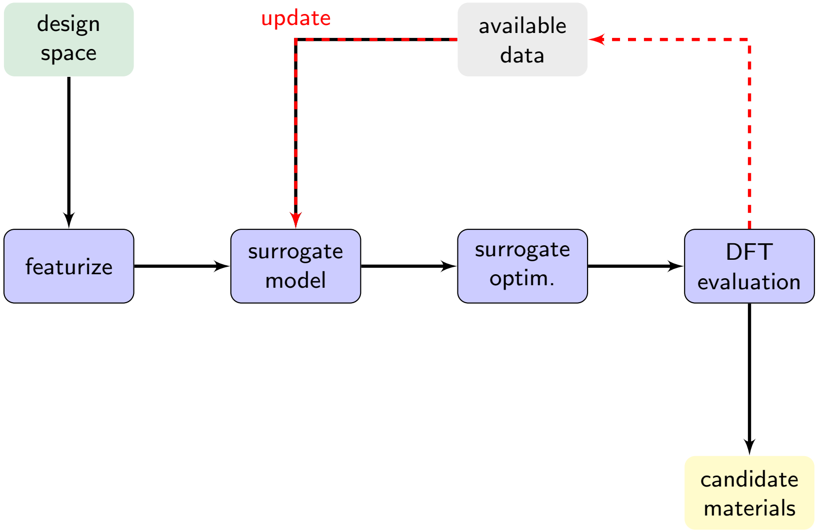

First-principles calculations

train on $\sim$ 100–2000 DFT calculations:

First-principles calculations

train on ∼ 100–2000 DFT calculations:

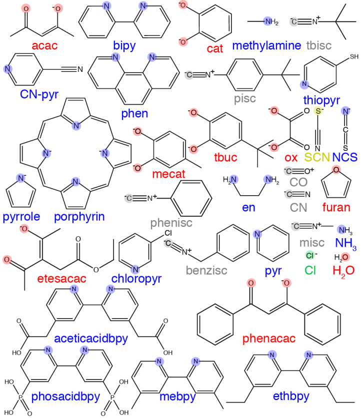

First-principles calculations

train on ∼ 100–2000 DFT calculations:

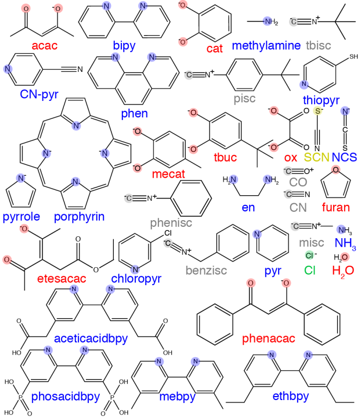

Cr	Mn	Fe	Co

First-principles calculations

train on ~ 100–2000 DFT calculations:

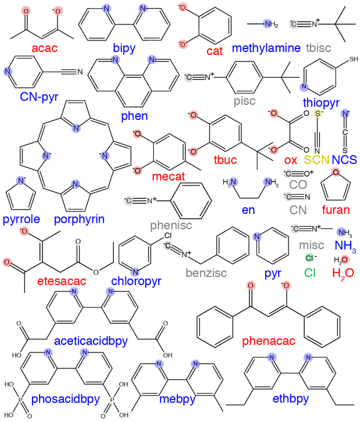

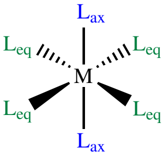

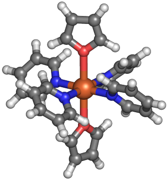

Cr	Mn	Fe	Co

First-principles calculations

train on ∼ 100–2000 DFT calculations:

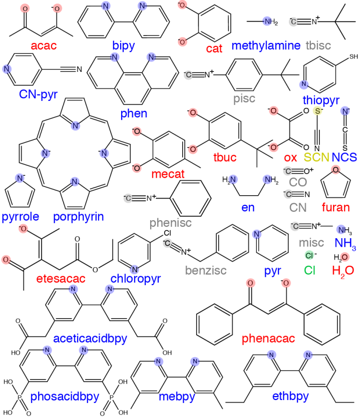

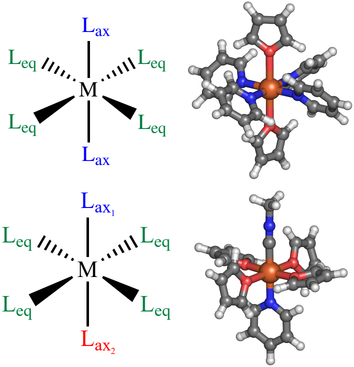

Cr	Mn	Fe	Co

First-principles calculations

train on ∼ 100–2000 DFT calculations:

Details:
•B3LYP-like DFT
•gas phase optimizaton
•LANL2DZ/6-31G*
•COSMO solvents
•high- and low-spin M(II)/(III)

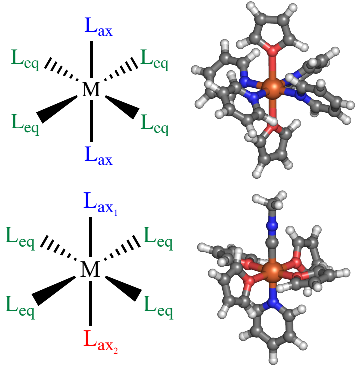

Cr	Mn	Fe	Co

First-principles calculations

train on ~ 100–2000 DFT calculations:

Details:

- B3LYP-like DFT
- gas phase optimizaton
- LANL2DZ/6-31G*
- COSMO solvents
- high- and low-spin M(II)/(III)

HF exchange varied 0–30%

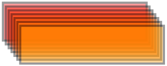

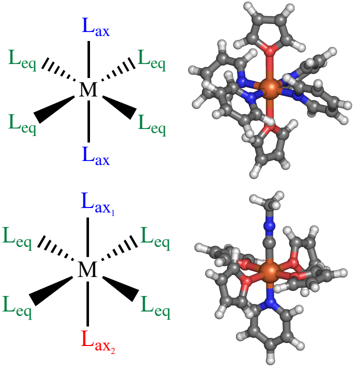

Cr	Mn	Fe	Co

Featurization with RACs

Graph-based features designed for TM complexes

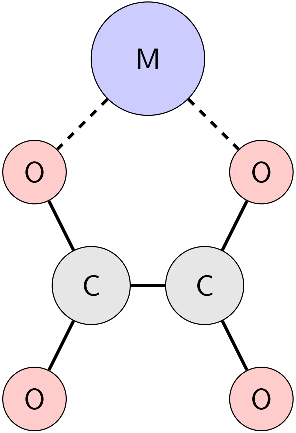

Janet, J.P., and Kulik, H.J., *J. Phys. Chem. A*, 121(46):8939–8954, 2017.

Featurization with RACs

Graph-based features designed for TM complexes

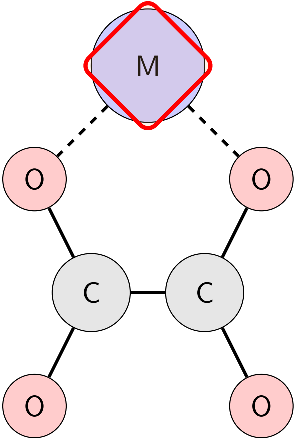

Janet, J.P., and Kulik, H.J., *J. Phys. Chem. A*, 121(46):8939–8954, 2017.

Featurization with RACs

Graph-based features designed for TM complexes

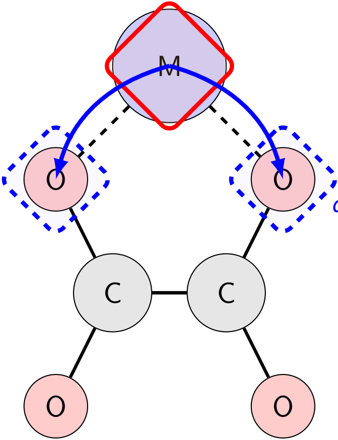

$d_1 : \sum_{M,O} Z_M Z_O$

Janet, J.P., and Kulik, H.J., *J. Phys. Chem. A*, 121(46):8939–8954, 2017.

Featurization with RACs

Graph-based features designed for TM complexes

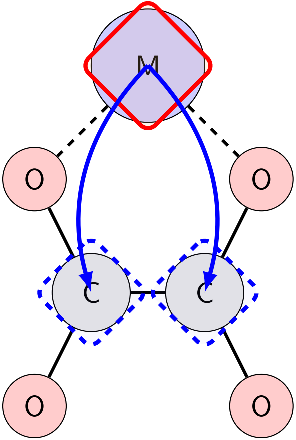

$$d_1 : \sum_{M,O} Z_M Z_O$$

$$d_2 : \sum_{M,C} Z_M Z_C$$

Janet, J.P., and Kulik, H.J., *J. Phys. Chem. A*, 121(46):8939–8954, 2017.

Featurization with RACs

Graph-based features designed for TM complexes

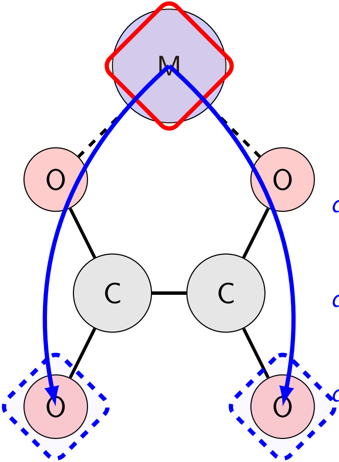

$d_1 : \sum_{M,O} Z_M Z_O$

$d_2 : \sum_{M,C} Z_M Z_C$

$d_3 : \sum_{M,O} Z_M Z_O$

Janet, J.P., and Kulik, H.J., *J. Phys. Chem. A*, 121(46):8939–8954, 2017.

Featurization with RACs

Graph-based features designed for TM complexes

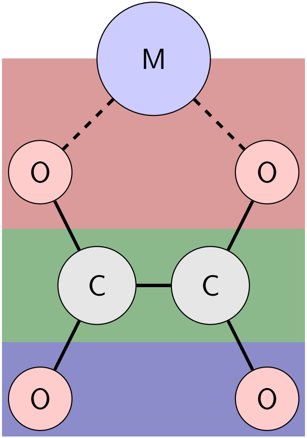

Janet, J.P., and Kulik, H.J., *J. Phys. Chem. A*, 121(46):8939–8954, 2017.

Featurization with RACs

Graph-based features designed for TM complexes

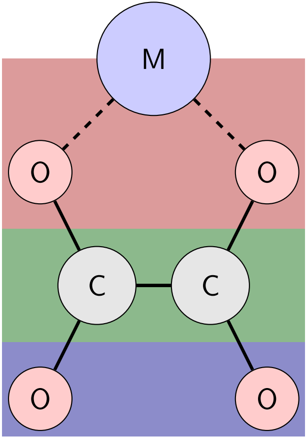

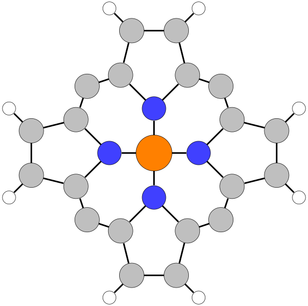

Janet, J.P., and Kulik, H.J., *J. Phys. Chem. A*, 121(46):8939–8954, 2017.

Featurization with RACs

Graph-based features designed for TM complexes

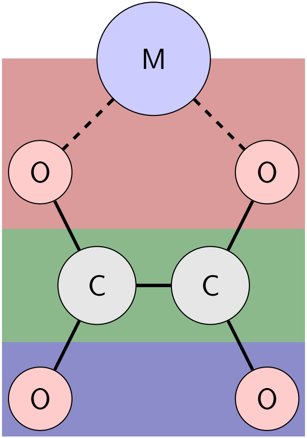

spin splitting ΔE_{H-L}

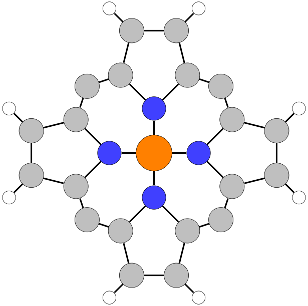

redox ΔG_{solv}

Janet, J.P., and Kulik, H.J., *J. Phys. Chem. A*, 121(46):8939–8954, 2017.

Featurization with RACs

Graph-based features designed for TM complexes

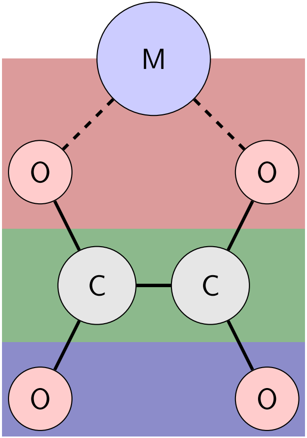

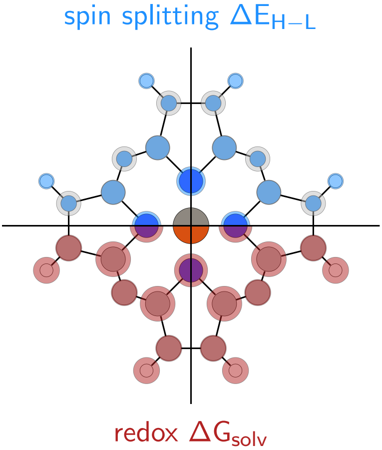

Janet, J.P., and Kulik, H.J., *J. Phys. Chem. A*, 121(46):8939–8954, 2017.

Featurization with RACs

Graph-based features designed for TM complexes

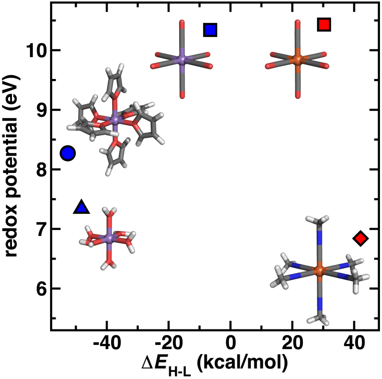

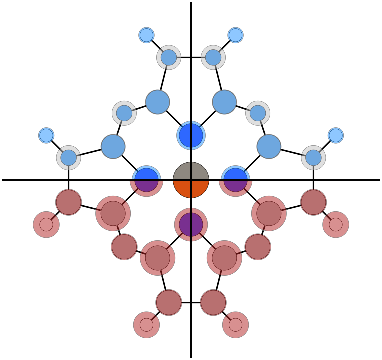

Janet, J.P., and Kulik, H.J., *J. Phys. Chem. A*, 121(46):8939–8954, 2017.

Janet, J.P. *et al.*, *Inorg. Chem.*, 58(16):10592–10606, 2019.

Property inference with ANNs

Estimate properties using small artifical neural networks (ANNs)

Property inference with ANNs

Estimate properties using small artifical neural networks (ANNs)

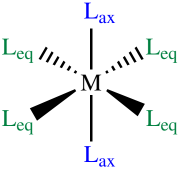

Property inference with ANNs

Estimate properties using small artifical neural networks (ANNs)

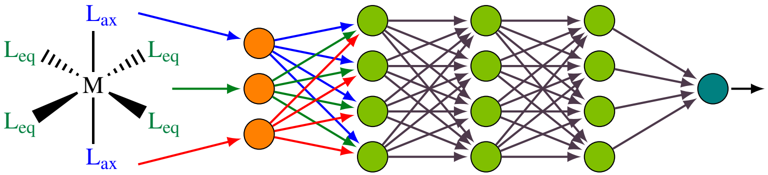

Property inference with ANNs

Estimate properties using small artifical neural networks (ANNs)

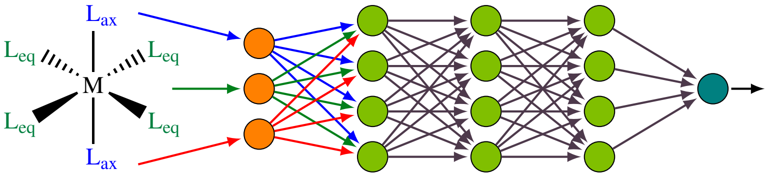

spin splitting energies

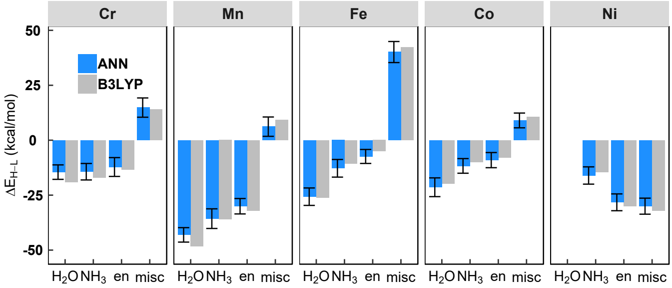

Janet, J.P. and Kulik, H.J., *Chem. Sci.*, 8:5137–5152, 2017. 50 × 50 tanh nodes fully connected ANN

Property inference with ANNs

Estimate properties using small artifical neural networks (ANNs)

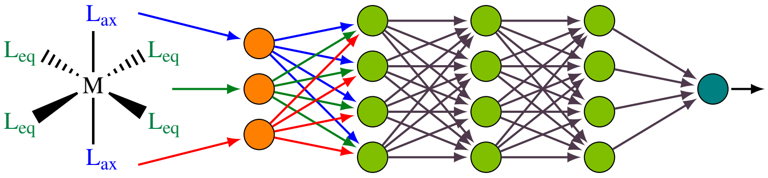

frontier orbital properties

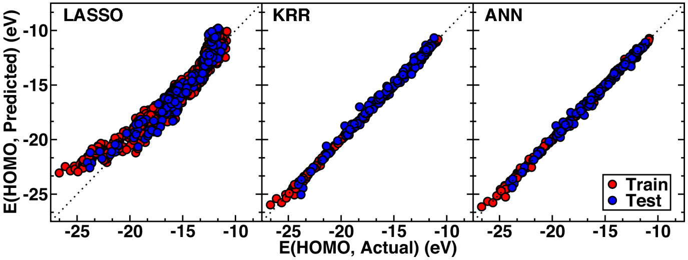

ANN: 500 × 500 ReLU nodes, fully connected

Nandy, A. *et al.*, *Ind. Eng. Chem. Res.*, 57(42):13973–13986, 2018. KRR: RFB + feature selection

Property inference with ANNs

Estimate properties using small artifical neural networks (ANNs)

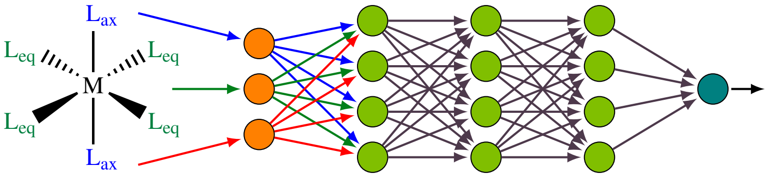

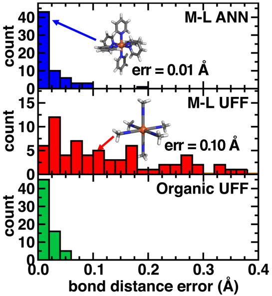

DFT equilibrium bond lengths

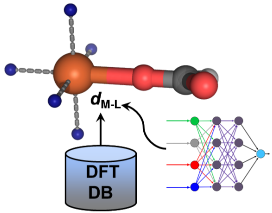

Janet, J.P. *et al.*, *Ind. Eng. Chem. Res.*, 56(17):4898–4910, 2017.

Janet, J.P. *et al.*, *Inorg. Chem.*, 58(16):10592–10606, 2019.

300 × 200 × 200 tanh nodes, fully connected

Beyond prediction: live job management

In high-throughput DFT screening, job failure is a frequent issue:

Duan, C., Janet, J.P. *et al.*, *J. Chem. Theory. Comp.*, 15(4):2331–2345, 2019.

Beyond prediction: live job management

In high-throughput DFT screening, job failure is a frequent issue:

new lead

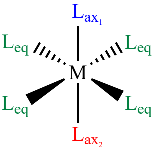

Duan, C., Janet, J.P. *et al.*, *J. Chem. Theory. Comp.*, 15(4):2331–2345, 2019.

Beyond prediction: live job management

In high-throughput DFT screening, job failure is a frequent issue:

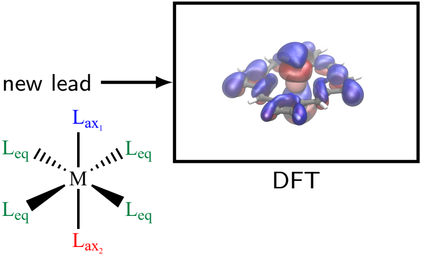

Duan, C., Janet, J.P. *et al.*, *J. Chem. Theory. Comp.*, 15(4):2331–2345, 2019.

Beyond prediction: live job management

In high-throughput DFT screening, job failure is a frequent issue:

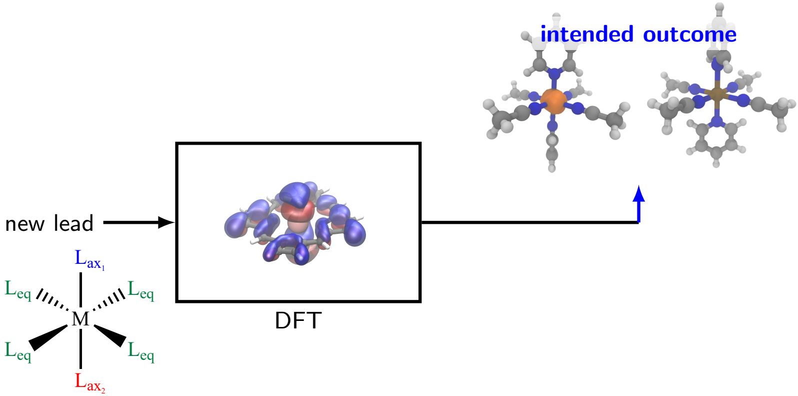

Duan, C., Janet, J.P. *et al.*, *J. Chem. Theory. Comp.*, 15(4):2331–2345, 2019.

Beyond prediction: live job management

In high-throughput DFT screening, job failure is a frequent issue:

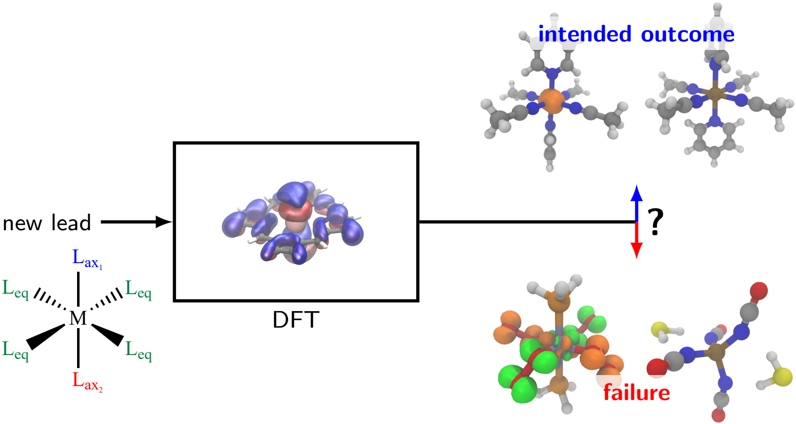

Duan, C., Janet, J.P. *et al.*, *J. Chem. Theory. Comp.*, 15(4):2331–2345, 2019.

Beyond prediction: live job management

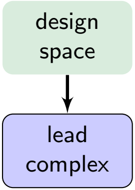

Duan, C., Janet, J.P. *et al.*, *J. Chem. Theory. Comp.*, 15(4):2331–2345, 2019.

Beyond prediction: live job management

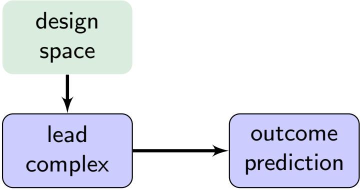

Duan, C., Janet, J.P. *et al.*, *J. Chem. Theory. Comp.*, 15(4):2331–2345, 2019.

Beyond prediction: live job management

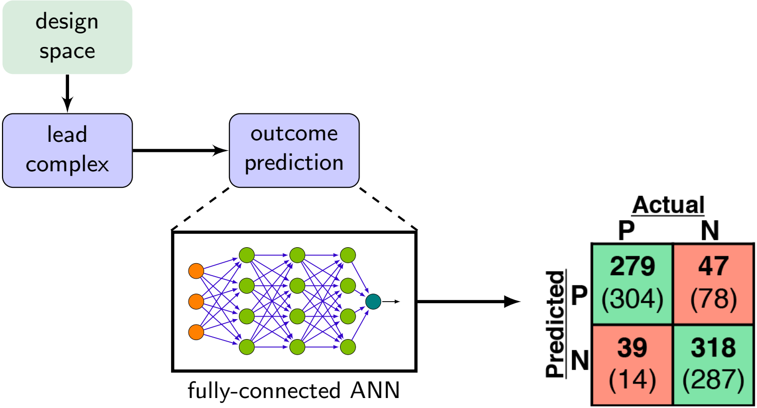

2 $\times$ 200 ReLU nodes, fully connected

Duan, C., Janet, J.P. *et al.*, *J. Chem. Theory. Comp.*, 15(4):2331–2345, 2019.

Beyond prediction: live job management

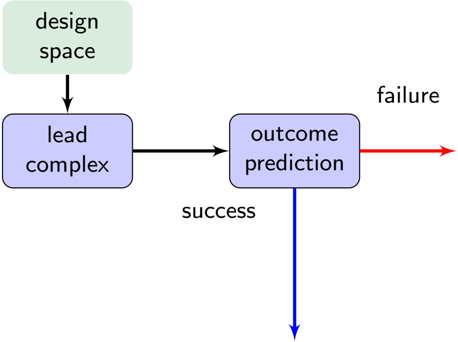

Duan, C., Janet, J.P. *et al.*, *J. Chem. Theory. Comp.*, 15(4):2331–2345, 2019.

Beyond prediction: live job management

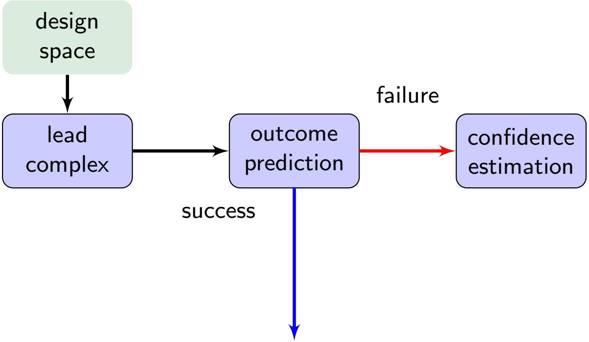

Duan, C., Janet, J.P. *et al.*, *J. Chem. Theory. Comp.*, 15(4):2331–2345, 2019.

Beyond prediction: live job management

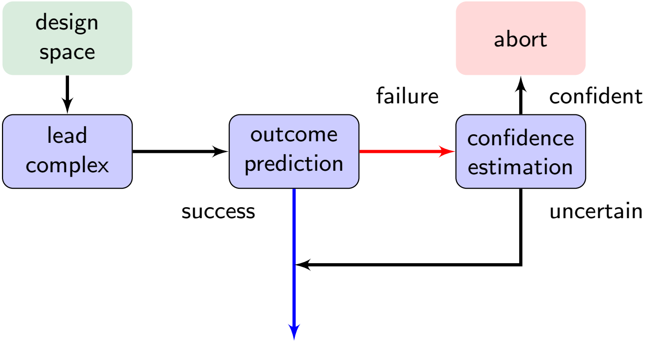

Duan, C., Janet, J.P. *et al.*, *J. Chem. Theory. Comp.*, 15(4):2331–2345, 2019.

Beyond prediction: live job management

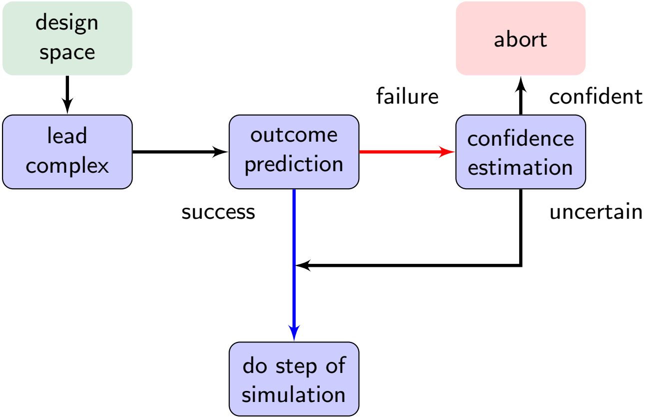

Duan, C., Janet, J.P. *et al.*, *J. Chem. Theory. Comp.*, 15(4):2331–2345, 2019.

Beyond prediction: live job management

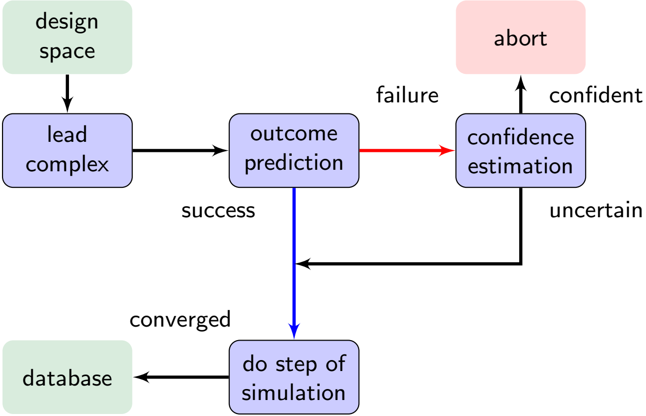

Duan, C., Janet, J.P. *et al.*, *J. Chem. Theory. Comp.*, 15(4):2331–2345, 2019.

Beyond prediction: live job management

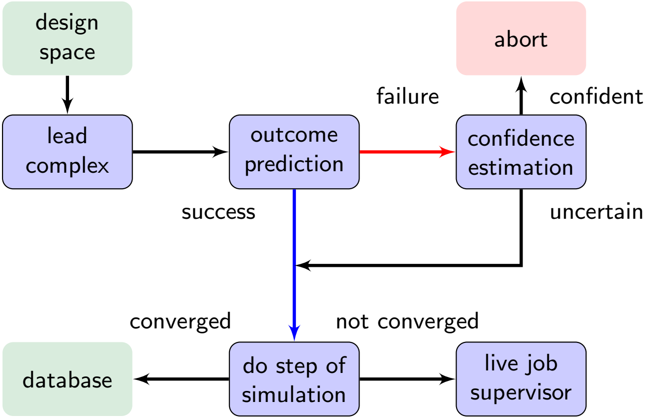

Duan, C., Janet, J.P. *et al.*, *J. Chem. Theory. Comp.*, 15(4):2331–2345, 2019.

Beyond prediction: live job management

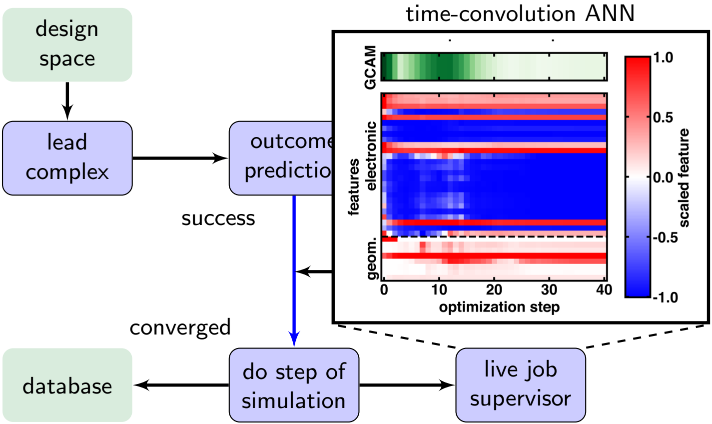

45 time convolution + 2 × 100 ReLU nodes

Duan, C., Janet, J.P. *et al.*, *J. Chem. Theory. Comp.*, 15(4):2331–2345, 2019.

Beyond prediction: live job management

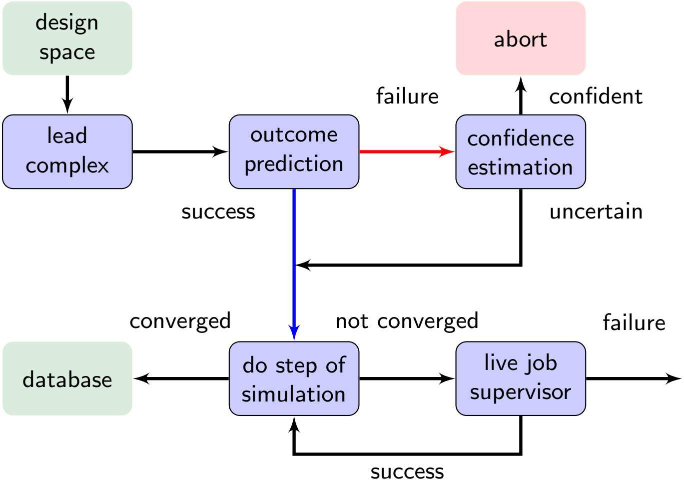

Duan, C., Janet, J.P. *et al.*, *J. Chem. Theory. Comp.*, 15(4):2331–2345, 2019.

Beyond prediction: live job management

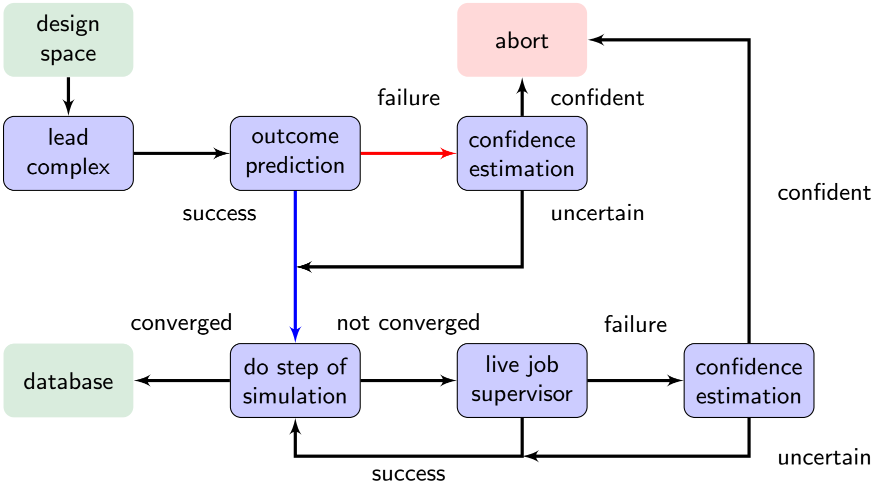

Duan, C., Janet, J.P. *et al.*, *J. Chem. Theory. Comp.*, 15(4):2331–2345, 2019.

Beyond prediction: live job management

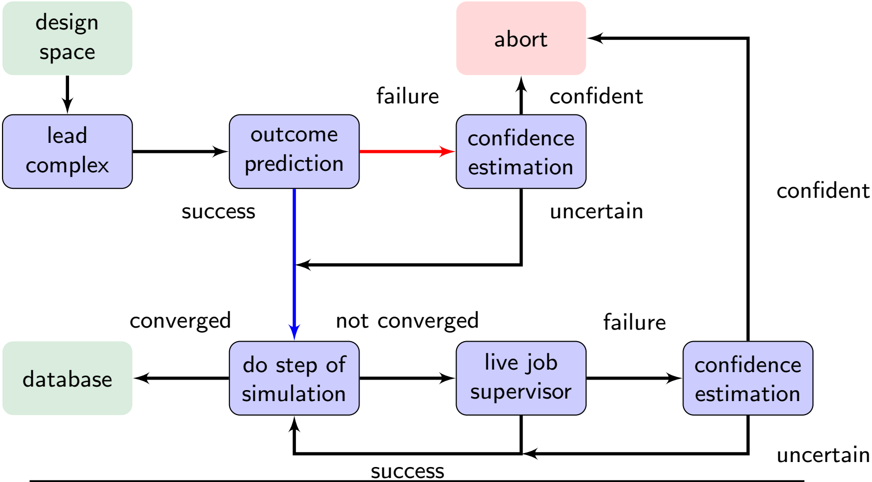

This leads to about **40% time savings** and can abort almost all failures.

Duan, C., Janet, J.P. *et al.*, *J. Chem. Theory. Comp.*, 15(4):2331–2345, 2019.

Model transferability

Test-set performance is not necessarily a good metric for general transferability:

Janet, J.P., and Kulik, H.J., *Chem. Sci.*, 8:5137–5152, 2017.

50 $\times$ 50 tanh nodes fully connected ANN

Model transferability

Test-set performance is not necessarily a good metric for general transferability:

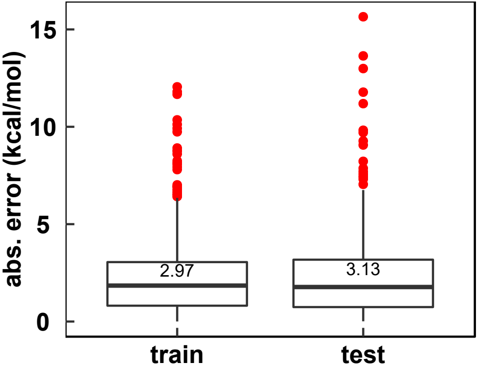

Janet, J.P., and Kulik, H.J., *Chem. Sci.*, 8:5137–5152, 2017.

50 × 50 tanh nodes fully connected ANN

Model transferability

Test-set performance is not necessarily a good metric for general transferability:

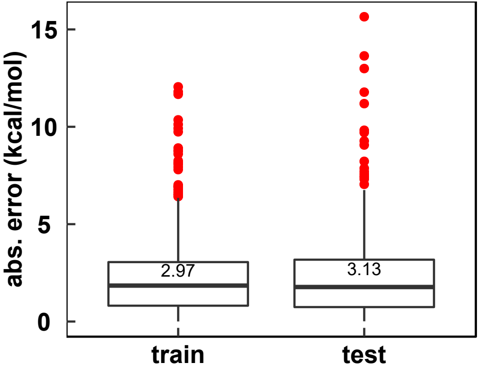

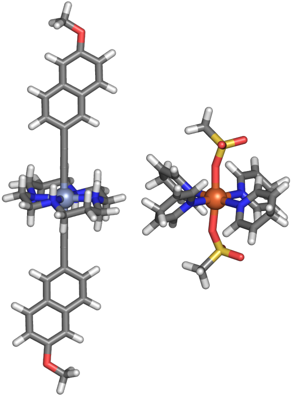

Janet, J.P., and Kulik, H.J., *Chem. Sci.*, 8:5137–5152, 2017.

50 × 50 tanh nodes fully connected ANN

Model transferability

Test-set performance is not necessarily a good metric for general transferability:

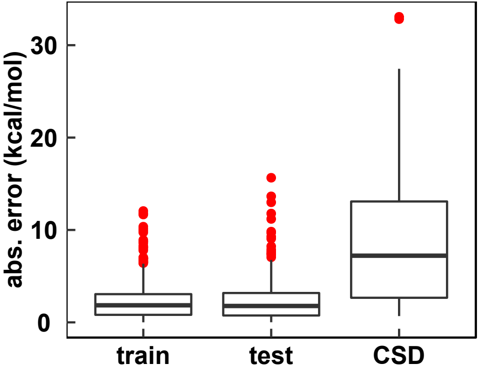

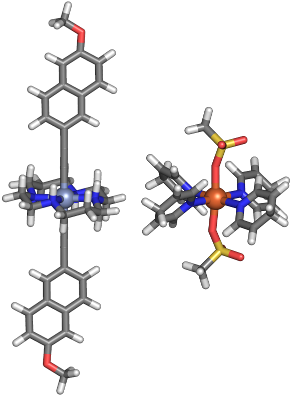

Janet, J.P., and Kulik, H.J., *Chem. Sci.*, 8:5137–5152, 2017.

50 × 50 tanh nodes fully connected ANN

Model transferability

Test-set performance is not necessarily a good metric for general transferability:

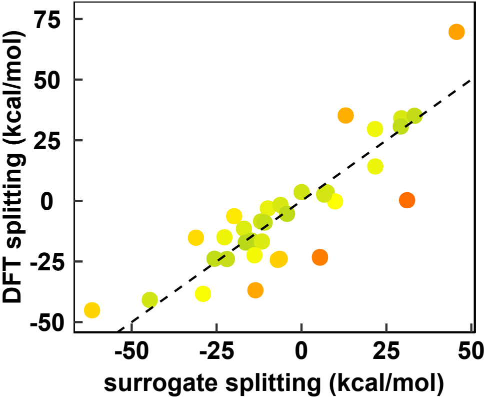

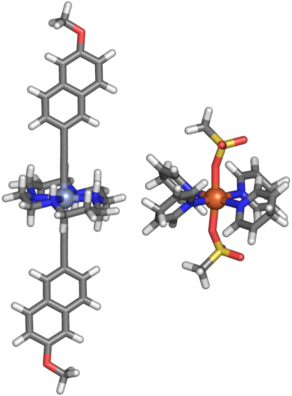

Janet, J.P., and Kulik, H.J., *Chem. Sci.*, 8:5137–5152, 2017.

50 × 50 tanh nodes fully connected ANN

How far can we extrapolate?

'Out-of-distribution' test: spin-splitting energies of 116 structures from the CSD, from training-like to very different.

How far can we extrapolate?

'Out-of-distribution' test: spin-splitting energies of 116 structures from the CSD, from training-like to very different.

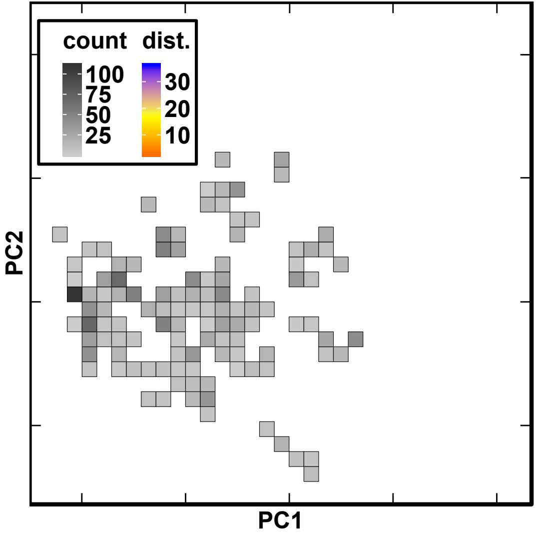

How far can we extrapolate?

'Out-of-distribution' test: spin-splitting energies of 116 structures from the CSD, from training-like to very different.

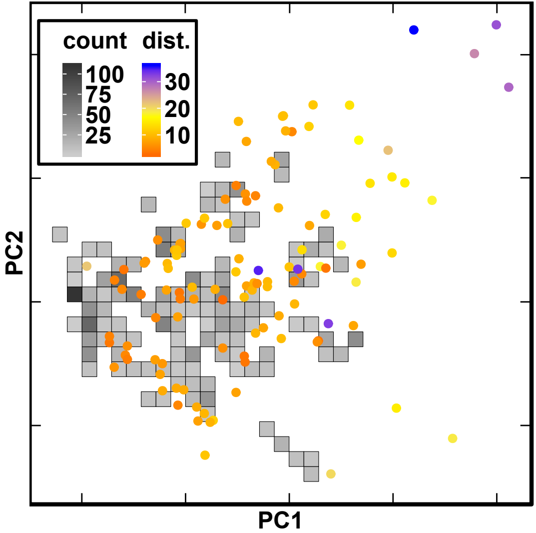

How far can we extrapolate?

'Out-of-distribution' test: spin-splitting energies of 116 structures from the CSD, from training-like to very different.

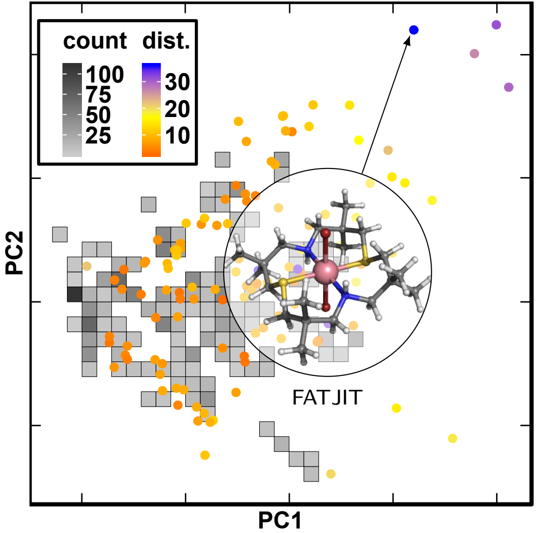

How far can we extrapolate?

'Out-of-distribution' test: spin-splitting energies of 116 structures from the CSD, from training-like to very different.

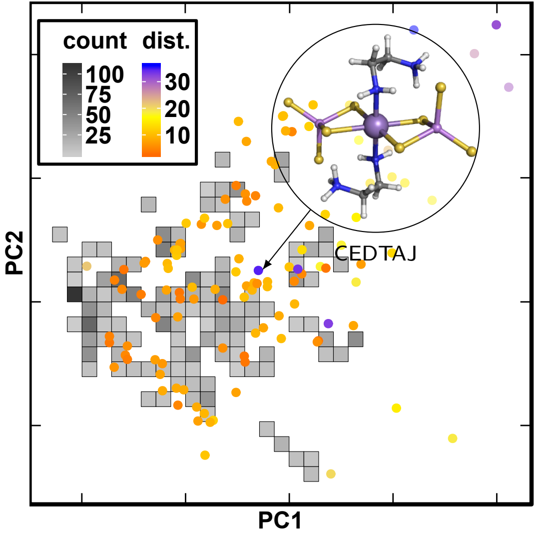

How far can we extrapolate?

'Out-of-distribution' test: spin-splitting energies of 116 structures from the CSD, from training-like to very different.

Train 3-layer fully connected ANN on 1900 DFT results on simple ligands:

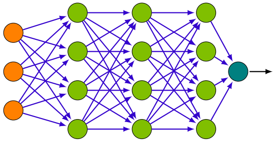

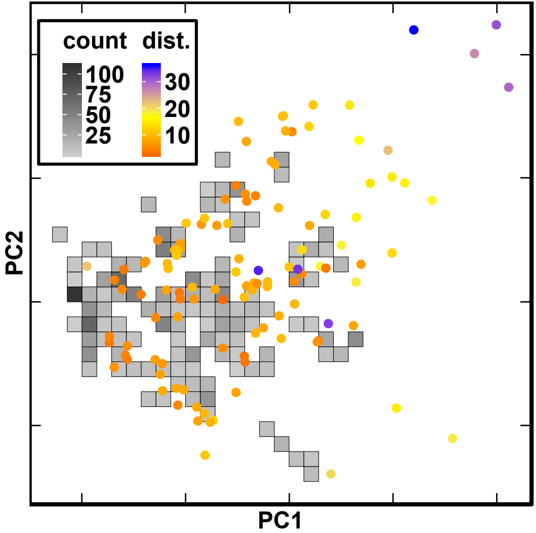

How far can we extrapolate?

'Out-of-distribution' test: spin-splitting energies of 116 structures from the CSD, from training-like to very different.

Train 3-layer fully connected ANN on 1900 DFT results on simple ligands:

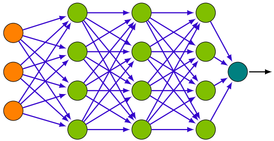

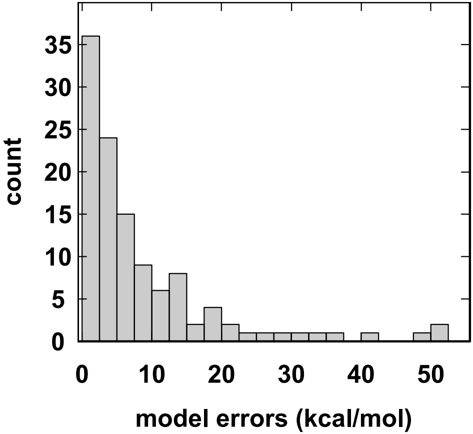

Latent distance similarity

Latent distance similarity

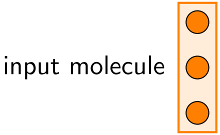

Latent distance similarity

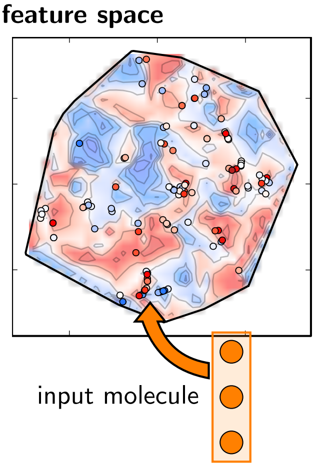

Latent distance similarity

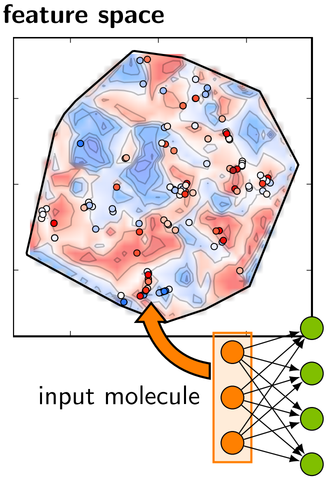

Latent distance similarity

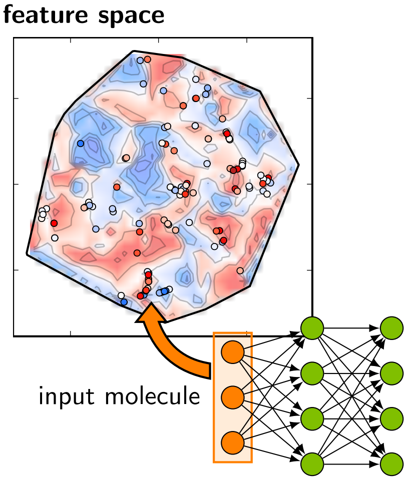

Latent distance similarity

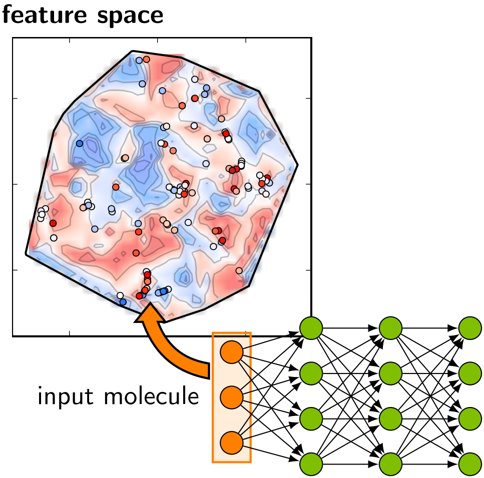

Latent distance similarity

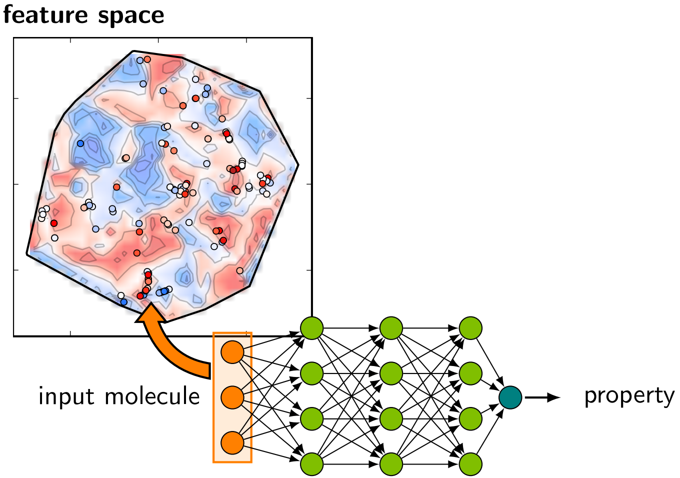

Latent distance similarity

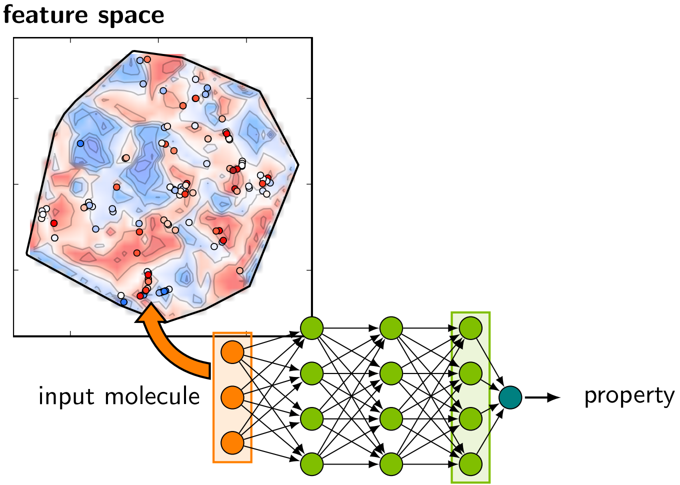

Latent distance similarity

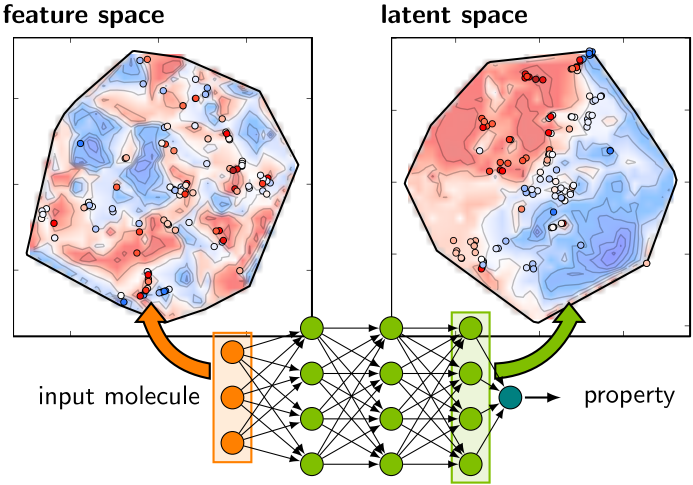

Latent distance similarity

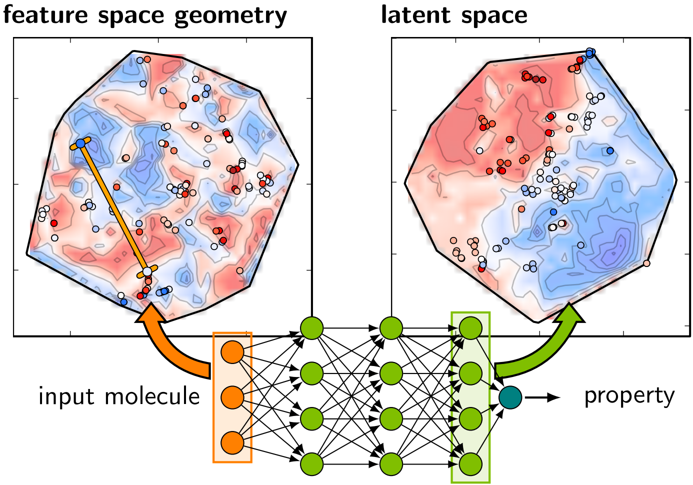

Latent distance similarity

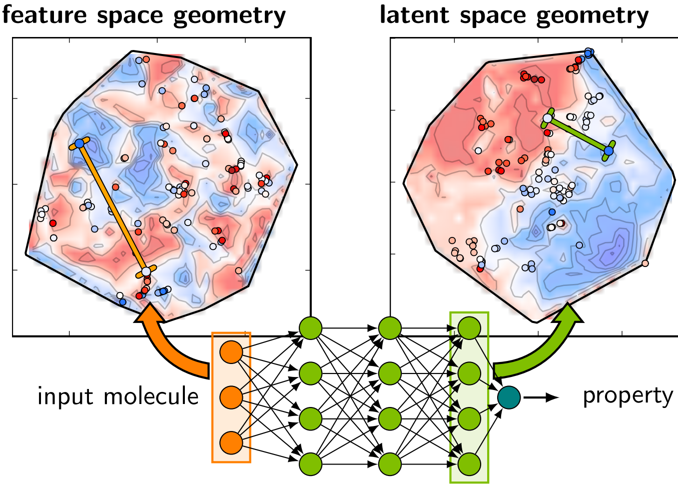

From distance to energy

Propose a simple conditionally-Gaussian model for predicting error distribution with latent distance, d:

$$\varepsilon(d) \sim \mathcal{N}\left(0, \sigma_1^2 + d\sigma_2^2\right)$$

From distance to energy

Propose a simple conditionally-Gaussian model for predicting error distribution with latent distance, d:

$$\varepsilon(d) \sim \mathcal{N}\left(0, \sigma_1^2 + d\sigma_2^2\right)$$

Estimate σ_1, σ_2 by max log likelihood, stably estimated even using few out-of-sample points

From distance to energy

Propose a simple conditionally-Gaussian model for predicting error distribution with latent distance, d:

$$\varepsilon(d) \sim \mathcal{N}\left(0, \sigma_1^2 + d\sigma_2^2\right)$$

Estimate σ_1, σ_2 by max log likelihood, stably estimated even using few out-of-sample points

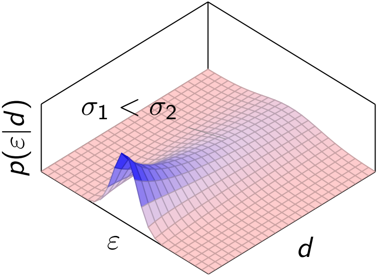

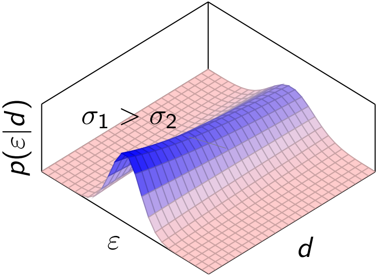

Other UQ metrics

1) Data-sampling ensembles:

Other UQ metrics

1) Data-sampling ensembles:

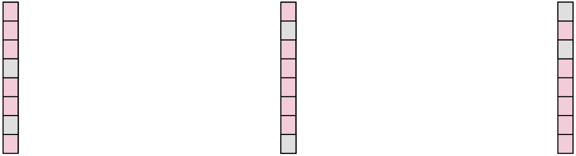

Other UQ metrics

1) Data-sampling ensembles:

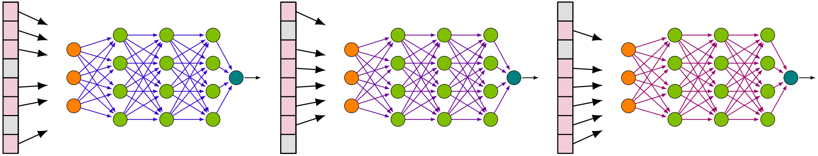

Other UQ metrics

1) Data-sampling ensembles:

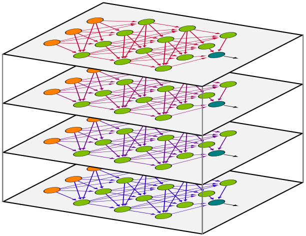

Other UQ metrics

1) Data-sampling ensembles:

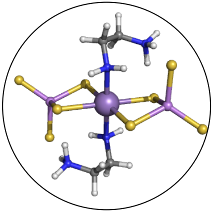

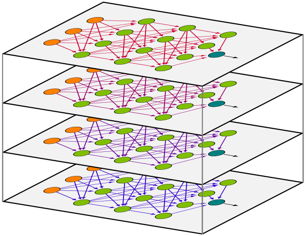

Other UQ metrics

1) Data-sampling ensembles:

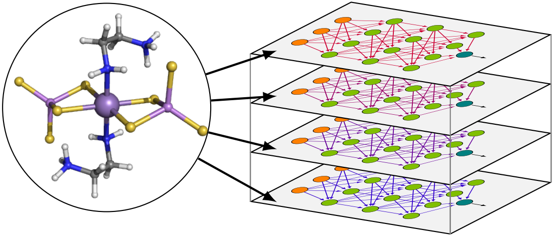

Other UQ metrics

1) Data-sampling ensembles:

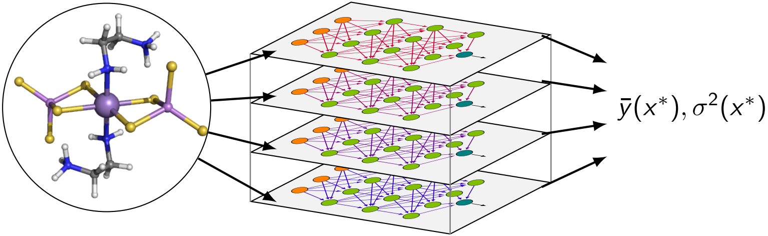

Other UQ metrics

1) Data-sampling ensembles:

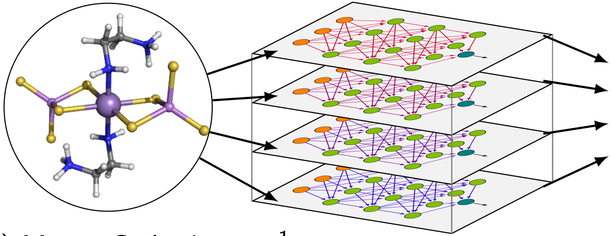

$\bar{y}(x^*), \sigma^2(x^*)$

2) Monte Carlo dropout[1]:

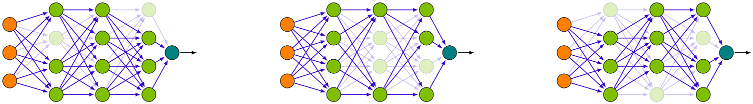

[1]:Gal, Y. and Ghahramani, Z., *ICMLR*, 1050–1059, 2016.

Other UQ metrics

1) Data-sampling ensembles:

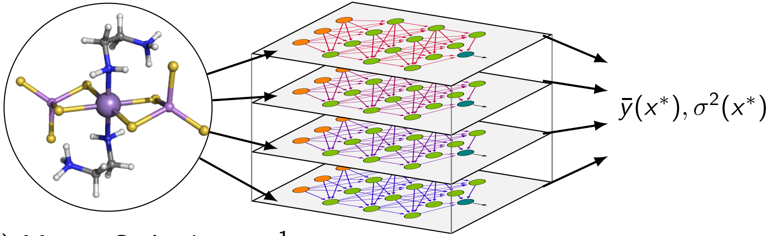

2) Monte Carlo dropout[1]:

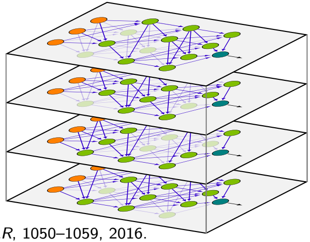

[1]:Gal, Y. and Ghahramani, Z., *ICMLR*, 1050–1059, 2016.

Other UQ metrics

1) Data-sampling ensembles:

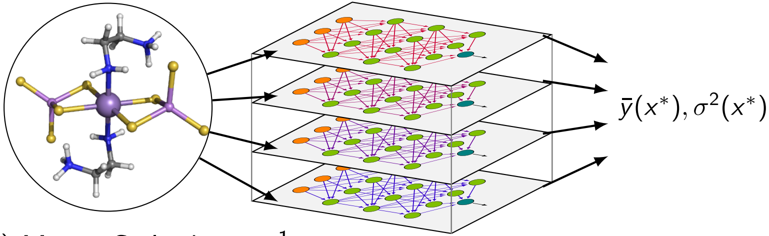

2) Monte Carlo dropout[1]:

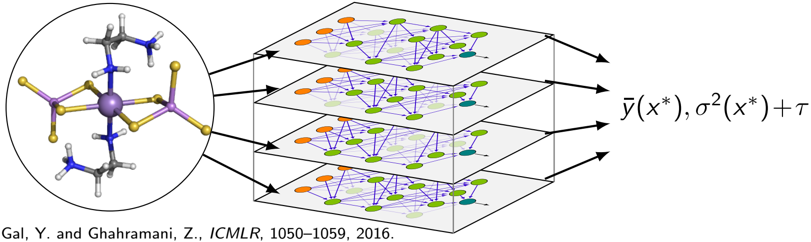

[1]:Gal, Y. and Ghahramani, Z., *ICMLR*, 1050–1059, 2016.

How do these distributions compare?

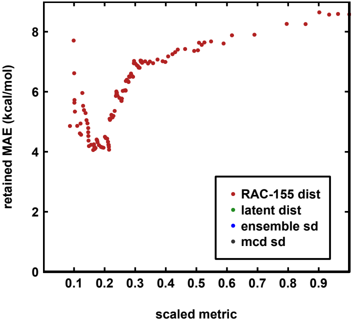

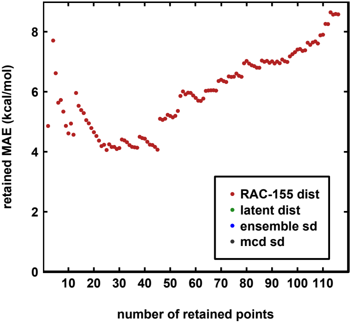

Janet, J.P., *et al.*, *Chem. Sci.*, 10:7913–7922 , 2019.

3×200 ReLU nodes, fully connected

How do these distributions compare?

latent distances are superior to feature space distances

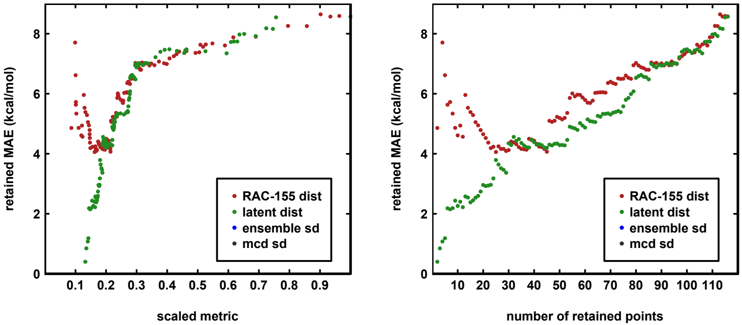

Janet, J.P., *et al.*, *Chem. Sci.*, 10:7913–7922 , 2019.

3×200 ReLU nodes, fully connected

How do these distributions compare?

latent distances are superior to feature space distances

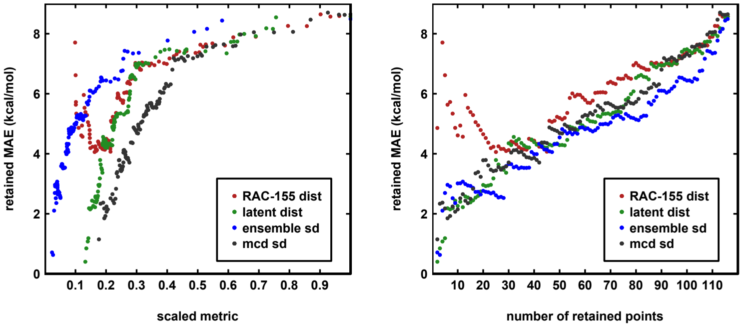

comparable with ensembles and mc dropout

Janet, J.P., *et al.*, *Chem. Sci.*, 10:7913–7922 , 2019.

3 × 200 ReLU nodes, fully connected

How do these distributions compare?

Comparison in energy units: $\varepsilon(d) \sim \mathcal{N}\left(0, \sigma_1^2 + d\sigma_2^2\right)$

latent distances are superior to feature space distances

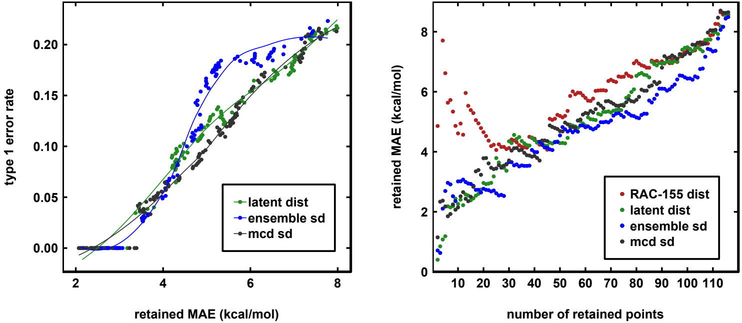

comparable with ensembles and mc dropout

Janet, J.P., *et al.*, *Chem. Sci.*, 10:7913–7922 , 2019. 3 × 200 ReLU nodes, fully connected

How do these distributions compare?

Comparison in energy units: $\varepsilon(d) \sim \mathcal{N}\left(0, \sigma_1^2 + d\sigma_2^2\right)$

latent distances are superior to feature space distances

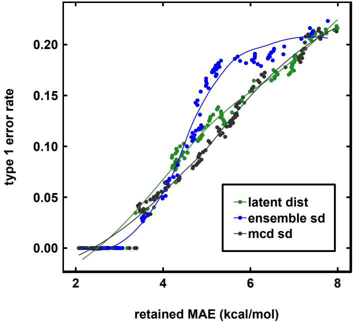

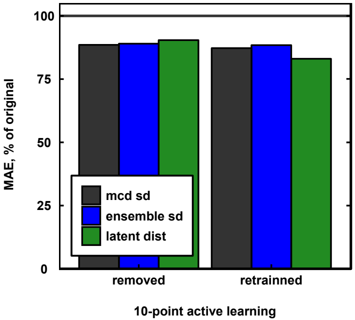

comparable with ensembles and mc dropout

Janet, J.P., *et al.*, *Chem. Sci.*, 10:7913–7922 , 2019.

3×200 ReLU nodes, fully connected

How do these distributions compare?

Comparison in energy units: $\varepsilon(d) \sim \mathcal{N}\left(0, \sigma_1^2 + d\sigma_2^2\right)$

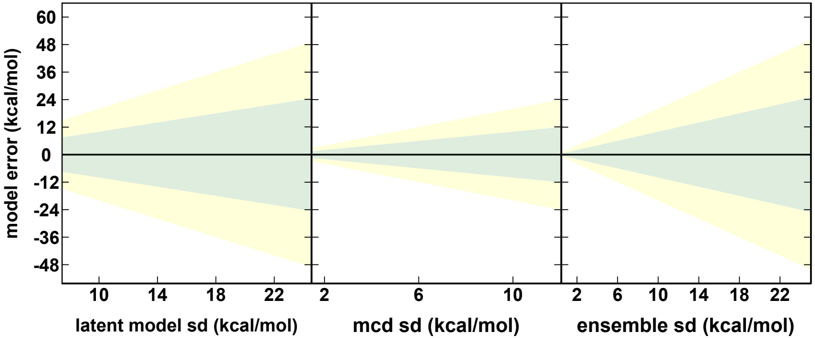

Janet, J.P., *et al.*, *Chem. Sci.*, 10:7913–7922 , 2019. 3×200 ReLU nodes, fully connected

How do these distributions compare?

Comparison in energy units: $\varepsilon(d) \sim \mathcal{N}\left(0, \sigma_1^2 + d\sigma_2^2\right)$

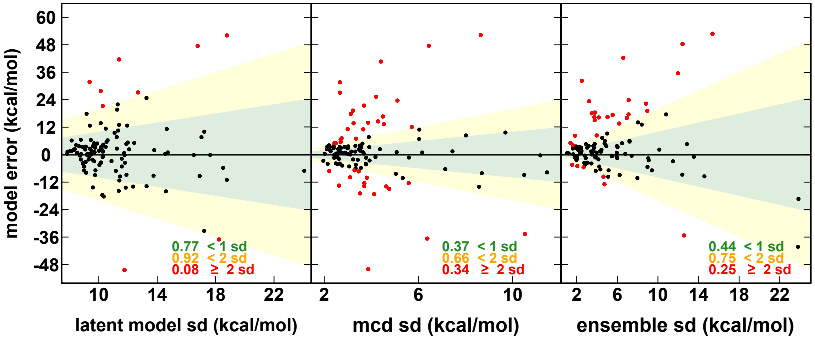

Janet, J.P., *et al.*, *Chem. Sci.*, 10:7913–7922 , 2019. 3×200 ReLU nodes, fully connected

How do these distributions compare?

Comparison in energy units: QM9 atomization energy data

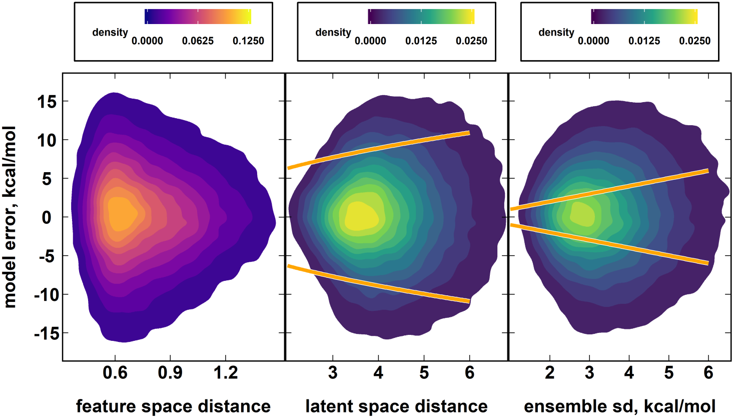

Janet, J.P., *et al.*, *Chem. Sci.*, 10:7913–7922 , 2019. 2 × 100 ReLU nodes, skip connections

Targeted data acquisition

Lack of data is a persistent issue. We can exploit knowledge of feature importance to generate data:

Gugler, S., Janet, J.P., and Kulik, H.J., *Mol. Sys. Des. Eng.*, Advance Article, 2019.

Targeted data acquisition

Lack of data is a persistent issue. We can exploit knowledge of feature importance to generate data:

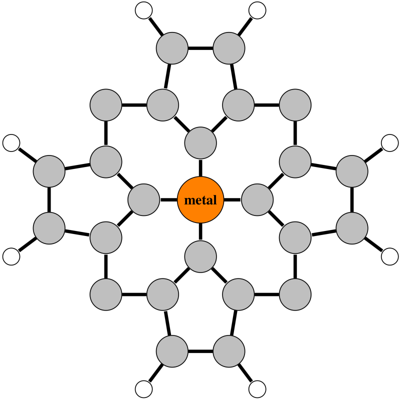

Gugler, S., Janet, J.P., and Kulik, H.J., *Mol. Sys. Des. Eng.*, Advance Article, 2019.

Targeted data acquisition

Lack of data is a persistent issue. We can exploit knowledge of feature importance to generate data:

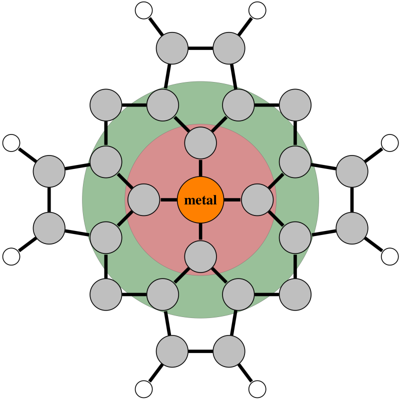

Gugler, S., Janet, J.P., and Kulik, H.J., *Mol. Sys. Des. Eng.*, Advance Article, 2019.

Targeted data acquisition

Lack of data is a persistent issue. We can exploit knowledge of feature importance to generate data:

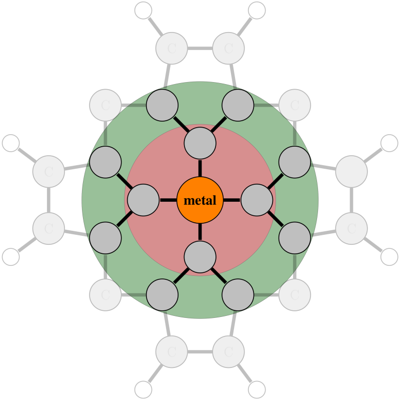

Gugler, S., Janet, J.P., and Kulik, H.J., *Mol. Sys. Des. Eng.*, Advance Article, 2019.

Targeted data acquisition

Lack of data is a persistent issue. We can exploit knowledge of feature importance to generate data:

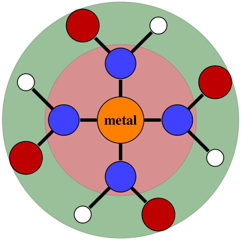

Gugler, S., Janet, J.P., and Kulik, H.J., *Mol. Sys. Des. Eng.*, Advance Article, 2019.

Targeted data acquisition

Lack of data is a persistent issue. We can exploit knowledge of feature importance to generate data:

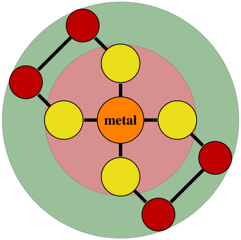

Gugler, S., Janet, J.P., and Kulik, H.J., *Mol. Sys. Des. Eng.*, Advance Article, 2019.

Targeted data acquisition

Lack of data is a persistent issue. We can exploit knowledge of feature importance to generate data:

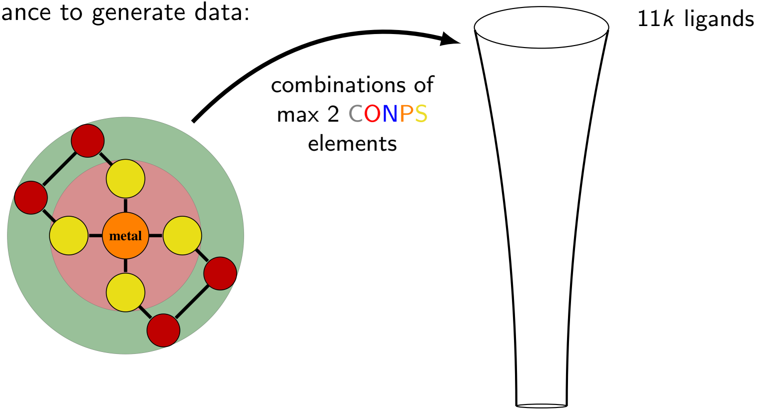

Gugler, S., Janet, J.P., and Kulik, H.J., *Mol. Sys. Des. Eng.*, Advance Article, 2019.

Targeted data acquisition

Lack of data is a persistent issue. We can exploit knowledge of feature importance to generate data:

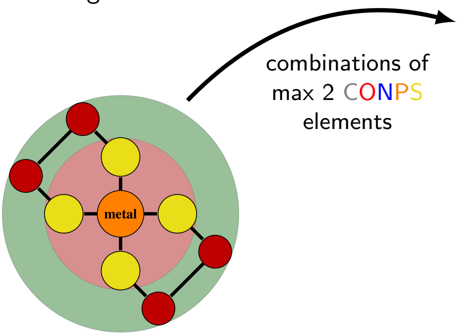

combinations of
max 2 CONPS
elements

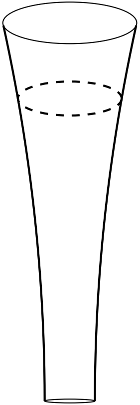

$11k$ ligands
filter
$2.6k$ ligands

Gugler, S., Janet, J.P., and Kulik, H.J., *Mol. Sys. Des. Eng.*, Advance Article, 2019.

Targeted data acquisition

Lack of data is a persistent issue. We can exploit knowledge of feature importance to generate data:

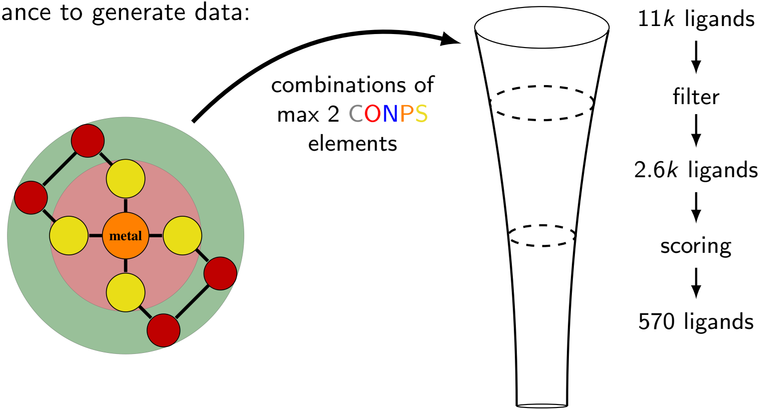

Gugler, S., Janet, J.P., and Kulik, H.J., *Mol. Sys. Des. Eng.*, Advance Article, 2019.

Targeted data acquisition

Lack of data is a persistent issue. We can exploit knowledge of feature importance to generate data:

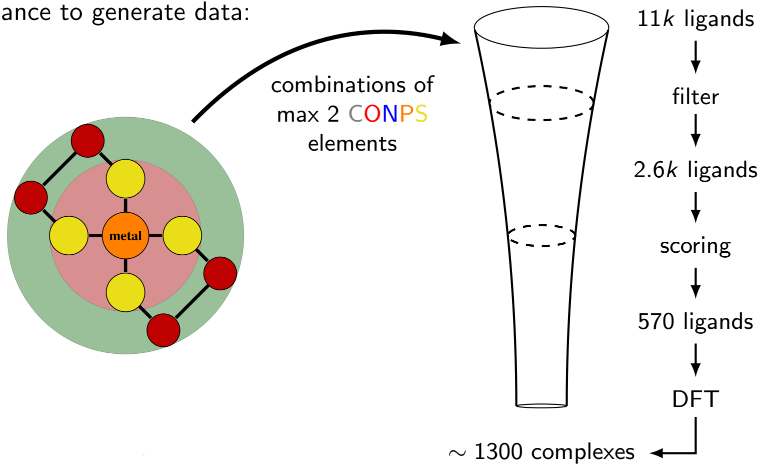

Gugler, S., Janet, J.P., and Kulik, H.J., *Mol. Sys. Des. Eng.*, Advance Article, 2019.

Targeted data acquisition

Lack of data is a persistent issue. We can exploit knowledge of feature importance to generate data:

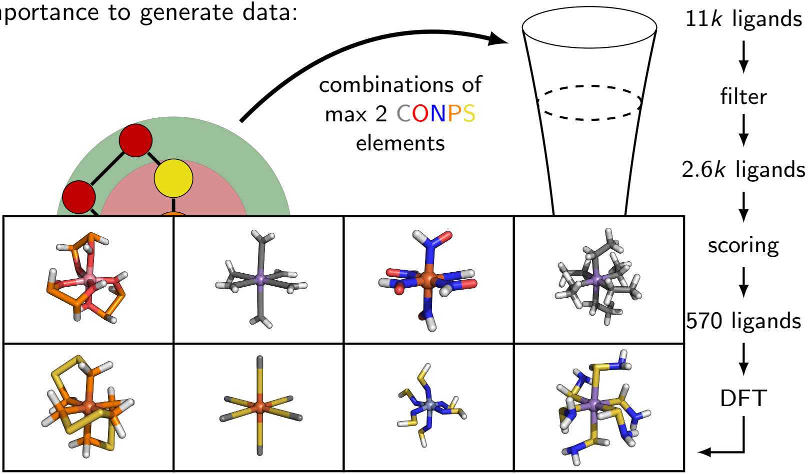

Gugler, S., Janet, J.P., and Kulik, H.J., *Mol. Sys. Des. Eng.*, Advance Article, 2019.

Targeted data acquisition

Lack of data is a persistent issue. We can exploit knowledge of feature importance to generate data:

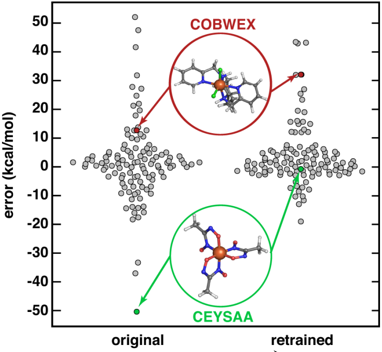

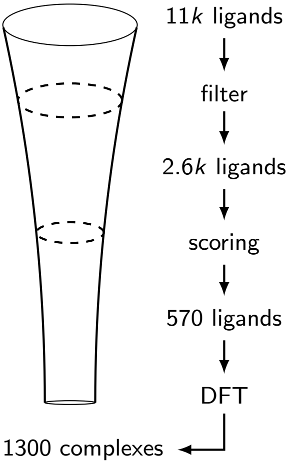

add to surrogate model

3×100 tanh nodes, fully connected ANN

Gugler, S., Janet, J.P., and Kulik, H.J., *Mol. Sys. Des. Eng.*, Advance Article, 2019.

Targeted data acquisition

Lack of data is a persistent issue. We can exploit knowledge of feature importance to generate data:

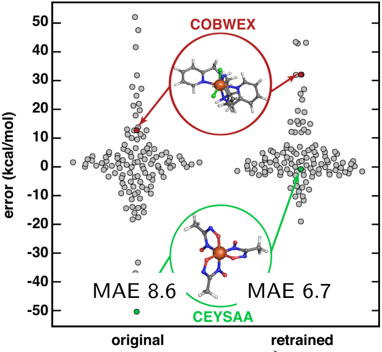

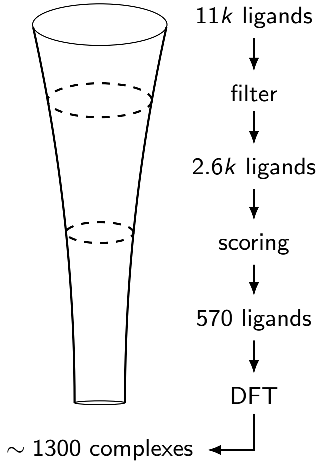

add to surrogate model

3 $\times$ 100 tanh nodes, fully connected ANN

Gugler, S., Janet, J.P., and Kulik, H.J., *Mol. Sys. Des. Eng.*, Advance Article, 2019.

Hedging against DFT uncertainty

Because we have trained our models with varying exact exchange, we can tune functionals for design:

Hedging against DFT uncertainty

Because we have trained our models with varying exact exchange, we can tune functionals for design:

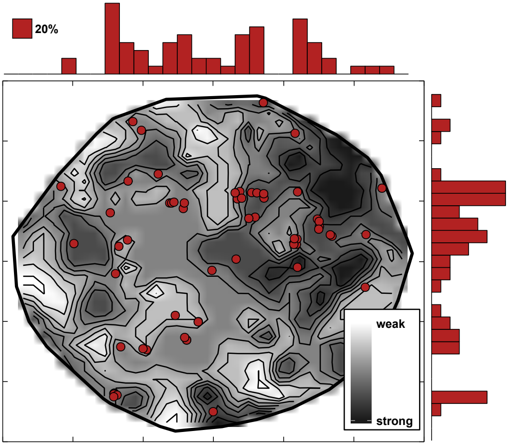

Janet, J.P. *et al.*, *Inorg. Chem.*, 58(16):10592–10606, 2019.

50 × 50 tanh nodes fully connected ANN

Hedging against DFT uncertainty

Because we have trained our models with varying exact exchange, we can tune functionals for design:

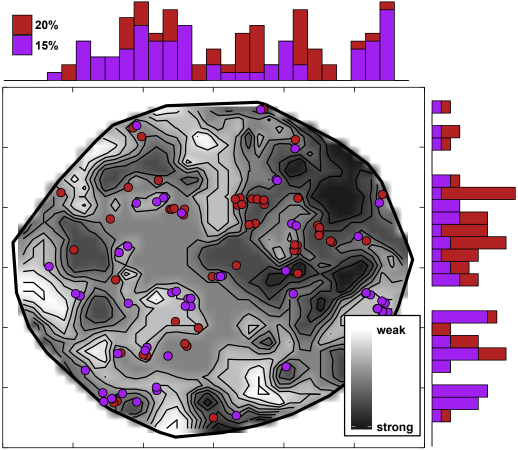

Janet, J.P. *et al.*, *Inorg. Chem.*, 58(16):10592–10606, 2019.

50 × 50 tanh nodes fully connected ANN

Hedging against DFT uncertainty

Because we have trained our models with varying exact exchange, we can tune functionals for design:

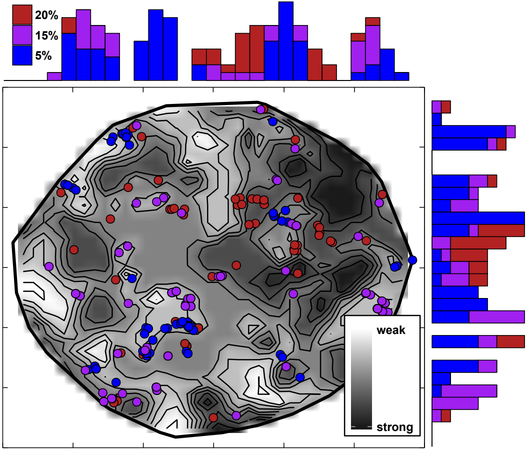

Janet, J.P. *et al.*, *Inorg. Chem.*, 58(16):10592–10606, 2019.

50 × 50 tanh nodes fully connected ANN

Using models for discovery

We utilize evolutionary algorithms to conduct design, guided by uncertainty metrics

Using models for discovery

We utilize evolutionary algorithms to conduct design, guided by uncertainty metrics

$$F_{s+d}(x) := \exp\left[-\left(\frac{\Delta E_{\text{H-L}}(x)}{p_{\Delta E_{\text{H-L}}}}\right)^2\right]$$

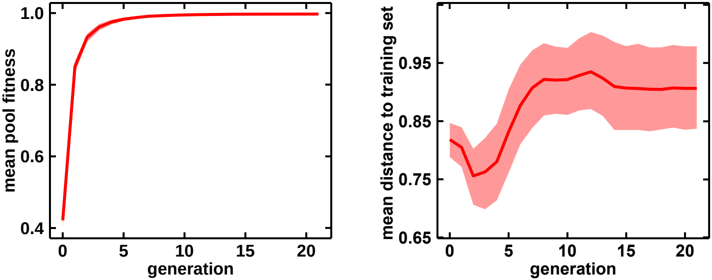

Using models for discovery

We utilize evolutionary algorithms to conduct design, guided by uncertainty metrics

$$F_{s+d}(x) := \exp\left[-\left(\frac{\Delta E_{\text{H-L}}(x)}{p_{\Delta E_{\text{H-L}}}}\right)^2\right] \exp\left[-\left(\frac{d(x)}{p_d}\right)^2\right]$$

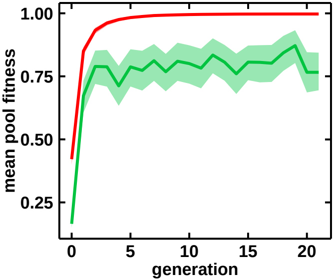

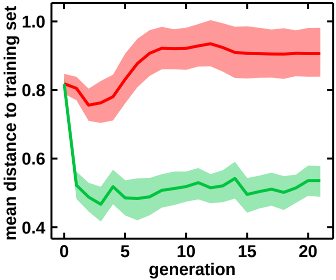

Using models for discovery

We utilize evolutionary algorithms to conduct design, guided by uncertainty metrics

$$F_{s+d}(x) := \exp\left[-\left(\frac{\Delta E_{\text{H-L}}(x)}{p_{\Delta E_{\text{H-L}}}}\right)^2\right] \exp\left[-\left(\frac{d(x)}{p_d}\right)^2\right]$$

Using models for discovery

We utilize evolutionary algorithms to conduct design, guided by uncertainty metrics

$$F_{s+d}(x) := \exp\left[-\left(\frac{\Delta E_{\text{H-L}}(x)}{p_{\Delta E_{\text{H-L}}}}\right)^2\right] \exp\left[-\left(\frac{d(x)}{p_d}\right)^2\right]$$

spin crossover complexes

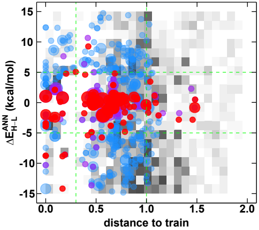

Janet, J.P., Chan, L. and Kulik, H.J., *J. Phys. Chem. Lett.*, 9(5):1064–1071, 2018.

Using models for discovery

We utilize evolutionary algorithms to conduct design, guided by uncertainty metrics

$$F_{s+d}(x) := \exp\left[-\left(\frac{\Delta E_{\text{H-L}}(x)}{p_{\Delta E_{\text{H-L}}}}\right)^2\right] \exp\left[-\left(\frac{d(x)}{p_d}\right)^2\right]$$

spin crossover complexes

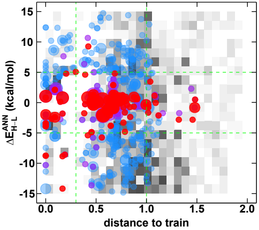

frontier orbital properties

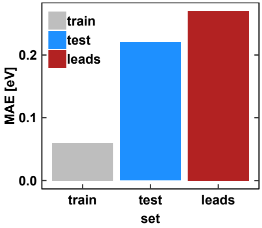

Janet, J.P., Chan, L. and Kulik, H.J., *J. Phys. Chem. Lett.*, 9(5):1064–1071, 2018.
Nandy, A. *et al.*, *Ind. Eng. Chem. Res.*, 57(42):13973–13986, 2018.

Using models for discovery

We utilize evolutionary algorithms to conduct design, guided by uncertainty metrics

$$F_{s+d}(x) := \exp\left[-\left(\frac{\Delta E_{\text{H-L}}(x)}{p_{\Delta E_{\text{H-L}}}}\right)^2\right] \exp\left[-\left(\frac{d(x)}{p_d}\right)^2\right]$$

spin crossover complexes

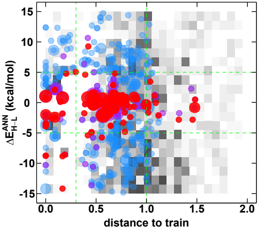

frontier orbital properties

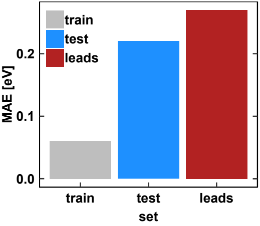

unusual catalytic reaction energies

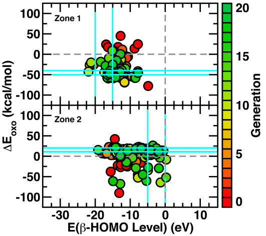

Janet, J.P., Chan, L. and Kulik, H.J., *J. Phys. Chem. Lett.*, 9(5):1064–1071, 2018.
Nandy, A. *et al.*, *Ind. Eng. Chem. Res.*, 57(42):13973–13986, 2018.
Nandy, A. *et al.*, *ACS Catal.*, 9(9):8243–8255, 2019.

More than just ML

Janet, J.P. *et al.*, *Inorg. Chem.*, 58(16):10592–10606, 2019.

More than just ML

target
properties

Janet, J.P. *et al.*, *Inorg. Chem.*, 58(16):10592–10606, 2019.

More than just ML

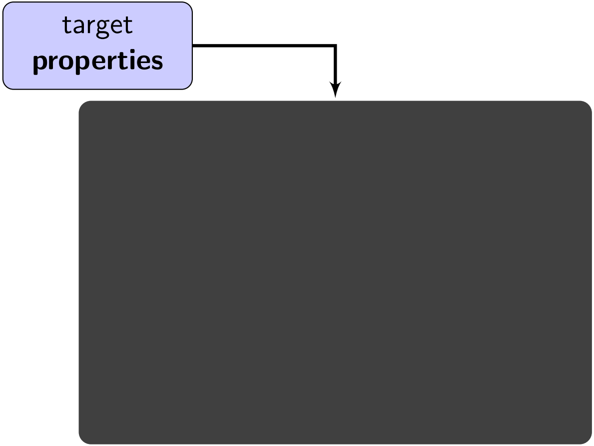

Janet, J.P. *et al.*, *Inorg. Chem.*, 58(16):10592–10606, 2019.

More than just ML

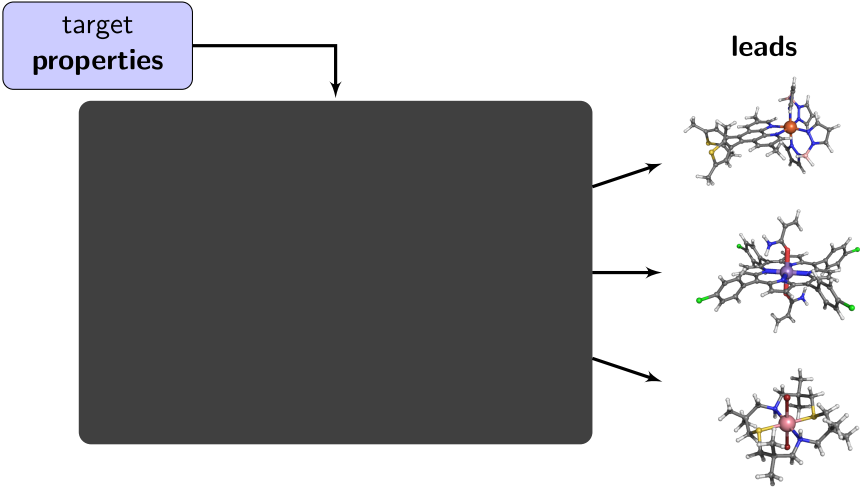

Janet, J.P. *et al.*, *Inorg. Chem.*, 58(16):10592–10606, 2019.

More than just ML

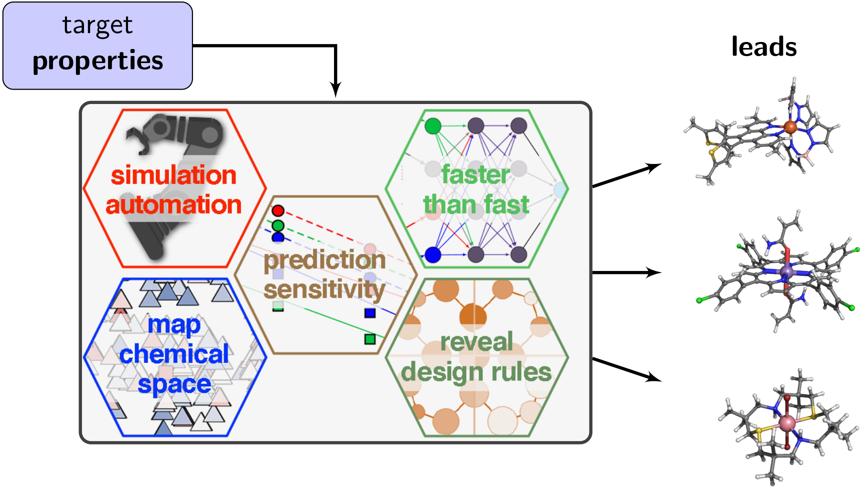

Janet, J.P. *et al.*, *Inorg. Chem.*, 58(16):10592–10606, 2019.

More than just ML

target **properties**

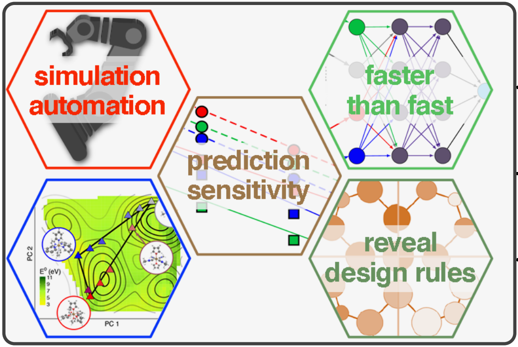

leads

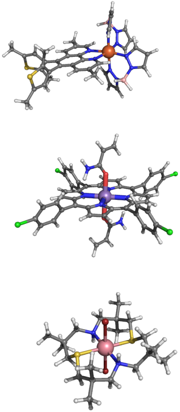

RAC features

Janet, J.P. *et al.*, *Inorg. Chem.*, 58(16):10592–10606, 2019.

More than just ML

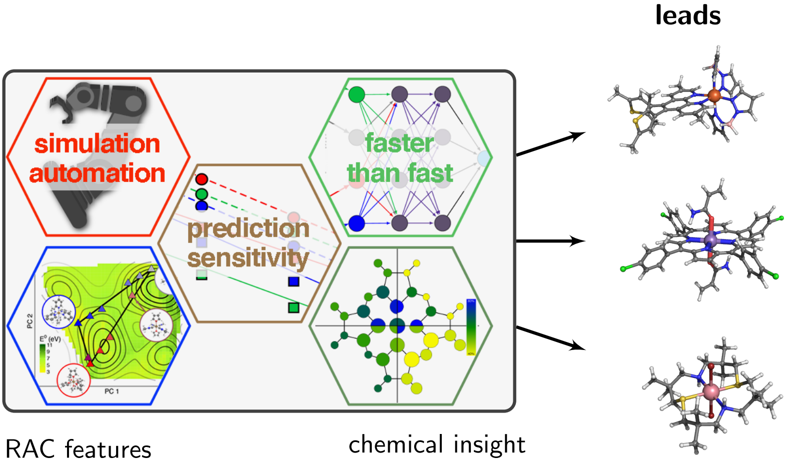

Janet, J.P. *et al.*, *Inorg. Chem.*, 58(16):10592–10606, 2019.

More than just ML

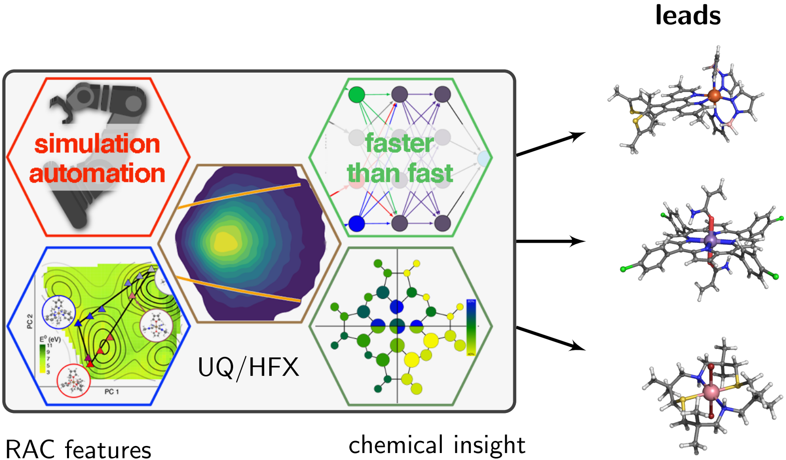

RAC features

chemical insight

Janet, J.P. *et al.*, *Inorg. Chem.*, 58(16):10592–10606, 2019.

More than just ML

design algorithms

leads

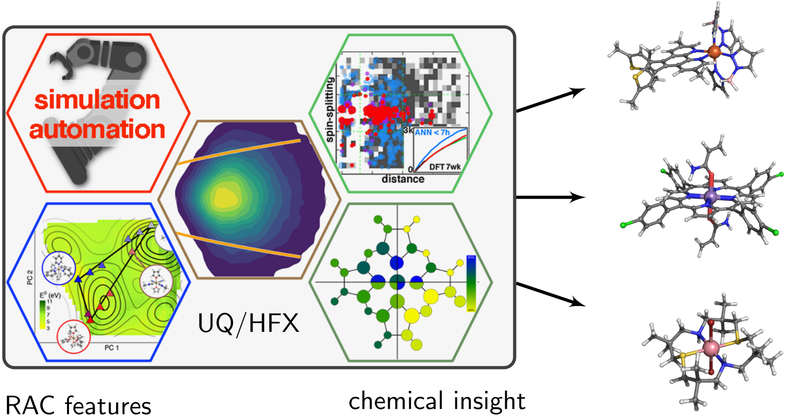

RAC features

chemical insight

Janet, J.P. *et al.*, *Inorg. Chem.*, 58(16):10592–10606, 2019.

More than just ML

github.com/hjkgrp

mAD/molSimplify

design algorithms

leads

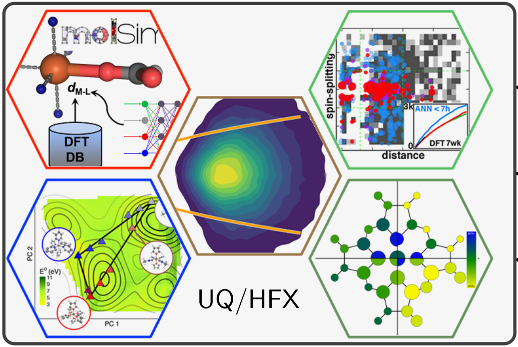

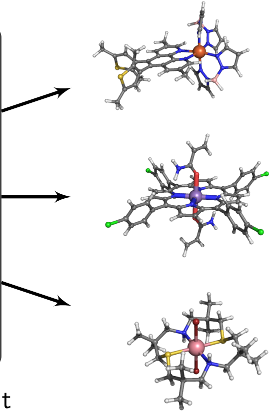

RAC features

chemical insight

Janet, J.P. *et al.*, *Inorg. Chem.*, 58(16):10592–10606, 2019.

More than just ML

github.com/hjkgrp

mAD/molSimplify

design algorithms

leads

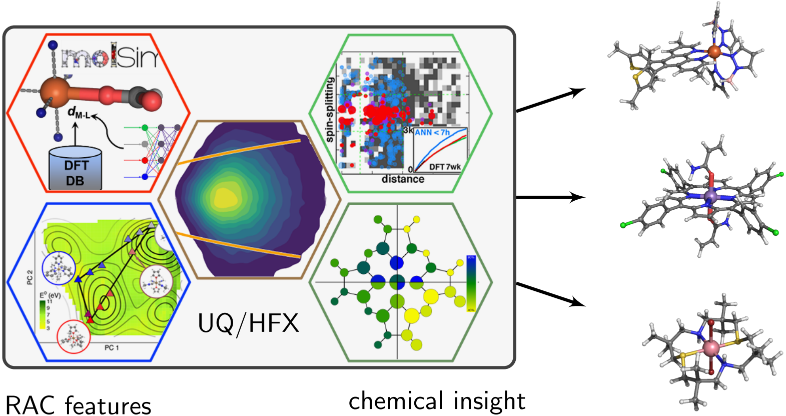

RAC features

chemical insight

An end-to-end approach for rational TM complex design

Case study: redox couples

Consider a multiobjective optimization problem:

Redox flow batteries (RFBs)
are a promising option for
scalable energy storage:

Case study: redox couples

Consider a multiobjective optimization problem:

Redox flow batteries (RFBs) are a promising option for scalable energy storage:

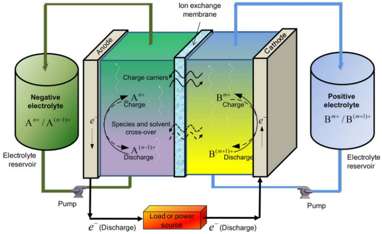

Perry, M.L. and Adam, Z., *J. Electrochem. Soc.*, 163(1):A5064–A5067, 2018.

Case study: redox couples

Consider a multiobjective optimization problem:

Redox flow batteries (RFBs) are a promising option for scalable energy storage:

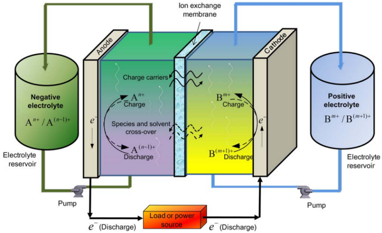

Perry, M.L. and Adam, Z., *J. Electrochem. Soc.*, 163(1):A5064–A5067, 2018.

Transition metal complexes make attractive redox couples for RFBs

Case study: redox couples

Consider a multiobjective optimization problem:

Redox flow batteries (RFBs) are a promising option for scalable energy storage:

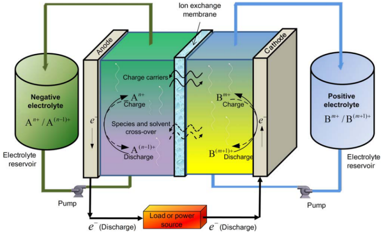

Perry, M.L. and Adam, Z., *J. Electrochem. Soc.*, 163(1):A5064–A5067, 2018.

Transition metal complexes make attractive redox couples for RFBs

- good ion stability (compared to organics)

Case study: redox couples

Consider a multiobjective optimization problem:

Redox flow batteries (RFBs) are a promising option for scalable energy storage:

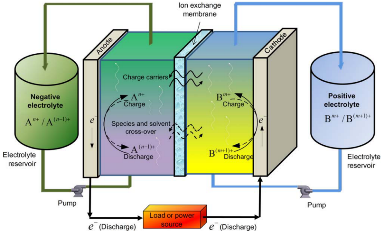

Perry, M.L. and Adam, Z., *J. Electrochem. Soc.*, 163(1):A5064–A5067, 2018.

Transition metal complexes make attractive redox couples for RFBs

- good ion stability (compared to organics)
- good range of redox potentials available

Case study: redox couples

Consider a multiobjective optimization problem:

Redox flow batteries (RFBs) are a promising option for scalable energy storage:

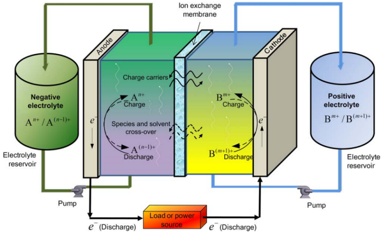

Perry, M.L. and Adam, Z., *J. Electrochem. Soc.*, 163(1):A5064–A5067, 2018.

Transition metal complexes make attractive redox couples for RFBs

- good ion stability (compared to organics)
- good range of redox potentials available
- solubility is an issue!

Case study: redox couples

Consider a multiobjective optimization problem:

Redox flow batteries (RFBs) are a promising option for scalable energy storage:

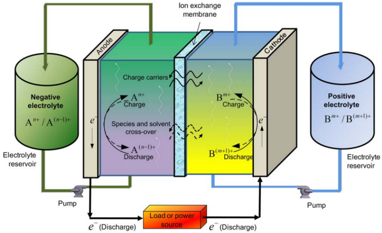

Perry, M.L. and Adam, Z., *J. Electrochem. Soc.*, 163(1):A5064–A5067, 2018.

Transition metal complexes make attractive redox couples for RFBs

- good ion stability (compared to organics)
- good range of redox potentials available
- solubility is an issue!

$$E_{\text{cell}} = 0.5 \times V_{\text{cell}} \times C \times n \times F$$

Case study: redox couples

Consider a multiobjective optimization problem:

Redox flow batteries (RFBs) are a promising option for scalable energy storage:

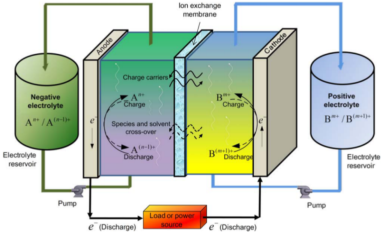

Perry, M.L. and Adam, Z., *J. Electrochem. Soc.*, 163(1):A5064–A5067, 2018.

Transition metal complexes make attractive redox couples for RFBs

- good ion stability (compared to organics)
- good range of redox potentials available
- solubility is an issue!

$$E_{\text{cell}} = 0.5 \times V_{\text{cell}} \times C \times n \times F$$

We need complexes that have high redox potential **and** good solubility

Design space construction

Design space construction

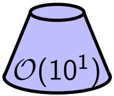

Design space construction

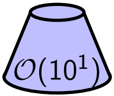

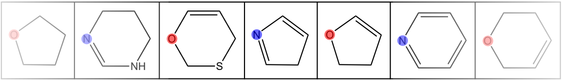

40 heterocycles

Design space construction

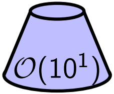

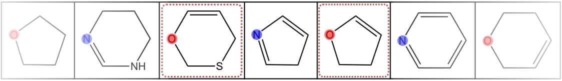

40 heterocycles

Design space construction

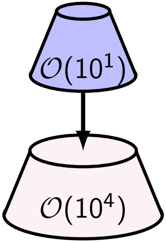

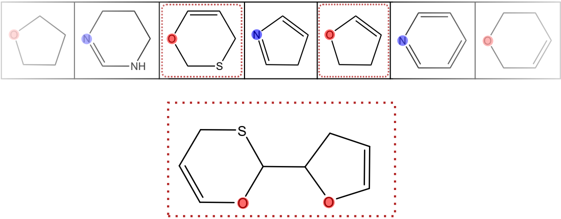

800 base ligands

Design space construction

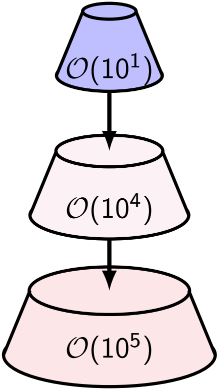

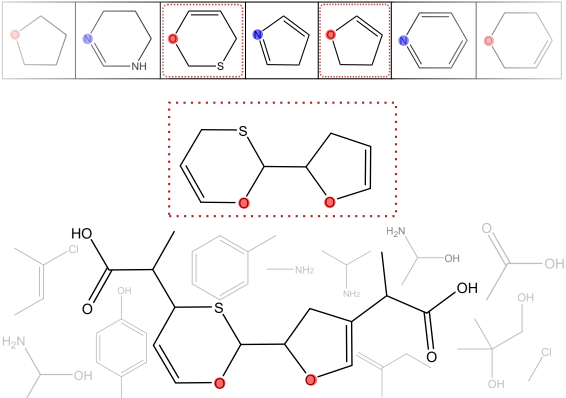

700k unique ligands

Design space construction

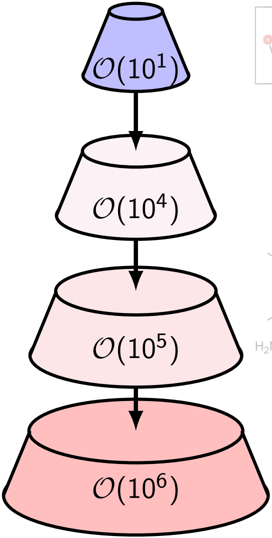

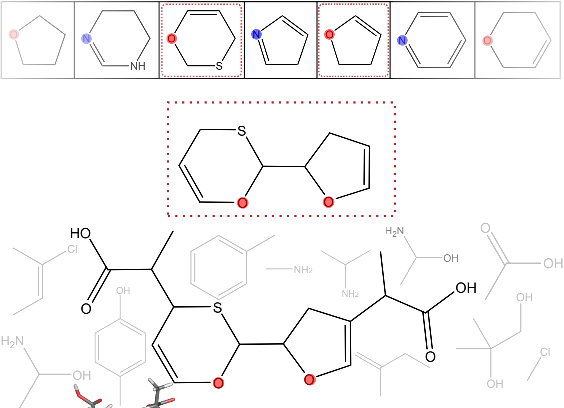

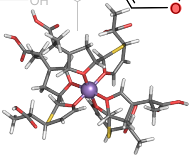

$\sim$ 3M complexes
with 4 metals

Multiobjective framework

We can predict quantites of interest for our RFBs:

Janet, J.P., *et al.*, *in preparation*.

3×100 tanh nodes, multitask, fully connected

Multiobjective framework

We can predict quantites of interest for our RFBs:

$$\Delta G_{\text{solv}} \approx \Delta E_{\text{III}-\text{II}} + \Delta\Delta G_s$$

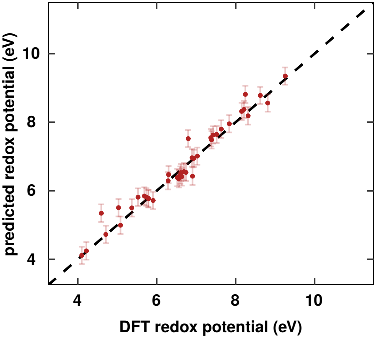

Janet, J.P., *et al.*, *in preparation*.

3 × 100 tanh nodes, multitask, fully connected

Multiobjective framework

We can predict quantites of interest for our RFBs:

$\Delta G_{\mathrm{solv}} \approx \Delta E_{\mathrm{III-II}} + \Delta\Delta G_s$

$\log P \approx \log \frac{\Delta G_{\mathrm{s,II,octanol}}}{\Delta G_{\mathrm{s,II,water}}}$

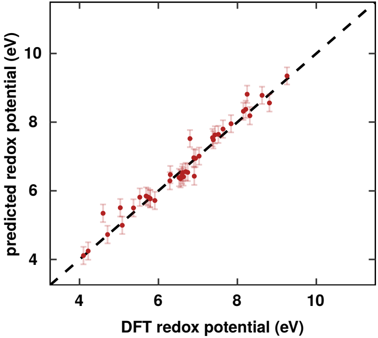

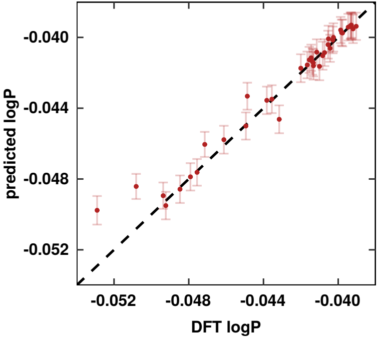

Janet, J.P., *et al.*, *in preparation*.

3 × 100 tanh nodes, multitask, fully connected

Multiobjective framework

We can predict quantites of interest for our RFBs:

$\Delta G_{\text{solv}} \approx \Delta E_{\text{III}-\text{II}} + \Delta\Delta G_s$

$\log \text{P} \approx \log \frac{\Delta G_{\text{s,II,octanol}}}{\Delta G_{\text{s,II,water}}}$

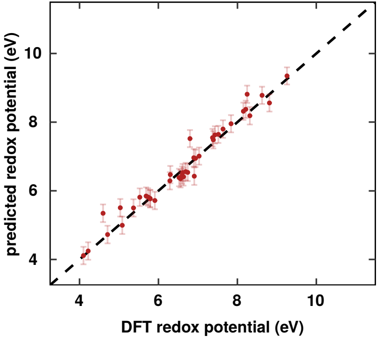

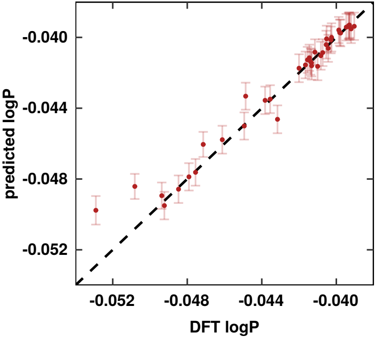

$$\begin{matrix}\Delta G_{\text{solv}} \\ \log \text{P}\end{matrix} = \begin{bmatrix}\hat{y}_1 \\ \hat{y}_2\end{bmatrix} \sim \mathcal{N}\left(\begin{bmatrix}\hat{\mu}_1 \\ \hat{\mu}_2\end{bmatrix}, \begin{bmatrix}\hat{\sigma}_1^2 & 0 \\ 0 & \hat{\sigma}_2^2\end{bmatrix}\right)$$

Janet, J.P., *et al.*, *in preparation*.

3 × 100 tanh nodes, multitask, fully connected

Multiobjective framework

We can predict quantites of interest for our RFBs:

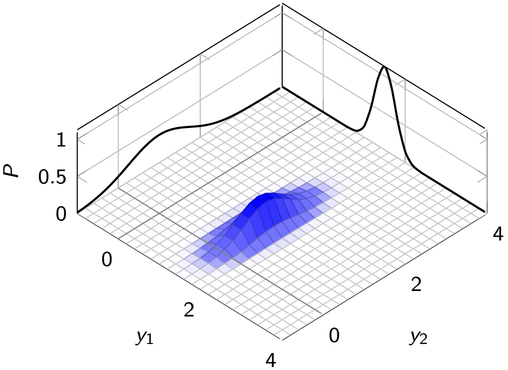

$$\begin{matrix}\Delta G_{\mathrm{solv}} \\ \log \mathrm{P}\end{matrix} = \begin{bmatrix}\hat{y}_1 \\ \hat{y}_2\end{bmatrix} \sim \mathcal{N}\left(\begin{bmatrix}\hat{\mu}_1 \\ \hat{\mu}_2\end{bmatrix}, \begin{bmatrix}\hat{\sigma}_1^2 & 0 \\ 0 & \hat{\sigma}_2^2\end{bmatrix}\right)$$

Janet, J.P., *et al.*, *in preparation*.

Multiobjective framework

We can predict quantites of interest for our RFBs:

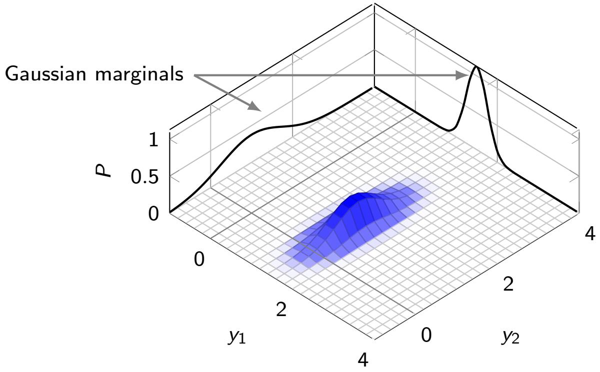

$$\begin{matrix}\Delta G_{\text{solv}} \\ \log \text{P}\end{matrix} = \begin{bmatrix}\hat{y}_1 \\ \hat{y}_2\end{bmatrix} \sim \mathcal{N}\left(\begin{bmatrix}\hat{\mu}_1 \\ \hat{\mu}_2\end{bmatrix}, \begin{bmatrix}\hat{\sigma}_1^2 & 0 \\ 0 & \hat{\sigma}_2^2\end{bmatrix}\right)$$

Janet, J.P., *et al.*, *in preparation*.

2D EGO Illustration

We will use a multiobjective expected improvement framework:

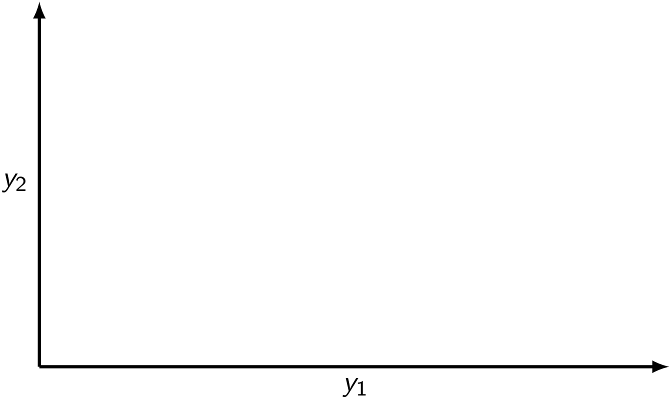

Keane, A. J., AIAA Journal, 44(4):879–891, 2006.

2D EGO Illustration

We will use a multiobjective expected improvement framework:

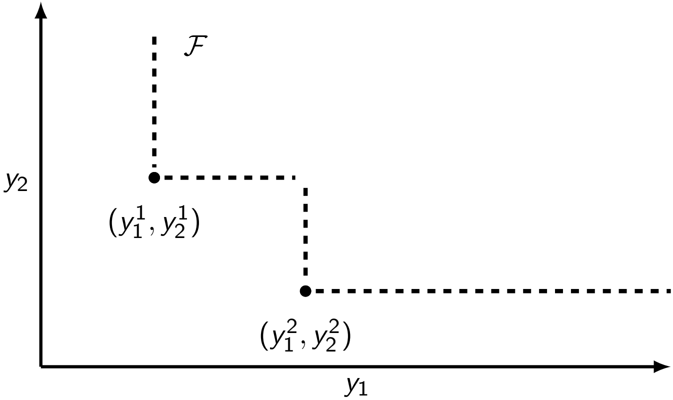

Keane, A. J., AIAA Journal, 44(4):879–891, 2006.

2D EGO Illustration

We will use a multiobjective expected improvement framework:

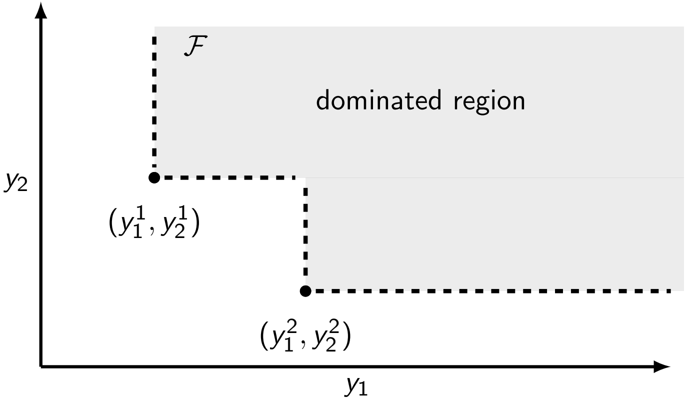

Keane, A. J., AIAA Journal, 44(4):879–891, 2006.

2D EGO Illustration

We will use a multiobjective expected improvement framework:

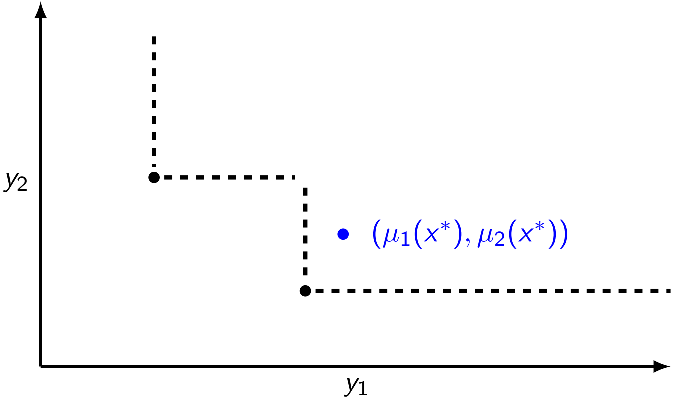

Keane, A. J., AIAA Journal, 44(4):879–891, 2006.

2D EGO Illustration

We will use a multiobjective expected improvement framework:

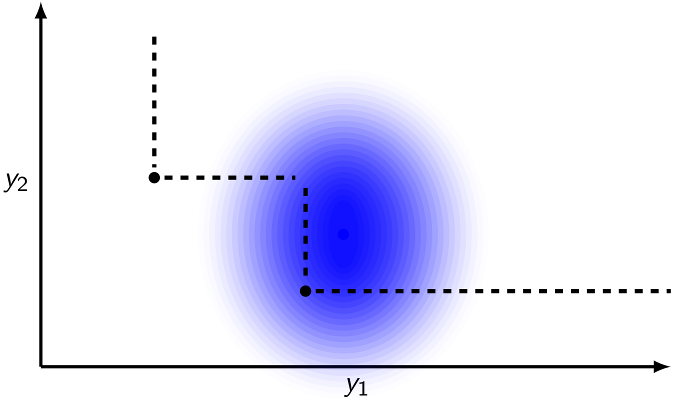

Keane, A. J., AIAA Journal, 44(4):879–891, 2006.

2D EGO Illustration

We will use a multiobjective expected improvement framework:

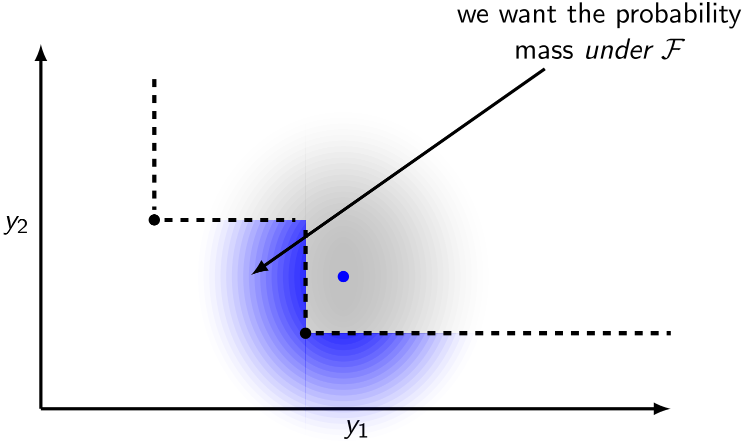

Keane, A. J., AIAA Journal, 44(4):879–891, 2006.

2D EGO Illustration

We will use a multiobjective expected improvement framework:

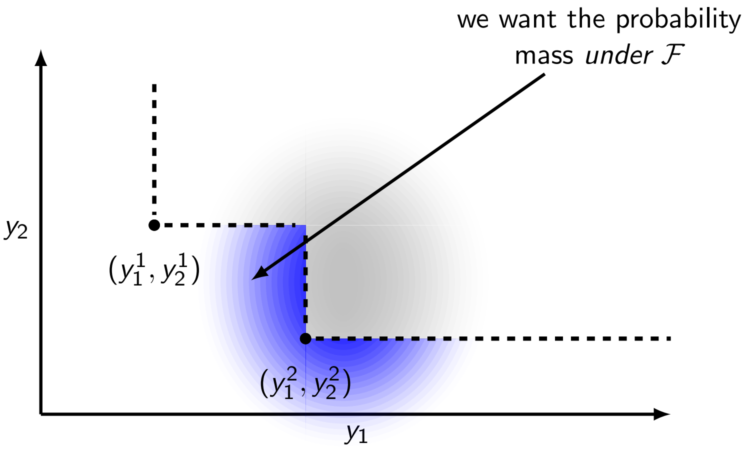

Keane, A. J., AIAA Journal, 44(4):879–891, 2006.

2D EGO Illustration

We will use a multiobjective expected improvement framework:

$$P(I) =$$

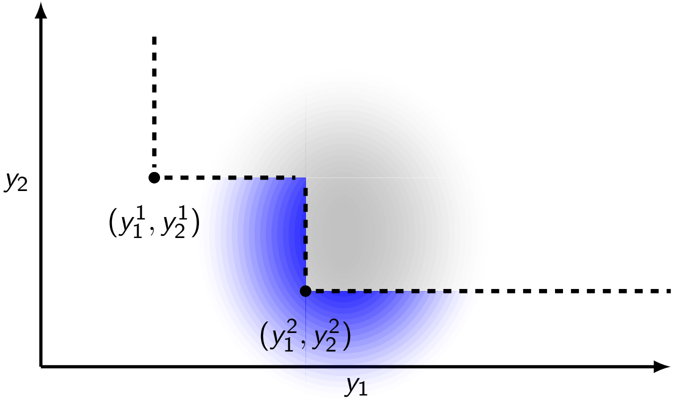

Keane, A. J., AIAA Journal, 44(4):879–891, 2006.

2D EGO Illustration

We will use a multiobjective expected improvement framework:

$$P(I) = \boxed{\int_{-\infty}^{y_1^1} \int_{-\infty}^{\infty} p(\hat{y}_1(x^*), \hat{y}_2(x^*)) dy_1 dy_2}$$

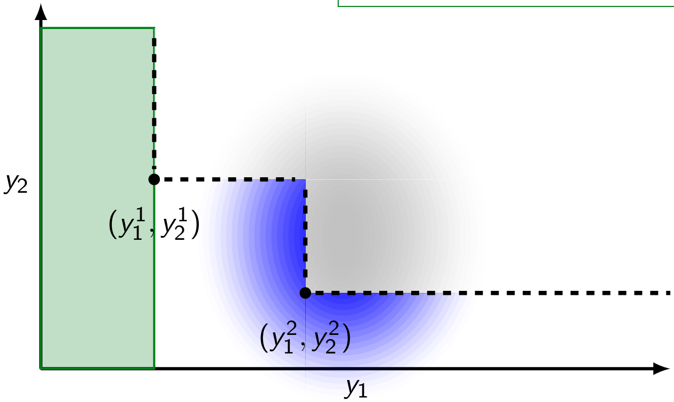

Keane, A. J., AIAA Journal, 44(4):879–891, 2006.

2D EGO Illustration

We will use a multiobjective expected improvement framework:

$$P(I) = \boxed{\int_{-\infty}^{y_1^1}\int_{-\infty}^{\infty} p(\hat{y}_1(x^*), \hat{y}_2(x^*))dy_1 dy_2}$$

$$+ \boxed{\int_{y_1^1}^{y_2^1}\int_{-\infty}^{y_2^1} p(\hat{y}_1(x^*), \hat{y}_2(x^*))dy_1 dy_2}$$

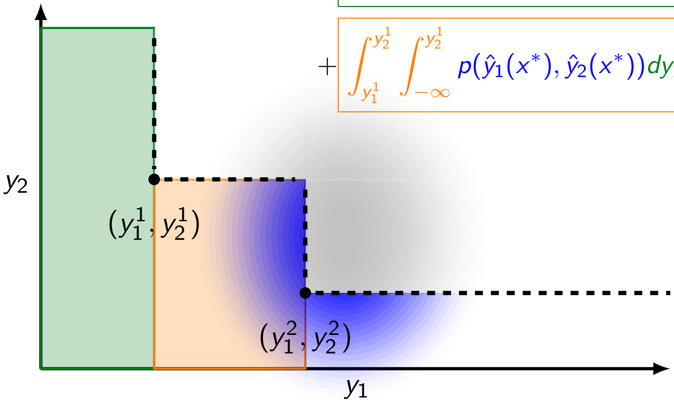

Keane, A. J., AIAA Journal, 44(4):879–891, 2006.

2D EGO Illustration

We will use a multiobjective expected improvement framework:

$$P(I) = \boxed{\int_{-\infty}^{y_1^1}\int_{-\infty}^{\infty} p(\hat{y}_1(x^*), \hat{y}_2(x^*))\,dy_1\,dy_2}$$

$$+ \boxed{\int_{y_1^1}^{y_2^1}\int_{-\infty}^{y_2^1} p(\hat{y}_1(x^*), \hat{y}_2(x^*))\,dy_1\,dy_2}$$

$$+ \boxed{\int_{y_1^2}^{\infty}\int_{-\infty}^{y_2^2} p(\hat{y}_1(x^*), \hat{y}_2(x^*))\,dy_1\,dy_2}$$

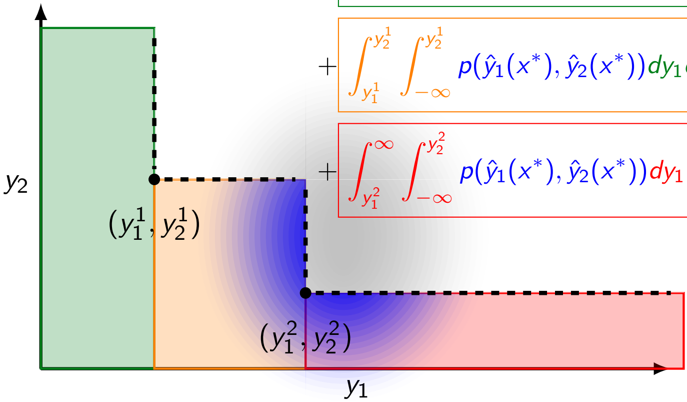

Keane, A. J., AIAA Journal, 44(4):879–891, 2006.

2D EGO Illustration

We will use a multiobjective expected improvement framework:

$$P(I) = \boxed{\int_{-\infty}^{y_1^1}\int_{-\infty}^{\infty} p(\hat{y}_1(x^*), \hat{y}_2(x^*))\,dy_1\,dy_2} + \boxed{\int_{y_1^1}^{y_2^1}\int_{-\infty}^{y_2^1} p(\hat{y}_1(x^*), \hat{y}_2(x^*))\,dy_1\,dy_2} + \boxed{\int_{y_1^2}^{\infty}\int_{-\infty}^{y_2^2} p(\hat{y}_1(x^*), \hat{y}_2(x^*))\,dy_1\,dy_2}$$

$$= f(\mu_1, \mu_2, \sigma_1, \sigma_2, \mathcal{F})$$

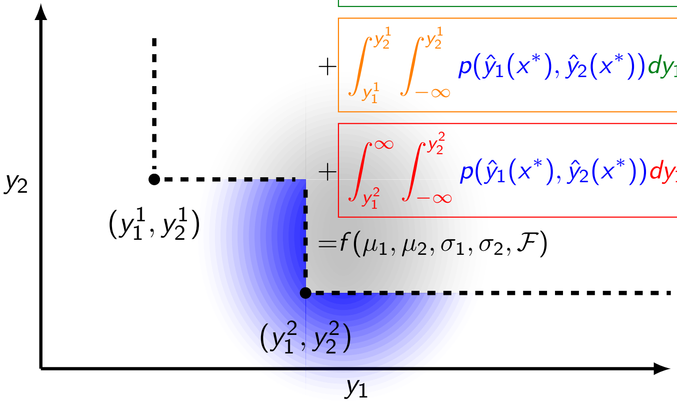

Keane, A. J., AIAA Journal, 44(4):879–891, 2006.

2D EGO Illustration

We will use a multiobjective expected improvement framework:

$$\mathbb{E}[I] = \int\int d(\hat{y}, \mathcal{F}) P[I(x^*)] d\hat{y}_1 d\hat{y}_2$$

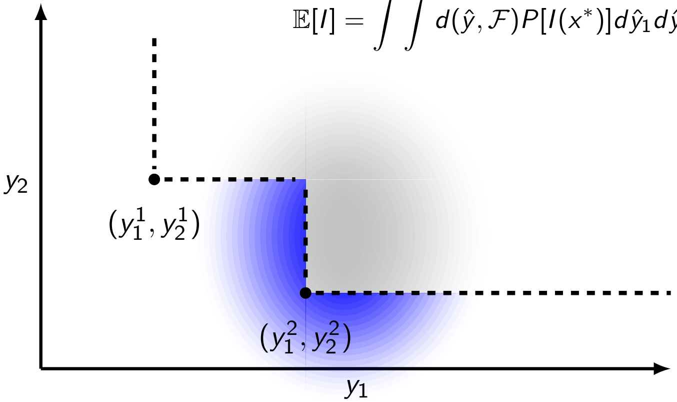

Keane, A. J., AIAA Journal, 44(4):879–891, 2006.

2D EGO Illustration

We will use a multiobjective expected improvement framework:

$$\mathbb{E}[I] = \int\int d(\hat{y}, \mathcal{F}) P[I(x^*)] d\hat{y}_1 d\hat{y}_2$$

$$\frac{\mathbb{E}[I]}{P(I)} = d(C, \mathcal{F})$$

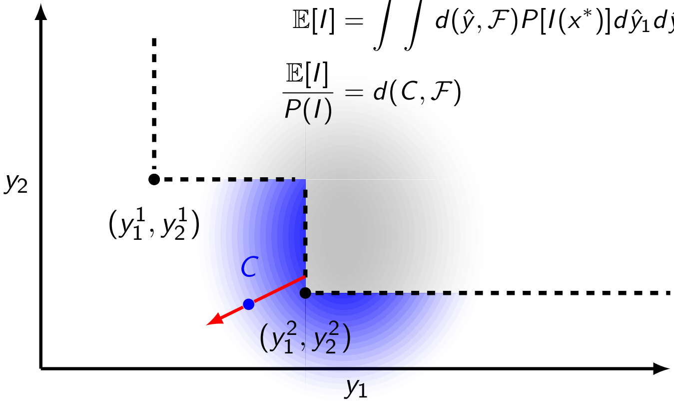

Keane, A. J., AIAA Journal, 44(4):879–891, 2006.

2D EGO Illustration

We will use a multiobjective expected improvement framework:

$$\mathbb{E}[I] = \int\int d(\hat{y}, \mathcal{F}) P[I(x^*)] d\hat{y}_1 d\hat{y}_2$$

$$\frac{\mathbb{E}[I]}{P(I)} = d(C, \mathcal{F})$$

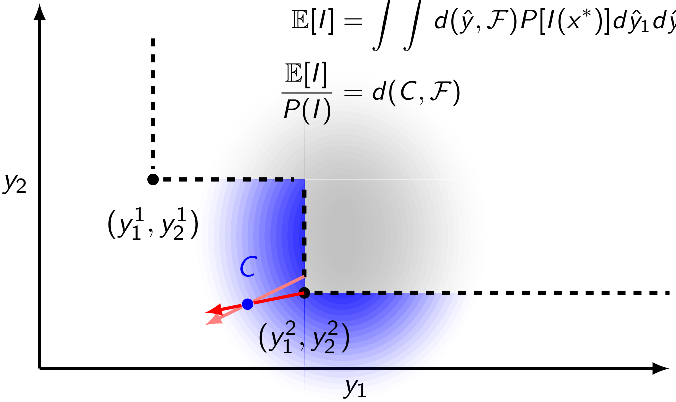

Keane, A. J., AIAA Journal, 44(4):879–891, 2006.

Design space and existing data

We observe poor overlap between existing data and design space:

Janet, J.P., *et al.*, *in preparation*.

Design space and existing data

We observe poor overlap between existing data and design space:

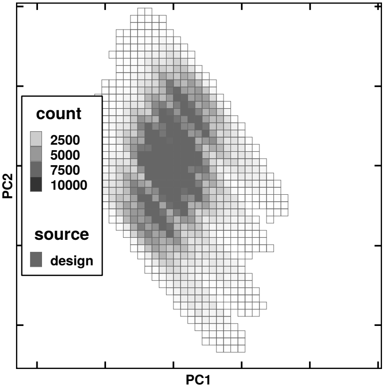

Janet, J.P., *et al.*, *in preparation*.

Design space and existing data

We observe poor overlap between existing data and design space:

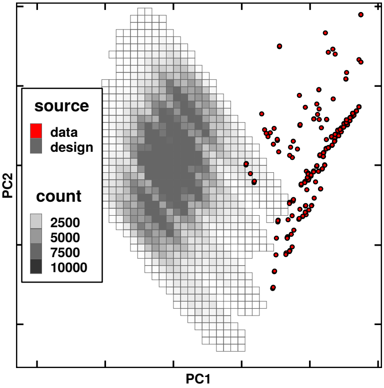

design space $\mathcal{O}(10^6)$

Janet, J.P., *et al.*, *in preparation*.

Design space and existing data

We observe poor overlap between existing data and design space:

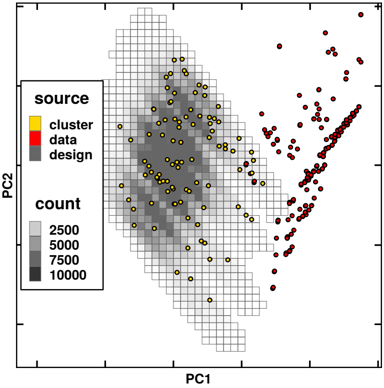

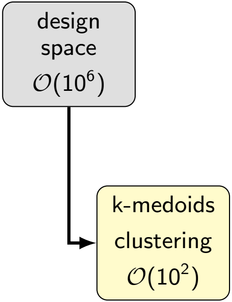

Janet, J.P., *et al.*, *in preparation*.

Design space and existing data

We observe poor overlap between existing data and design space:

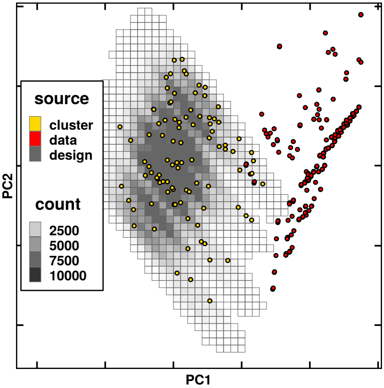

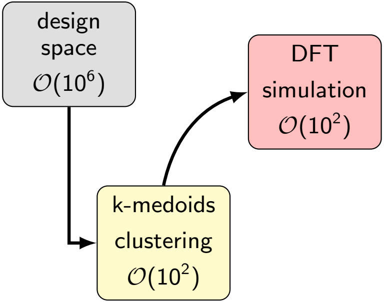

Janet, J.P., *et al.*, *in preparation*.

Design space and existing data

We observe poor overlap between existing data and design space:

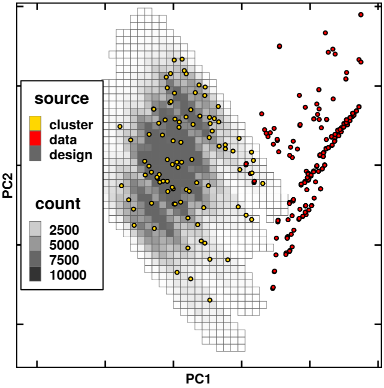

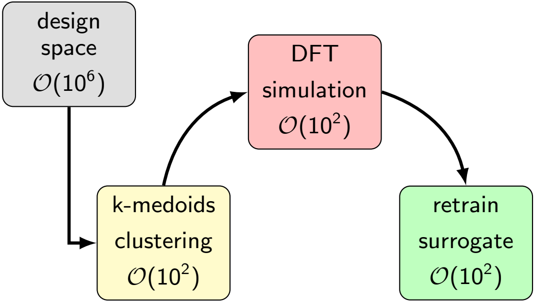

Janet, J.P., *et al.*, *in preparation*.

Design space and existing data

We observe poor overlap between existing data and design space:

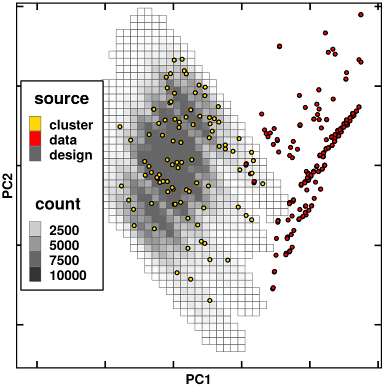

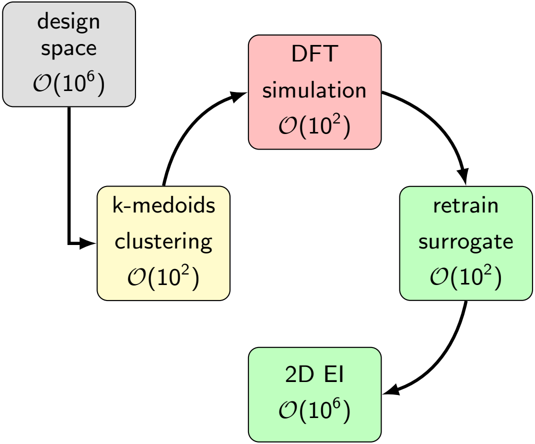

Janet, J.P., *et al.*, *in preparation*.

Design space and existing data

We observe poor overlap between existing data and design space:

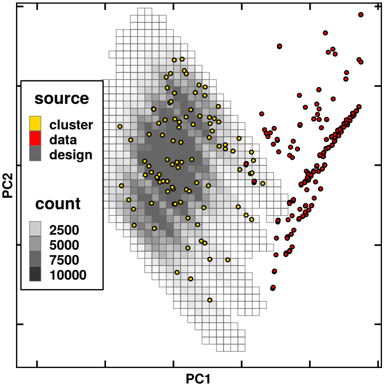

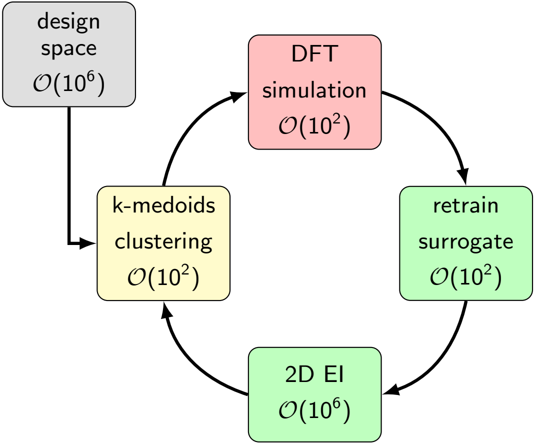

Janet, J.P., *et al.*, *in preparation*.

Design space and existing data

We observe poor overlap between existing data and design space:

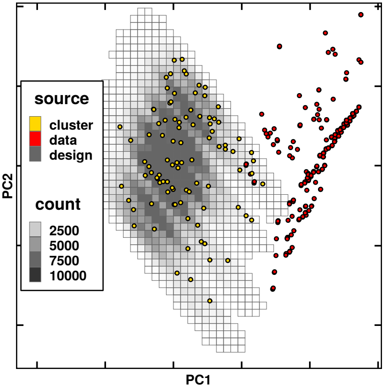

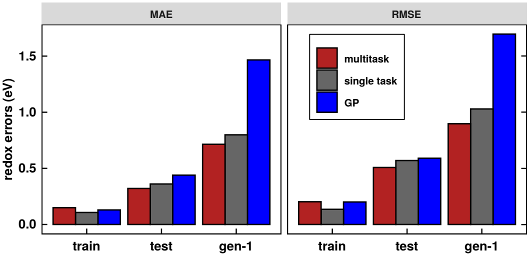

single task redox: 3 × 100 tanh nodes, fully connected
single task log P: 2 × 50 ReLU nodes, skip + residual connections
multitask: 2 × 100 tanh nodes, fully connected

Janet, J.P., *et al.*, *in preparation*.

Design space and existing data

We observe poor overlap between existing data and design space:

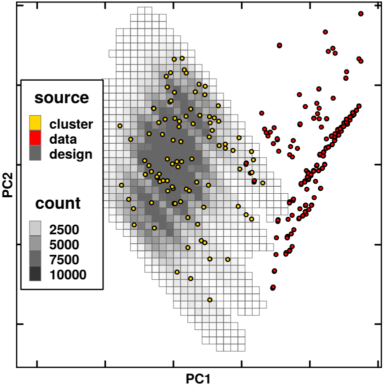

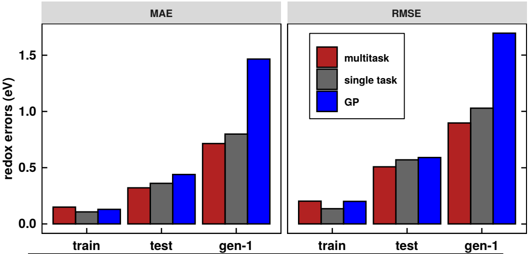

Therefore, we will use multitask ANN to drive the design process

single task redox: 3 × 100 tanh nodes, fully connected
single task log P: 2 × 50 ReLU nodes, skip + residual connections
multitask: 2 × 100 tanh nodes, fully connected

Janet, J.P., *et al.*, *in preparation*.

Active learning

We can monitor the evolution of the model as data is acquired

feature space

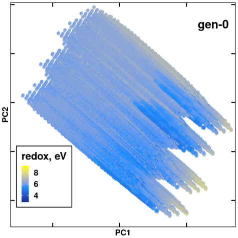

Active learning

We can monitor the evolution of the model as data is acquired

feature space

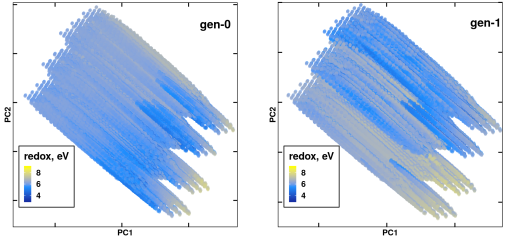

Active learning

We can monitor the evolution of the model as data is acquired

feature space

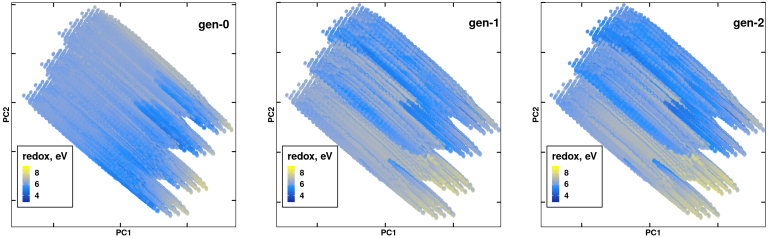

Active learning

We can monitor the evolution of the model as data is acquired

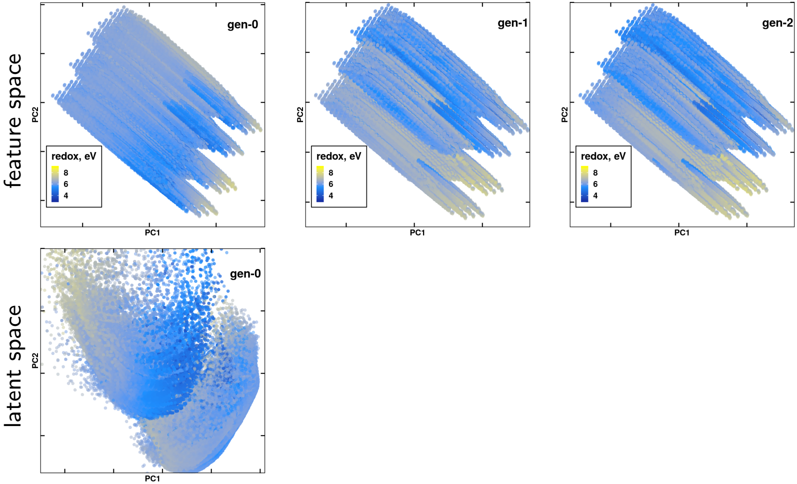

Active learning

We can monitor the evolution of the model as data is acquired

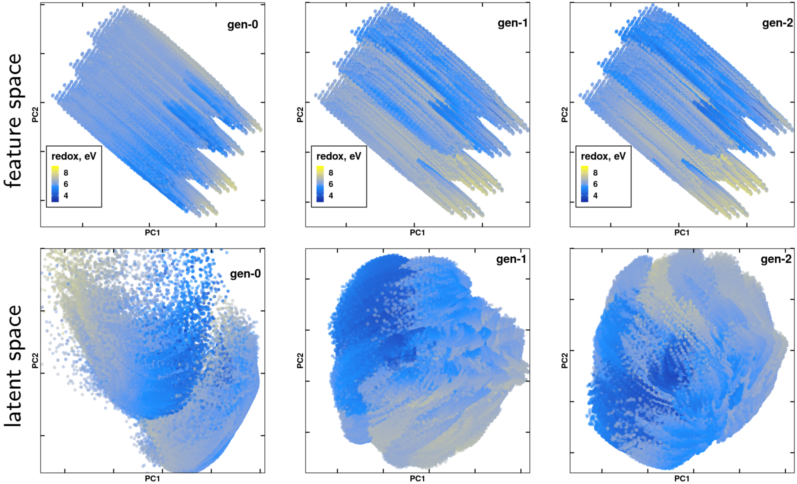

Active learning

We can monitor the evolution of the model as data is acquired

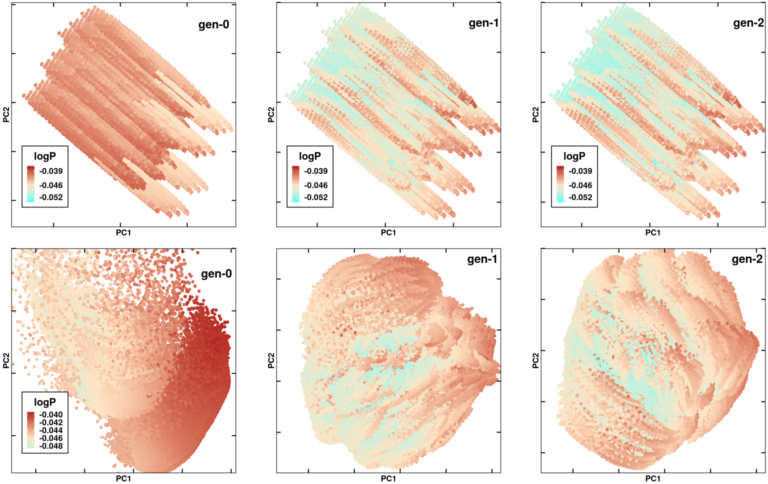

Active learning

We can monitor the evolution of the model as data is acquired

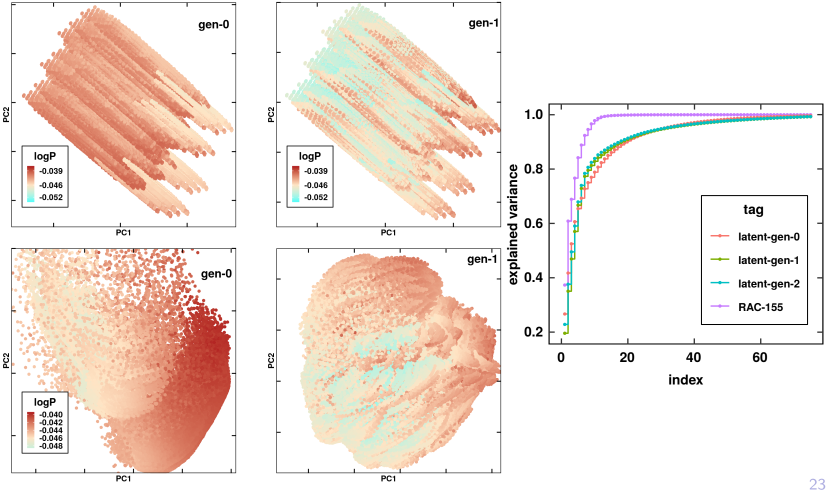

Mapping output space

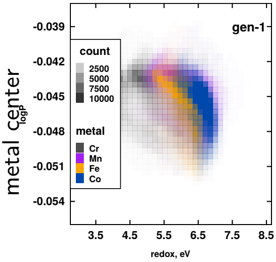

Mapping output space

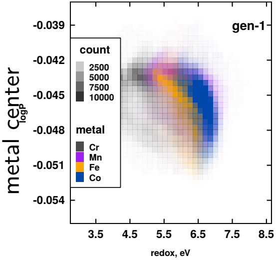

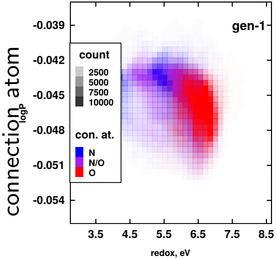

Mapping output space

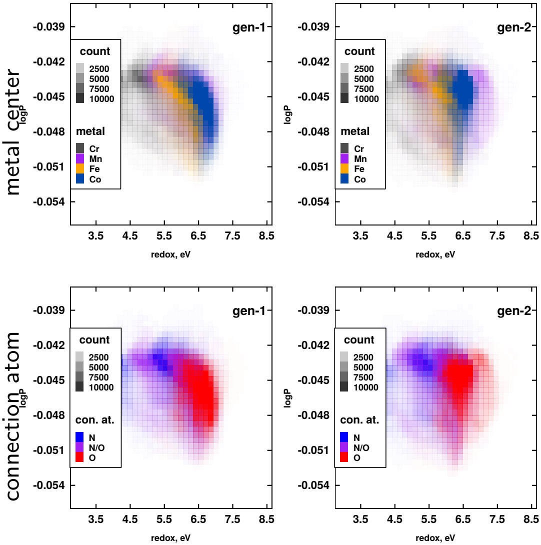

Mapping output space

metal center

connection atom

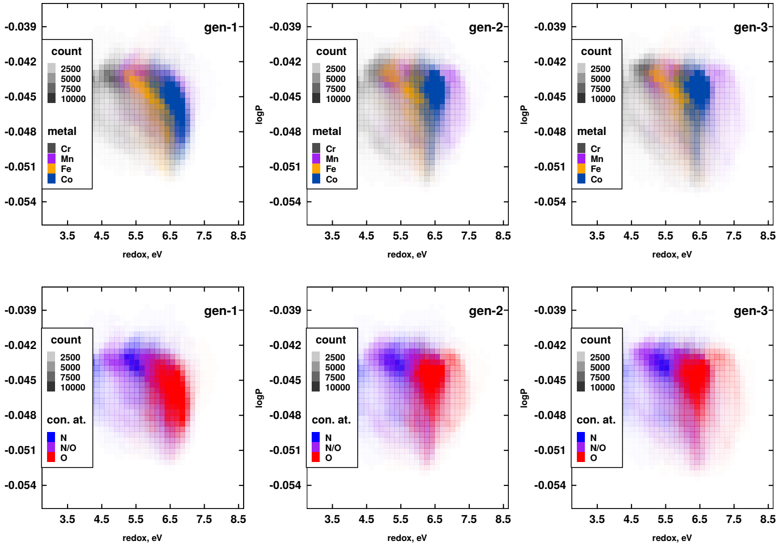

Mapping output space

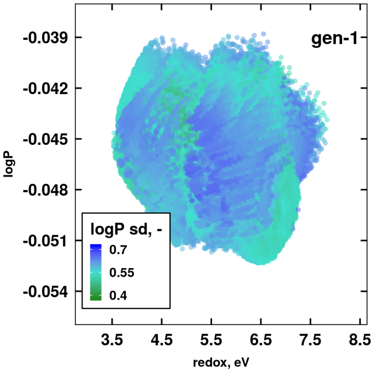

Mapping output space

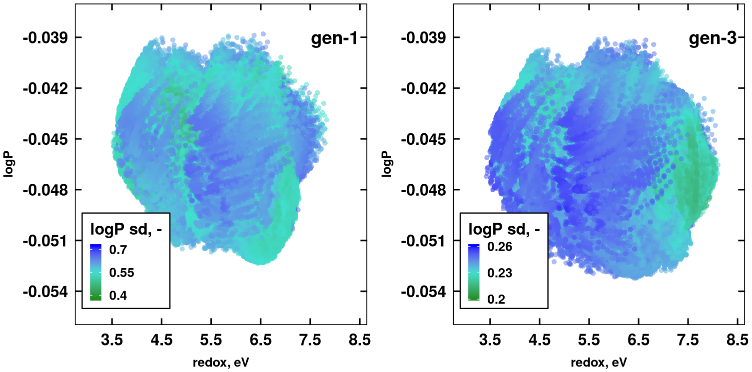

model confidence is localized in target region!

EGO results

probability of improvement

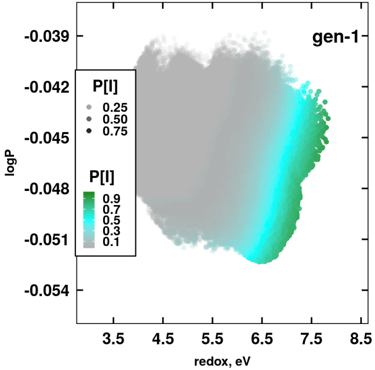

expected improvement

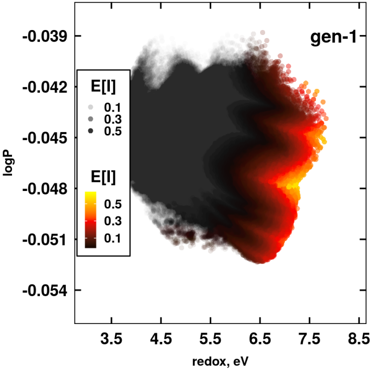

Janet, J.P., *et al.*, *in preparation*.

EGO results

probability of improvement

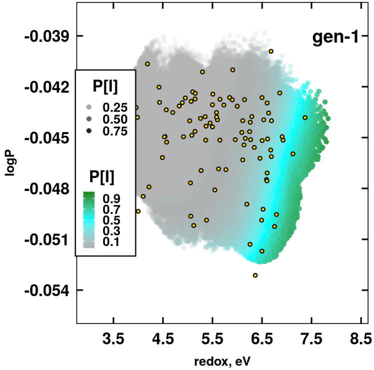

expected improvement

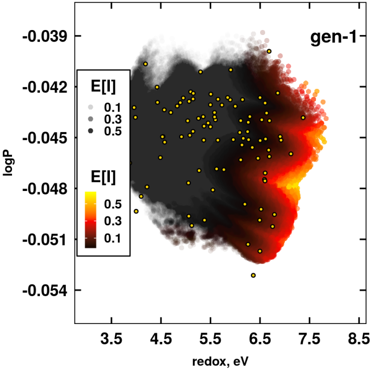

Janet, J.P., *et al.*, *in preparation*.

EGO results

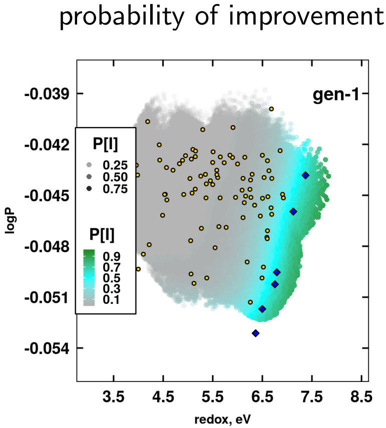

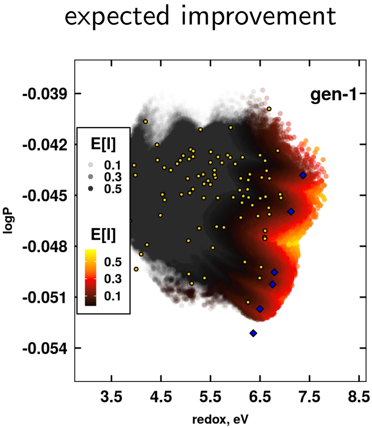

Janet, J.P., *et al.*, *in preparation*.

EGO results

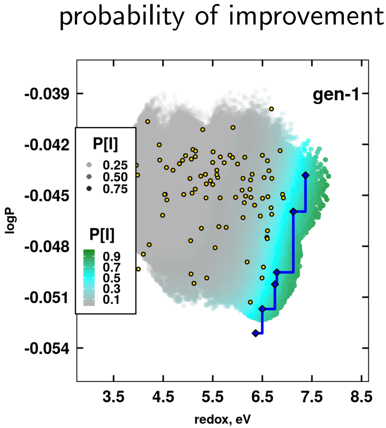

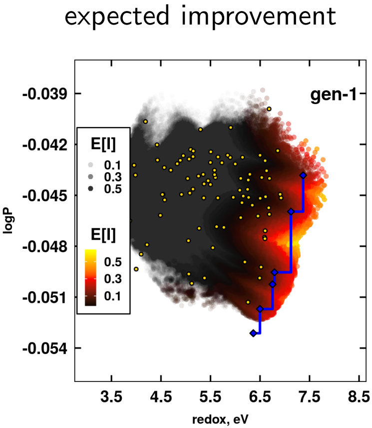

Janet, J.P., *et al.*, *in preparation*.

EGO results

probability of improvement

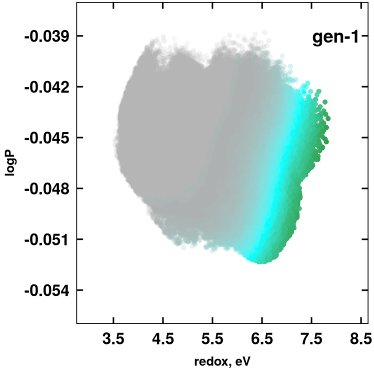

expected improvement

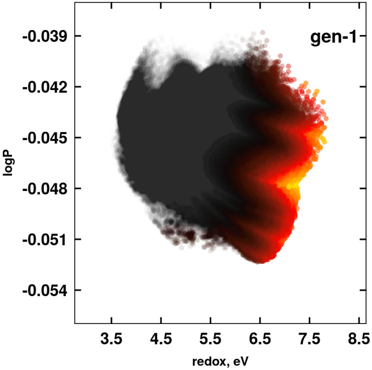

Janet, J.P., *et al.*, *in preparation*.

DFT results

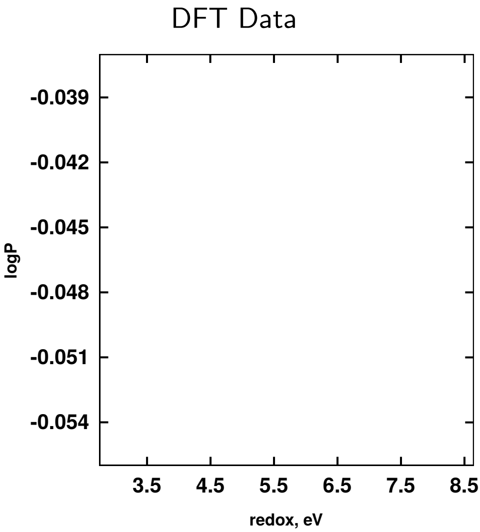

Janet, J.P., *et al.*, *in preparation*.

DFT results

k-medoids points (gen 1: 107 complexes)

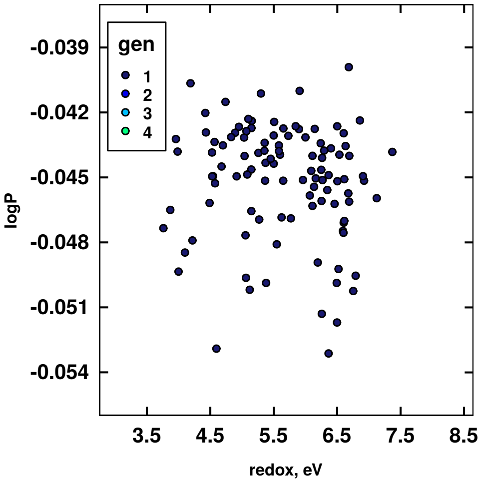

Janet, J.P., *et al.*, *in preparation*.

DFT results

pareto front (gen 1)

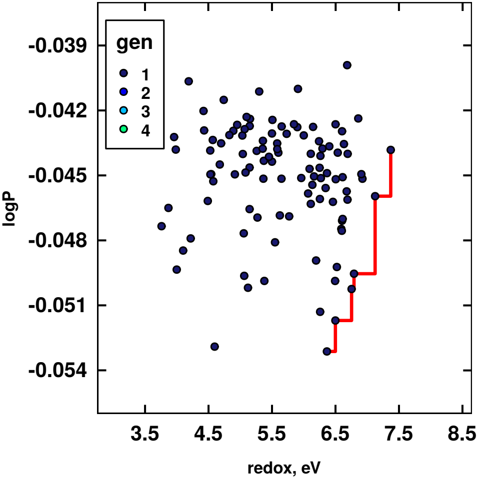

Janet, J.P., *et al.*, *in preparation*.

DFT results

EI points (gen 2: 34 complexes)

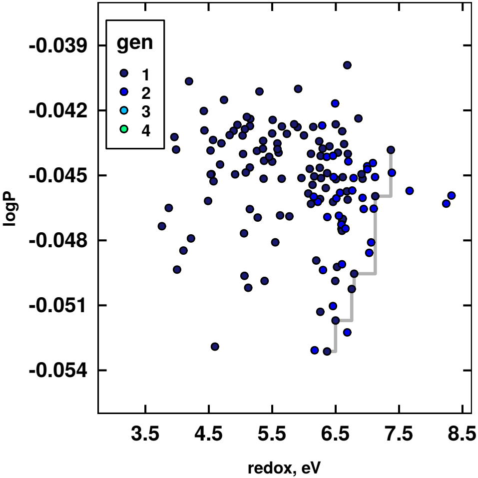

Janet, J.P., *et al.*, *in preparation*.

DFT results

pareto front (gen 2)

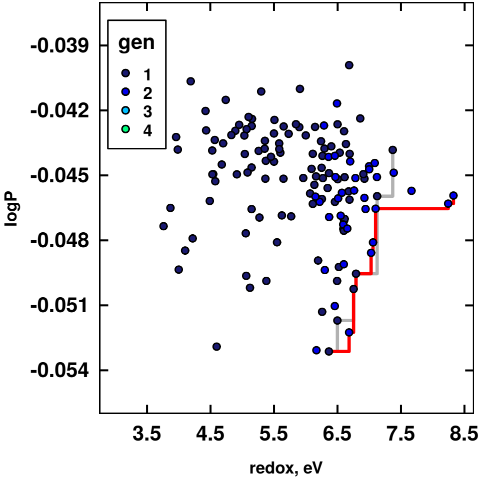

Janet, J.P., *et al.*, *in preparation*.

DFT results

EI points (gen 3: 24 complexes)

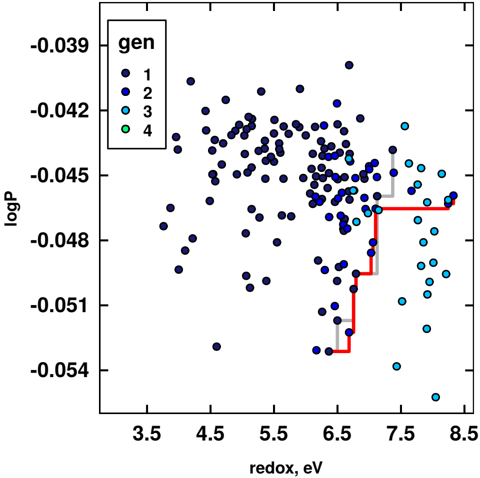

Janet, J.P., *et al.*, *in preparation*.

DFT results

pareto front (gen 3)

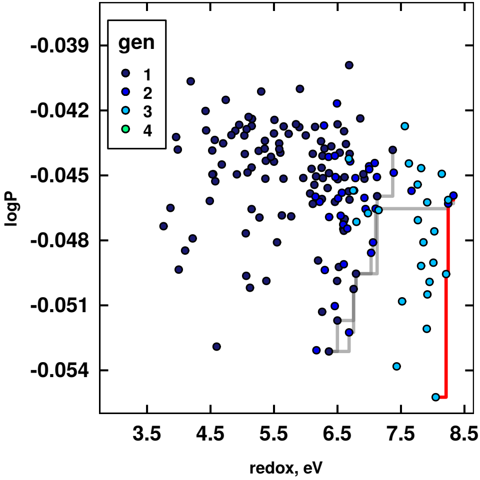

Janet, J.P., *et al.*, *in preparation*.

DFT results

EI points (gen 4: 15 complexes)

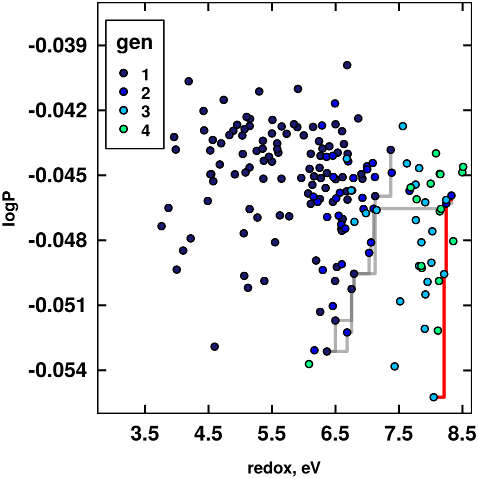

Janet, J.P., *et al.*, *in preparation*.

DFT results

pareto front (gen 4)

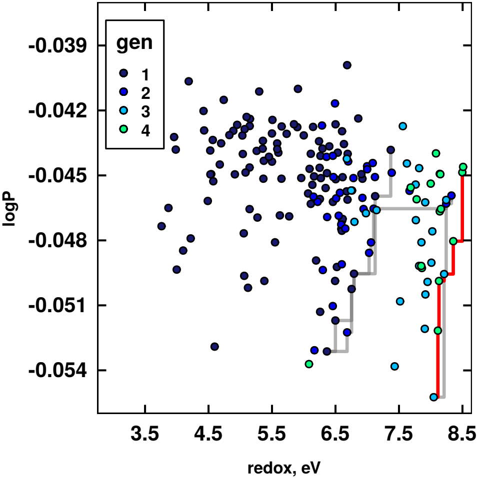

Janet, J.P., *et al.*, *in preparation*.

DFT results

convex hulls

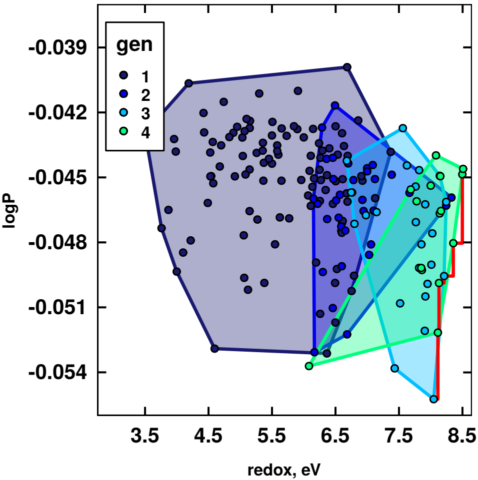

Janet, J.P., *et al.*, *in preparation*.

DFT results

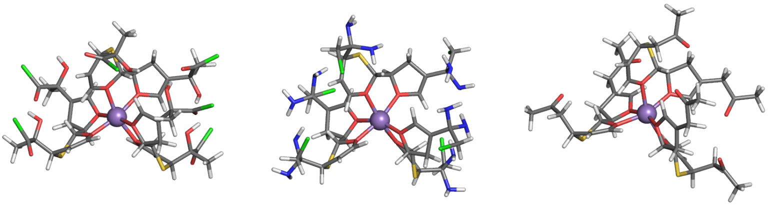

Janet, J.P., *et al.*, *in preparation*.

Case study conclusions

Janet, J.P., *et al.*, *in preparation*.

Case study conclusions

- EI framework provides high resolution in the region of interest (c.f. maximum uncertainty), converges quickly

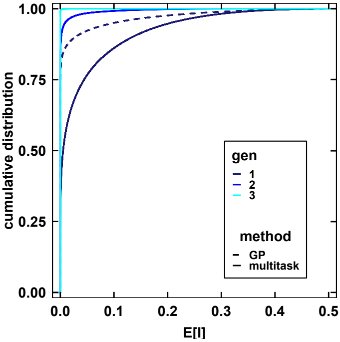

Janet, J.P., *et al.*, *in preparation*.

Case study conclusions

- EI framework provides high resolution in the region of interest (c.f. maximum uncertainty), converges quickly
- We are able to identify fruitful regions from large chemical spaces based on few DFT evaluations

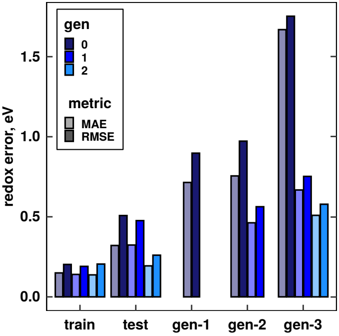

Janet, J.P., *et al.*, *in preparation*.

Case study conclusions

- EI framework provides high resolution in the region of interest (c.f. maximum uncertainty), converges quickly
- We are able to identify fruitful regions from large chemical spaces based on few DFT evaluations
- Multiobjective DFT optimization guided by data-driven method efficiency generates lead complexes

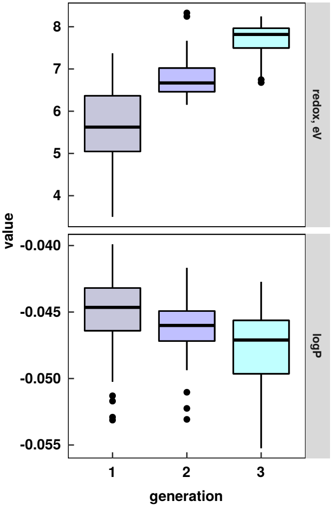

Janet, J.P., *et al.*, *in preparation*.

Acknowledgments

Thanks to the Kulik group and funding partners:

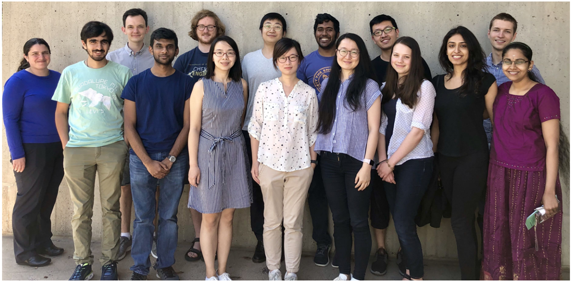

DARPA
MITei
DEPARTMENT OF ENERGY
UNITED STATES OF AMERICA
eni
Office of Naval Research
ONR
Science & Technology
NSF
BURROUGHS
WELLCOME
FUND

Thermodynamic cycle

$$\mathrm{M(III)}_s + e^- \xrightarrow[\Delta G_{\mathrm{solv}}]{} \mathrm{M(II)}_s$$

Thermodynamic cycle

$$M(III)_g + e^- \xrightarrow{\Delta G_{gas}} M(II)_g$$

$$M(III)_s + e^- \xrightarrow[\Delta G_{solv}]{} M(II)_s$$

Thermodynamic cycle

$$
\begin{tikzcd}
\mathrm{M(III)}_g + e^- \arrow[r, "\Delta \mathrm{G}_{\mathrm{gas}}"] \arrow[d, "\Delta \mathrm{G}_{\mathrm{s,III}}"'] & \mathrm{M(II)}_g \arrow[d, "\Delta \mathrm{G}_{\mathrm{s,II}}"] \\
\mathrm{M(III)}_s + e^- \arrow[r, "\Delta \mathrm{G}_{\mathrm{solv}}"'] & \mathrm{M(II)}_s
\end{tikzcd}
$$

Thermodynamic cycle

$$\begin{tikzcd}
M(III)_g + e^- \arrow[r, "\Delta G_{gas}"] \arrow[d, "\Delta G_{s,III}"'] & M(II)_g \arrow[d, "\Delta G_{s,II}"] \\
M(III)_s + e^- \arrow[r, "\Delta G_{solv}"'] & M(II)_s
\end{tikzcd}$$

$$\Delta G_{solv} = \Delta G_{gas} + \Delta\Delta G_s$$

Thermodynamic cycle

$$
\begin{tikzcd}
\mathrm{M(III)}_g + e^- \arrow[r, "\Delta \mathrm{G_{gas}}"] \arrow[d, "\Delta \mathrm{G_{s,III}}"'] & \mathrm{M(II)}_g \arrow[d, "\Delta \mathrm{G_{s,II}}"] \\
\mathrm{M(III)}_s + e^- \arrow[r, "\Delta \mathrm{G_{solv}}"'] & \mathrm{M(II)}_s
\end{tikzcd}
$$

$$
\begin{aligned}
\Delta \mathrm{G_{solv}} &= \Delta \mathrm{G_{gas}} + \Delta\Delta \mathrm{G}_s \\
&\approx \Delta \mathrm{E}_{\mathrm{gas},III-II} + \Delta\Delta \mathrm{G}_s
\end{aligned}
$$

Thermodynamic cycle

$$\begin{tikzcd}
M(III)_g + e^- \arrow[r, "\Delta G_{gas}"] \arrow[d, "\Delta G_{s,III}"'] & M(II)_g \arrow[d, "\Delta G_{s,"] \\
M(III)_s + e^- \arrow[r, "\Delta G_{solv}"'] & M(II)_s
\end{tikzcd}$$

$$\Delta G_{solv} = \Delta G_{gas} + \Delta\Delta G_s$$
$$\approx \Delta E_{gas,III-II} + \Delta\Delta G_s$$

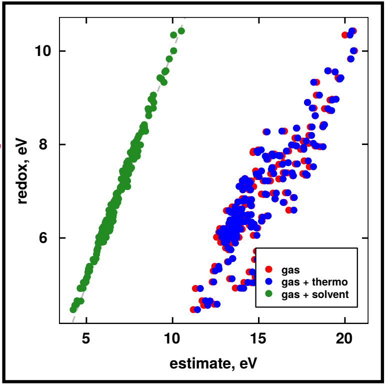

Thermodynamic cycle

$$
\begin{tikzcd}
\mathrm{M(III)}_g + e^- \arrow[r, "\Delta \mathrm{G}_{\mathrm{gas}}"] \arrow[d, "\Delta \mathrm{G}_{\mathrm{s,III}}"'] & \mathrm{M(II)}_g \arrow[d, "\Delta \mathrm{G}_{\mathrm{s,II}}"] \\
\mathrm{M(III)}_s + e^- \arrow[r, "\Delta \mathrm{G}_{\mathrm{solv}}"'] & \mathrm{M(II)}_s
\end{tikzcd}
$$

$$
\begin{aligned}
\Delta \mathrm{G}_{\mathrm{solv}} &= \Delta \mathrm{G}_{\mathrm{gas}} + \Delta\Delta \mathrm{G}_s \\
&\approx \Delta \mathrm{E}_{\mathrm{gas},III-II} + \Delta\Delta \mathrm{G}_s \\
\log \mathrm{P} &\approx \log \frac{\Delta \mathrm{G}_{\mathrm{s,II,octanol}}}{\Delta \mathrm{G}_{\mathrm{s,II,water}}}
\end{aligned}
$$

- Spin state taken as the M(II) ground state
- Need 3 geometry optimizations at minimum